

**UNIVERSITY OF SOUTH BOHEMIA IN ČESKÉ BUDĚJOVICE**  
**FACULTY OF AGRICULTURE**

**DISSERTATION**

**Analysis of matter and energy fluxes within the montane forest and  
grassland ecosystems based on spectral characteristics of vegetation**

Mgr. Alexander Ač

**2009**



**Supervisor:** prof. RNDr. Ing. Michal V. Marek, DrSc.  
Institute of Systems Biology and Ecology, Brno  
Academy of Sciences of the Czech Republic

**Consultants:** Dr. Zbyněk Malenovský  
Remote Sensing Laboratories, Department of Geography,  
University of Zürich  
Dr. Otmar Urban  
Institute of Systems Biology and Ecology, Brno  
Academy of Sciences of the Czech Republic

I would like to thank to **prof. RNDr. Ing. Michal V. Marek, DrSc.** and to my consultants **Dr. Zbyněk Malenovský and Dr. Otmar Urban** for their help and advices during my PhD studies.

I would like to thank to all of my colleagues at the Institute of Systems Biology and Ecology, at Ostrava University and at Wageningen University. Without their help, this work would not be possible.

Invaluable thanks are devoted to my family and close friends.

I declare that the dissertation thesis was written independently, based on my own ideas and with the help of the cited literature.

.....

In České Budějovice on 25. 9. 2009

## TABLE OF CONTENTS

<b>LIST OF FIGURES</b> .....	<b>VI</b>
<b>LIST OF TABLES</b> .....	<b>X</b>
<b>LIST OF ACRONYMS</b> .....	<b>XI</b>
<b>ABSTRAKT</b> .....	<b>XIII</b>
<b>SUMMARY</b> .....	<b>XIV</b>
<b>CHAPTER 1</b> .....	<b>15</b>
<b>GENERAL INTRODUCTION</b> .....	<b>15</b>
1.1 MOTIVATION .....	16
1.2 RESEARCH OBJECTIVES .....	17
1.3 REFERENCES .....	18
<b>CHAPTER 2</b> .....	<b>20</b>
<b>THEORY BACKGROUND</b> .....	<b>20</b>
2.1 BASICS OF IMAGING SPECTROSCOPY.....	21
2.2 XANTHOPHYLL CYCLE AND REMOTE SENSING.....	22
2.2.1 <i>Molecular basis and ecophysiology of xanthophyll cycle</i> .....	22
2.2.2 <i>Remote sensing of xanthophyll cycle and photosynthetic activity</i> .....	25
2.2.2.1 <i>Leaf to canopy level</i> .....	25
2.2.2.2 <i>Regional to satellite level</i> .....	26
2.3 REMOTE SENSING OF CHLOROPHYLL FLUORESCENCE .....	27
2.3.1 <i>Basics of chlorophyll fluorescence</i> .....	27
2.3.2 <i>Basic characteristics of selected chlorophyll fluorescence parameters</i> .....	28
2.3.3 <i>Measurements of chlorophyll fluorescence emission from reflectance</i> .....	29
2.3.4 <i>Chlorophyll fluorescence vegetation indices and their relation to chlorophyll fluorescence</i> .....	30
2.4 REFERENCES .....	31
<b>CHAPTER 3</b> .....	<b>41</b>
<b>DIFFERENCES IN PIGMENT COMPOSITION, PHOTOSYNTHETIC RATES AND CHLOROPHYLL FLUORESCENCE IMAGES OF SUN AND SHADE LEAVES OF FOUR TREE SPECIES</b> .....	<b>41</b>
3.1 INTRODUCTION.....	43
3.2 MATERIALS AND METHODS .....	44
3.2.1 <i>Site description</i> .....	44
3.2.2 <i>Plant material</i> .....	44
3.2.3 <i>Pigment analysis</i> .....	45
3.2.4 <i>Gas-exchange measurement</i> .....	45
3.2.5 <i>Chlorophyll fluorescence imaging</i> .....	45
3.2.6 <i>Statistical analysis</i> .....	46
3.3 RESULTS.....	46
3.3.1 <i>General leaf characteristics</i> .....	47
3.3.2 <i>Chlorophyll and carotenoid levels</i> .....	48
3.3.3 <i>Pigment ratios</i> .....	48
3.3.4 <i>Measurements of photosynthetic rates <math>P_N</math></i> .....	48
3.3.5 <i>Chlorophyll fluorescence imaging</i> .....	49
3.4 DISCUSSION.....	50
3.5 CONCLUSIONS .....	59
3.6 ACKNOWLEDGMENTS .....	60
3.7 REFERENCES .....	60
<b>CHAPTER 4</b> .....	<b>65</b>
<b>NEAR DISTANCE IMAGING SPECTROSCOPY INVESTIGATING CHLOROPHYLL FLUORESCENCE AND PHOTOSYNTHETIC ACTIVITY OF GRASSLAND IN THE DAILY COURSE</b> .....	<b>65</b>

4.1 INTRODUCTION.....	67
4.2 MATERIALS AND METHODS.....	69
4.2.1 <i>Study site description</i> .....	69
4.2.2 <i>Measurement of leaf chlorophyll fluorescence</i> .....	69
4.2.3 <i>Ground-based imaging spectroscopy</i> .....	70
4.2.3.1 <i>Leaf and canopy observational levels</i> .....	71
4.2.3.2 <i>“Shade-removal” experiment</i> .....	72
4.2.3.3 <i>Optical vegetation indexes</i> .....	72
4.2.4 <i>Statistical analysis</i> .....	72
4.3 RESULTS.....	72
4.3.1 <i>Chlorophyll fluorescence detection from image data</i> .....	73
4.3.2 <i>Interpretation of hyperspectral images at leaf level</i> .....	74
4.3.3 <i>Interpretation of hyperspectral images at canopy level</i> .....	77
4.4 DISCUSSION.....	78
4.4.1 <i>Remote detection of chlorophyll fluorescence signals</i> .....	78
4.4.2 <i>Fluorescence vegetation indexes – leaf image observations</i> .....	79
4.4.3 <i>Fluorescence vegetation indexes – canopy level</i> .....	81
4.5 CONCLUSIONS.....	82
4.6 ACKNOWLEDGEMENTS.....	82
4.7 REFERENCES.....	82
<b>CHAPTER 5.....</b>	<b>88</b>
<b>ARE SIMPLE REFLECTANCE RATIOS RELATED TO CHLOROPHYLL FLUORESCENCE ABLE TO TRACK CHANGES IN CARBON FLUXES OF GRASSLAND AND FOREST ECOSYSTEMS? ....</b>	<b>88</b>
5.1 INTRODUCTION.....	90
5.2 MATERIALS AND METHODS.....	92
5.2.1 <i>Study site</i> .....	92
5.2.1.1 <i>Grassland ecosystem</i> .....	92
5.2.1.2 <i>Forest ecosystem</i> .....	93
5.2.2 <i>Hyperspectral images</i> .....	93
5.2.2.1 <i>Image data processing</i> .....	93
5.2.3 <i>Measured parameters</i> .....	94
5.2.3.1 <i>Gas exchange measurements</i> .....	94
5.2.3.2 <i>Eddy-covariance measurements</i> .....	94
5.2.3.3 <i>Pigment analysis</i> .....	95
5.2.4 <i>Experimental setup</i> .....	95
5.2.5 <i>Statistical analysis</i> .....	97
5.3 RESULTS.....	97
5.3.1 <i>Steady-state experiment</i> .....	97
5.3.2 <i>“Shade removal” experiment</i> .....	98
5.3.3 <i>Daily course experiment</i> .....	98
5.4 DISCUSSION.....	102
5.5 CONCLUSIONS.....	104
5.6 ACKNOWLEDGEMENTS.....	105
5.7 REFERENCES.....	105
<b>CHAPTER 6.....</b>	<b>111</b>
<b>ANGULAR CHLOROPHYLL INDICES ESTIMATES DERIVED FROM GROUND-BASED DIURNAL COURSE DATA AND MULTIANGULAR CHRIS-PROBA DATA: TWO CASE STUDIES.....</b>	<b>111</b>
6.1 INTRODUCTION.....	113
6.2 METHODS.....	115
6.3 CASE STUDY I: SENSITIVITY OF MONTANE GRASSLAND VEGETATION INDICES USING DIURNAL AISA DATA MEASURED AT GROUND.....	116
6.3.1 <i>Data acquisition and study site</i> .....	116
6.3.2 <i>Classification and resampling</i> .....	116
6.4 RESULTS.....	117
6.4.1 <i>Diurnal course</i> .....	119
6.5 CASE STUDY II: SENSITIVITY OF CONIFEROUS FOREST VEGETATION INDICES USING MULTIANGULAR CHRIS-PROBA DATA AND FLIGHT MODELLING.....	121
6.5.1 <i>Data and study site</i> .....	121

6.6 RESULTS.....	123
6.6.1 <i>Chlorophyll indices sensitivity analysis</i> .....	124
6.7 CONCLUSIONS .....	126
6.8 REFERENCES .....	127
<b>CURRICULUM VITAE.....</b>	<b>130</b>
<b>LIST OF PUBLICATIONS.....</b>	<b>131</b>

## List of figures

- Figure 2.1. Typical spectral signature (y-axis - reflectance, relative signal) for healthy green leaf in a wavelength region from 400 to 1000 nm (x-axis) with a description of areas, where biophysical properties of vegetation can be estimated. (Adapted from Penuelas and Filella 1998, published with permission). ..... 21
- Figure 2.2. Schematic representation of the xanthophyll cycle. Through the action of the enzyme violaxanthin de-epoxidase (VDE), violaxanthin is converted to zeaxanthin in a two-step process, with antheraxanthin as intermediate. The Z can be epoxidized back to violaxanthin by zeaxanthin epoxidase (ZE). (Adapted from Szabo et al. 2005, published with permission). ..... 23
- Figure 2.3. Fates of sunlight absorbed in the light-harvesting chlorophyll complexes. Chl, chlorophyll; 1Chl\*, excited singlet chlorophyll; 3Chl\*, excited triplet chlorophyll; P, photochemistry (green); D, safe dissipation of excess excitation energy as heat (red); F, fluorescence; 3T, triplet pathway, leading to the formation of singlet oxygen ( $1O_2^*$ ) and photo-oxidative damage. (Adapted from Demmig-Adams and Adams 2000, published with permission). ..... 27
- Figure 2.4. A) Reflectance spectrum of a *Helianthus annuus* (sunflower) leaf in the dark state (solid line) and 10 minutes after exposure to the white light (dotted line). B) differential spectrum (reflectance in dark state minus reflectance in light state, i.e.  $\Delta R$ ) derived from the spectra A). (Adapted from Gamon and Surfus 1999, published with permission). ..... 29
- Figure 3.1 Differences in needle thickness ( $\mu\text{m}$ ) between sun and shade needles of fir (*Abies alba*) of different needle years. The values are given for 1<sup>st</sup>, 2<sup>nd</sup>, 3<sup>rd</sup>, 4<sup>th</sup> and 5<sup>th</sup> year needles. Needles from three branches of two trees ( $n = 18$  for each needle year and condition). Columns represent mean values and bars standard deviations. The differences are highly significant ( $p < 0.001$ ). ..... 47
- Figure 3.2. A,B. Relative water content (RWC; A) and specific leaf area (SLA; B) in sun (white columns) and shade leaves (black columns) of deciduous *Acer pseudoplatanus*, *Fagus sylvatica*, *Tilia cordata* and coniferous *Abies alba*. All differences between sun and shade leaves are statistically highly significant ( $p < 0.01$ ). Columns represent mean values and bars standard deviations.  $n = 8$ . ..... 47
- Figure 3.3. A-D. Total chlorophyll (Chl (a+b); A, B), and carotenoid content (Cars (x/c); C, D) expressed per leaf area unit (A, C) and dry weight unit (B, D). Sun (white columns) and shade leaves (black columns) of deciduous *Acer pseudoplatanus*, *Fagus sylvatica*, *Tilia cordata* and coniferous *Abies alba* are presented. Columns represent mean values and bars standard deviations. \*\* and \* represent the statistically significant differences at  $p < 0.01$  and  $p < 0.05$  level, respectively.  $n = 8$ . ..... 49
- Figure 3.4. A,B. Ratio of Chl a to Chl b (Chl a/b; A) and weight ratio of total chlorophylls to total carotenoids (Chls/Cars; B) in sun (white columns) and shade leaves (black columns) of deciduous *Acer pseudoplatanus*, *Fagus sylvatica*, *Tilia cordata* and coniferous *Abies alba* are



presented. All differences between sun and shade leaves are statistically highly significant ( $p < 0.01$ ). Columns represent mean values and bars the standard deviations.  $n = 8$ ..... 51

Figure 3.5. A-C. Maximum of light-saturated CO<sub>2</sub> assimilation rate ( $P_{Nmax}$ ) expressed on a projected leaf area basis (A), on a chlorophyll ( $a+b$ ) basis (B), and on a leaf dry weight basis (C). Mean values (columns) and standard deviations (bars) of sun (white columns) and shade leaves and needles (black columns) of *Acer pseudoplatanus*, *Fagus sylvatica*, *Tilia cordata*, and *Abies alba* are presented. All differences between sun and shade leaves are statistically highly significant ( $p < 0.01$ ), except  $P_{Nmax}$  expressed on a leaf dry weight basis (C) in *A. pseudoplatanus*.  $n = 8$ ..... 52

Figure 3.6. Relationship between maximum CO<sub>2</sub> assimilation rate ( $P_{Nmax}$ ) and maximum stomatal conductance for water vapor ( $G_{Smax}$ ) at saturating photosynthetic photon flux density (PPFD $\approx$ 1500  $\mu\text{mol m}^{-2} \text{s}^{-1}$ ). Symbols represent the mean of five measurements of sun and shade leaves of *A. pseudoplatanus*, *F. sylvatica*, *T. cordata*, and shoots of *A. alba*. All data were fitted using linear regression. The perpendicular broken line was drawn to indicate the values of sun leaves (upper right part) and shade leaves (lower left part). ..... 52

Figure 3.7. A-D. Images of the maximum Chl-F at a saturating light pulse ( $F_m$ ; A), and at steady state Chl-F after 5 min of continuous saturating light ( $F_s$ ; B), and the Chl-F decrease ratio ( $R_{Fd}$ ) in sun (C) and shade leaves (B) of *Fagus sylvatica*. The differences in the relative Chl-F yield of the different leaf parts are indicated by false colors with red for high and blue for low Chl-F. In case of the  $R_{Fd}$  ratio images (C, D) the colors indicate the absolute values of the ratio. See scale in (D). ..... 55

Figure 3.8. A-D. Images of the maximum Chl-F (red band near 690 nm) at a saturating pulse ( $F_M$ ; A), the steady state Chl-F after 5 min of continuous saturating light ( $F_s$ ; B), and the Chl-F decrease ratio ( $R_{Fd}$ ) in first-year sun (C) and shade needles (B) of *Abies alba*. The differences in the relative Chl fluorescence yield of the different needle parts are indicated by false colors with red for high and blue for low Chl-F. The fluorescence images of the  $R_{Fd}$  ratio are given in false colors that state the absolute values of the ratio. See scale in (D). ..... 56

Figure 3.9. A-D. Histograms of the relative frequency distribution of the Chl-F decrease ratio ( $R_{Fd}$ ) measured in sun (empty symbols) and shade leaves and needles (filled symbols) of *Acer pseudoplatanus* (A), *Fagus sylvatica* (B), *Tilia cordata* (C), and *Abies alba* (D). The  $R_{Fd}$  value distributions are based on several ten thousand leaf and needle pixels as indicated in Section 2. The relative frequency is indicated here as percentage, which allows to better compare the results of the four trees, since the absolute pixel numbers were not the same for all leaves. .. 57

Figure 3.10. Correlation between the red (band near 690 nm) chlorophyll fluorescence decrease ratio ( $R_{Fd}$ ) and the maximum CO<sub>2</sub> assimilation rate ( $P_{Nmax}$ ) at saturating photosynthetic photon flux density (PPFD $\approx$ 1500  $\mu\text{mol m}^{-2} \text{s}^{-1}$ ) of sun and shade leaves/needles of *Acer pseudoplatanus*, *Fagus sylvatica*, *Tilia cordata*, and *Abies alba*. All data were fitted using linear regression. The perpendicular broken line was drawn to indicate the values of the sun leaves (upper right part) and the shade leaves (lower left part). ..... 58

Figure 4.1. Experimental set-up of daily hyperspectral measurements performed with the visible and near-infrared AISA Eagle imaging spectroradiometer. The extent of the experimental plot was approximately 1.5 x 4.0 m; a black blanket was covering part of the experimental grassland plot (referred to as “mantled plot” in the text). Legend: 1 – extent of

sensed experimental plot; 2 – AISA hyperspectral sensor head, 3 – PAM Chlorophyll Fluorometer; 4 – PAM optical cable with a leaf clip; 5 – SPAD Chlorophyllmeter , 6 – AISA Eagle acquisition unit. .... 71

Figure 4.2. Reflectance difference ( $\Delta R$ ) spectra observed when subtracting the reflectance of green sun exposed pixels of the mantled plot acquired at the 5<sup>th</sup> and 90<sup>th</sup> s (●) and at the 90<sup>th</sup> and 200<sup>th</sup> s (●) after removal of a non-transparent blanket inducing the dark-adapted state of the canopy within 480-800 nm (A) intervals; vertical lines indicate SD (n > 400 000). The results of July 4<sup>th</sup> are presented; nevertheless, similar results were also obtained on July 19<sup>th</sup>. The intensity of zeaxanthin and chlorophyll fluorescence signals (numbers indicate peak wavelengths) in the daily course acquired on July 4<sup>th</sup> is indicated (B). .... 73

Figure 4.3. Determination coefficients ( $R^2$ ) found for the best-fit relationships between PRI (A),  $R_{686}/R_{630}$  (B),  $R_{740}/R_{800}$  (C) and physiological parameters of interest on July 19<sup>th</sup> 2007 during the daily course, n = 14-18. Bold numbers indicate the average  $R^2$  for a given parameter during the whole daily course and asterisks indicate level of statistical significance:  $p < 0.01$  (\*),  $p < 0.001$  (\*\*) and  $< 0.0001$  (\*\*\*). (Chl  $a+b$  – total chlorophyll content on area basis;  $F_V/F_M$  – maximum yield of chlorophyll fluorescence;  $F_S$  – Steady-state chlorophyll fluorescence;  $\Phi_{II}$  – actual quantum yield of chlorophyll fluorescence.)..... 74

Figure 4.4. Best fit regressions between the physiological parameters [total chlorophyll content (Chl  $a+b$ ), maximum yield of chlorophyll fluorescence ( $F_V/F_M$ ), steady-state chlorophyll fluorescence ( $F_S$ ) and actual quantum yield of chlorophyll fluorescence ( $\Phi_{II}$ )] and vegetation indexes (PRI and  $R_{686}/R_{630}$ ) (A–H). The numbers indicate local time of the fit during the daily course. The respective determination coefficients ( $R^2$ ) of the regressions are summarized in figure 3. N = 14-18. .... 76

Figure 4.5. Daily courses of vegetations indexes derived from the region of interest (ROI) (●) and from sun-exposed pixels of the whole image (○) for: (A) PRI, (B)  $R_{686}/R_{630}$ , and  $R_{740}/R_{800}$  (C). ROI represents the average of all measured leaves (N=150-180), and the image represents the average of all green sun-exposed pixels (n > 400 000).  $R^2$  coefficients of determination for the linear regression between the given vegetation index derived from the whole image and steady-state chlorophyll fluorescence ( $F_S$ ). Actual quantum yields of  $F_S$  ( $\Phi_{II}$ ) are indicated. Graph (D) shows the daily course of  $F_S$  (○) and the actual quantum yield of Chl-F (●) measured on sample leaves (ROI). Asterisks denote the significance at the probability level  $p < 0.001$ (\*\*). .... 78

Figure 5.1. Midday relationships between light-saturated  $CO_2$  assimilation rate ( $A_{max}$ ) and selected vegetation indices (A -  $R_{686}/R_{630}$ , B – PRI (Physiological Reflectance Index), C –  $R_{740}/R_{800}$ ) under saturating steady state light conditions (open dots); and the relative change of the vegetation indices ( $\Delta$ ) during the dynamic transition of plants form dark-to-light adapted state (closed dots). Each point represents mean value of five measurements for  $A_{max}$  and 8-10 measurements (pixels) for the reflectance indices. Error bars represent standard deviations. NS means non significant relationship. .... 97

Figure 5.2. Diurnal courses of de-epoxidation state of xanthophylls cycle pigments [DEPS =  $(Z+A)/(V+A+Z)$ ], where Z is zeaxanthin, A is antheraxanthin and V is violaxanthin] (A) and total chlorophyll pigment content (Chl  $a+b$ ) (B) of grassland and forest ecosystem (black and white columns, respectively). DEPS values represent a mean value of current, 1- and 2-years old needles) (n = 24), Chl  $a+b$  values represent mean values of current needles (n = 6). Error bars indicate standard deviations. .... 98

Figure 5.3. Daily courses of modelled net ecosystem exchange of CO<sub>2</sub> (NEE, A) and Light Use Efficiency (LUE, B) in grassland ecosystem and corresponding daily course of PRI (C) and R<sub>686</sub>/R<sub>630</sub> (D) vegetation indices over experimental plot of 4 m<sup>2</sup> measured by hyperspectral imaging sensor AISA Eagle (Specim, Finland). Each data point of eddy-covariance parameters represents an average of half-hour measurement. The PRI (Physiological Reflectance Index) and R<sub>686</sub>/R<sub>630</sub> data points represent average of more than 400 000 image (i.e., average of one image scan acquired in half and one hour intervals). ..... 99

Figure 5.4. Daily courses of modelled net ecosystem exchange of CO<sub>2</sub> (NEE, A) and radiation use efficiency (LUE, B) in forest ecosystem during two consecutive days with corresponding daily courses of R<sub>686</sub>/R<sub>630</sub> (C) and PRI (D) vegetation indexes (VIs) measured by hyperspectral imaging sensor AISA Eagle (Specim, Finland). Data points of eddy-covariance parameters represent averages of half-hour measurements (A,B) and data points of VIs (C,D) represent average of more than 400 000 image pixels (i.e., average of one image scan acquired in half and one hour intervals). ..... 100

Figure 6.1. Automatic classification of the representative area in diurnal course (pixel size of 0.1 x 0.2m; N=8145 pixels). The overall classification accuracy was between 83.1-87.8% with kappa coefficient between 0.78 – 0.83. .... 117

Figure 6.2. Histogram showing diurnal variation in defined classes. .... 118

Figure 6.3. Sensitivity of PRI (A), TCARI/OSAVI (B), SIPI (C) and NDVI (D) to deep shade (DS, blue), shade (S, green) and non-photosynthetic vegetation (NPV, red) at 12:30 (local time). .... 118

Figure 6.4. Noon-normalized diurnal courses of VIs for all pixels (A) and for sun-exposed pixels only (B). .... 120

Figure 6.5. Polar plot of CHRIS acquisition and illumination geometry as of June 27, 2004. PP: principal plane ..... 121

Figure 6.6. Averaged angular PRI and SIPI from forest acquired by CHRIS with error bars of ± 1 SEM (a). PRI derived from FLIGHT-BRFs with varying fractions of PV and NPV along the CHRIS viewing geometry (b). (%NPV= 100-%PV)..... 124

Figure 6.7. Normalized angular signatures of PRI, SIPI, TCARI/OSAVI and NDVI calculated from FLIGHT-BRFs for stands various PV-NPV mixtures..... 125

Figure 6.8. Standard deviations of VIs calculated from the (a) per-angle PV-NPV variability and (b) per-PV-NPV mixture angular variability..... 125

## List of tables

Table 2.1. Vegetation indices (VIs) used for quantification of chlorophyll fluorescence (Chl-F). Earlier VIs used for vegetation stress detection are also included as they are using the wavelengths where the effects of Chl-F on the apparent reflectance were later demonstrated. ....	30
Table 4.1 Best-fit regressions between vegetation indexes and tested physiological parameters. Legend: Total chlorophyll content – Chl <i>a+b</i> , Potential yield of chlorophyll fluorescence – $F_V/F_M$ ; Steady-state chlorophyll fluorescence – Chl-Fs; Actual quantum yield of chlorophyll fluorescence - $\Phi_{II}$ .....	77
Table 5.1. Vegetation indices (VIs) used in this study. Legend: $R_\lambda$ is reflectance at a wavelength $\lambda$ in nm, Light use efficiency - LUE; <i>Steady-state</i> chlorophyll fluorescence – $F_s$ .	94
Table 5.2. Summary of coefficients of determination ( $R^2$ ) found for the linear relations between vegetation indices (VIs) and physiological parameters derived from eddy-covariance measurements in (a) grassland and (b) forest. Gross primary production (GPP [ $\mu\text{mol}(\text{CO}_2) \text{ m}^2 \text{ s}^{-1}$ ] = NEE + R); Net ecosystem exchange of $\text{CO}_2$ (NEE [ $\mu\text{mol}(\text{CO}_2) \text{ m}^{-2} \text{ s}^{-1}$ ]); Gross Light Use Efficiency (gLUE = GPP/PPFD [ $\text{g C MJ}^{-1}$ ]); Radiation use efficiency (LUE = NEE/PPFD [ $\text{g C MJ}^{-1}$ ]). Values of eddy-covariance derived parameters are half-hour averages and values of VIs are averages of more than 400 000 pixels (i.e., average of one image scan acquired in half to one hour intervals), R is reflectance at subscripted wavelength and PRI is calculated as $(R_{532}-R_{570})/(R_{532}+R_{570})$ . * denotes for $p<0.1$ and ** for $p<0.05$ . ....	101
Table 6.1. Selected VIs used in this study with a central wavelength corresponding to both, AISA and CHRIS-PROBA bands. ....	115
Table 6.2. AISA sensor configuration during diurnal measurement.....	116
Table 6.3. Slopes of linear regressions of compared VIs in the diurnal course. Asterisks show statistical significance of linear regression at $p<0.05$ (*) and $p< 0.01$ (**) levels.....	119
Table 6.4. Normalized standard deviations as calculated from values in figure 6.4.....	120
Table 6.5. CHRIS configurations for Land Mode 3.....	121
Table 6.6. Averaged input variables for FLIGHT parameterization collected at four test sites. (Remaining input variables are described in Flight, 1996) .....	123
Table 6. 7. Ranked SDs of the in Figure 6.8 calculated SDs. ....	126

## List of acronyms

- [A] Antheraxanthin
- [AISA] Airborne Imaging Spectrometer for Applications
- [ $A_{\max}$ ] Carbon assimilation under saturating light condition
- [ANOVA] ANalysis Of VAriance
- [AVIRIS] Airborne Visible InfraRed Imaging Spectrometer
- [BRF] Bidirectional Reflectance Factor
- [Cars] Total carotenoids
- [CCD] Charge-Coupled Device
- [Chls] Total chlorophylls
- [CO<sub>2</sub>] Carbon dioxide
- [DA] Dark Adapted state
- [DEPS] De-epoxidation state
- [DS] Deep Shade
- [DW] Dry Weight
- [EPS] EPoxidation State
- [EC] Eddy-Covariance
- [EM] ElectroMagnetic
- [ $F_d$ ] Chl fluorescence decrease from  $F_M$  to  $F_S$
- [FRI] Fluorescence-Reflectance Index
- [FLIGHT] Forest LIGHT interaction model
- [ $F_M$ ] Maximum chlorophyll fluorescence of dark adapted leaf
- [ $F_M'$ ] Maximum chlorophyll fluorescence of light adapted leaf
- [ $F_S$ ] Steady-state chlorophyll fluorescence
- [ $F_V$ ] Variable chlorophyll fluorescence
- [ $F_V/F_M$ ] Potential yield of chlorophyll fluorescence
- [FW] Fresh Weight
- [ $\Phi_{II}$ ] Actual quantum yield of chlorophyll fluorescence
- [GCC] Global Climate Changes
- [gNDVI] green Normalized difference vegetation index
- [GPP] Gross Primary Production
- [ $G_S$ ] Stomatal conductance
- [ $G_{S\max}$ ] Maximum Stomatal Conductance
- [HDRF] Hemispherical-Directional Reflectance Factor
- [HPLC] High performance liquid chromatography
- [Chls] Total chlorophylls
- [Chl *a*] Chlorophyll a
- [Chl *b*] Chlorophyll b
- [Chl *a+b*] Chlorophyll a+b
- [Chl *a/b*] ratio of chlorophyll a to chlorophyll b
- [Chl-F] Chlorophyll fluorescence
- [CHRIS] Compact High Resolution Imaging Spectrometer
- [CUR] CURvature Index
- [GCC] Global Climate Changes
- [IPCC] Intergovernmental Panel on Climate Change
- [LAI] Leaf Area Index
- [LAp] projected Leaf Area
- [LHCII] Light Harvesting Complex II

[LUE] Light Use Efficiency  
 [gLUE] gross Light Use Efficiency  
 [MODIS] MODerate resolution Imaging Spectroradiometer  
 [N] Nitrogen  
 [NDVI] Normalized Difference Vegetation Index  
 [NEE] Net Ecosystem Exchange  
 [NIR] Near-InfraRed region of the electromagnetic spectrum  
 [NPP] Net Primary Production  
 [NPQ] Non-Photochemical Quenching of chlorophyll fluorescence  
 [NPV] Non-Photosynthetic Vegetation  
 [OSAVI] Optimized Soil-Adjusted Vegetation Index  
 [PPFD] Photosynthetic Photon Flux Density  
 [PROBA] PRoject for OnBoard Anatomy  
 [PRI] Plant (Physiological, Photochemical) Reflectance index  
 [PV] Photosynthetic Vegetation  
 [ $P_{Nmax}$ ] Maximum net photosynthetic CO<sub>2</sub> assimilation  
 [PS2] Photosystem 2  
 [R] Reflectance  
 [ $R_{xxx}$ ] Reflectance at a subscripted wavelength  $_{xxx}$  in nanometers  
 [RC] Reaction Centers  
 [ROI] Regions Of Interest  
 [RUE] Radiation Use Efficiency  
 [RWC] Relative Water Content  
 [ $R^2$ ] Coefficient of determination  
 [ $R_{Fd}$ ] Relative fluorescence decrease ratio  
 [ $\Delta R$ ] Reflectance at light adapted state minus reflectance at dark adapted state  
 [S] Shade  
 [SD] Standard Deviation  
 [SIPI] Structure Insensitive Pigment Index  
 [SLA] Specific Leaf Area  
 [SNP] Swiss National Park  
 [SP] Saturating Pulse  
 [SZA] Sun Zenith Angle  
 [TCARI] Transformed Chlorophyll Absorption in Reflectance index  
 [V] Violaxanthin  
 [VAZ] Xanthophyll cycle pigments  
 [VDE] Violaxanthin De-Epoxidase  
 [VI] Vegetation Index  
 [VIS] VISible region of the electromagnetic spectrum  
 [Z] Zeaxanthin  
 [ZE] Zeaxanthin Epoxidase

## ABSTRAKT

Globální oteplování a následná klimatická změna podle očekávání přinesou další narušení dlouhodobého charakteru počasí, na které byly rostliny adaptovány v průběhu minulých generací. Takovéto narušení může potenciálně vést k významným změnám v uhlíkovém cyklu, v závislosti na intenzitě změny v daném ekosystému. Podrobné porozumění těmto změnám je důležité pro předpovědi budoucího vývoje uhlíkového cyklu, a poskytne užitečné informace pro strategie minimalizující jejich negativní dopady.

Tato práce přispěla k lepšímu pochopení vztahů mezi rychlými fotochemickými a fotosyntetickými procesy a dálkově měřeným signálem fluorescence chlorofylu na úrovni listu, pomocí metod zobrazovací fluorescence a gazometrické metody výměny plynů. Konkrétně jsme ukázali, že poměrně jednoduchý fluorescenční parametr  $R_{Fd}$  je v úzkém lineárním vztahu s celkovou rychlostí fotosyntetické asimilace, bez ohledu na typ adaptace rostliny (slunné nebo stinné listy, respektive jehlice), potvrzujíc tak potenciál chlorofylové fluorescence pro odhad fotosyntetických procesů. Rovněž jsme našli statisticky významný rozdíl v prostorové distribuci parametru  $R_{Fd}$  slunných a stinných listů, přičemž stinné listy měli homogennější distribuci  $R_{Fd}$ .

V dalším kroku jsme ukázali, že „steady-state“ chlorofylová fluorescence ( $F_S$ ) je měřitelná s použitím zobrazovacího spektrometru za přirozených podmínek a v průběhu denního cyklu. Rovněž jsme našli statisticky významný vztah mezi jednoduchými vegetačními indexy (Fyziologickým Reflektančním Indexem - PRI a poměrem  $R_{686}/R_{630}$ ) odvozenými z měření spektrální reflektance na úrovni koruny a měřeními parametru  $F_S$  na úrovni listů. Zároveň ale platí, že vztah mezi rychlostí asimilace při saturačním světle na úrovni listů a vegetačními indexy je komplikovanější a vyžaduje dalšího zkoumání.

Dále jsme našli statisticky významné vztahy, zejména mezi Celkovou Ekosystémovou Výměnou (NEE) odvozenou pomocí měření vířivé kovariance, a vegetačními indexy (PRI a  $R_{686}/R_{630}$ ) odvozenými ze spektroskopických měření z věže. Tyto vztahy byly platné v denním chodu a i v travnatém a lesním ekosystému.

Nakonec jsme porovnali přesnost rozličných chlorofylových vegetačních indexů ve dvou případových studiích: pozemních měření zobrazovací spektroskopie v denním chodu a multi-uhlových satelitních měření Chris PROBA. V obou studiích jsme zjistili, že PRI index je poměrně senzitivní k ne-fyziologickým faktorům.

## SUMMARY

Global warming and subsequent climate change are expected to bring further disruption in long-term weather patterns, to which plants were adapted in the past generations. Such disturbances may potentially lead to significant changes in carbon cycling within terrestrial ecosystems, depending on the magnitude of the change within given ecosystem. Detailed understanding of these changes is important for predicting the future of the carbon cycle, and would provide useful information for mitigation strategies.

This work has contributed to better understanding of leaf level relationships between fast photochemical and photosynthetic processes and remotely sensed chlorophyll fluorescence signal, by means of chlorophyll fluorescence imaging and gas-exchange measurements. Specifically, we have shown that relatively simple  $R_{Fd}$  chlorophyll fluorescence parameter scales linearly with area-based net photosynthetic rate, irrespective of the plant adaptation (sun or shade leaves or needles, respectively), confirming potential of chlorophyll fluorescence for estimation of photosynthetic processes. There is also statistically significant difference between spatial distribution of  $R_{Fd}$  of sun and shade leaves, with the latter ones having more homogeneous  $R_{Fd}$  distribution.

In the next step we have shown, that the “steady-state” chlorophyll fluorescence signal ( $F_S$ ) is measurable by means of imaging spectrometer under natural conditions and in diurnal course. We have also found statistically significant relationship between simple vegetation indices (Physiological Reflectance Index - PRI and ratio  $R_{686}/R_{630}$ ) derived from canopy level spectral reflectance measurements and leaf level  $F_S$  measurements. At the same time relationship between leaf level light saturated photosynthetic rate and vegetation indices is more complicated, requiring further investigation.

Further, we have found statistically significant relationships between eddy-covariance based canopy level Net Ecosystem Exchange (NEE) and vegetation indices (PRI and  $R_{686}/R_{630}$ ) derived from tower-based spectroscopic measurements during the daily course and in both, grassland and forest ecosystem.

Finally, we compared the accuracy of various chlorophyll vegetation indices in two case studies: ground-based diurnal imaging spectroscopy measurements and Chris PROBA multi-angular satellite measurements. In both studies PRI has been found as relatively sensitive to non-physiological factors.



# **CHAPTER 1**

## General Introduction

## 1.1 Motivation

The greenhouse gases, predominantly CO<sub>2</sub>, have been identified as a primary cause of the observed increase of the global temperatures and subsequent climate change (Houghton 2004; IPCC 2007). In 2007, humans have emitted around 40 gigatons of CO<sub>2</sub> into atmosphere (Global Carbon Project 2008) and concentration of this gas reached the highest levels during the last 2.1 millions years (Hönisch et al. 2009), while the rate of this increase is probably at least 10 times faster than at any time during the past 10 000 years (Joos and Spahni 2008). Even if all of the anthropogenic CO<sub>2</sub> emissions were stopped immediately, the global temperature will most likely further rise by approximately 0.6°C to 2.4°C as a result of induced Earth energy imbalance (Hansen et al. 2005; Ramanathan and Feng 2008). As a consequence, the interaction of human civilization with the surrounding environment has led some scientists to define our era as “*anthropocene*” (Crutzen and Steffen 2003).

While there is no definition of “*optimal climate*”, there is a climate which all current plants and animals are adapted to in a fluctuating dynamic equilibrium state. Therefore, even a small change in the temperature and/or precipitation will lead to a forced adaptive response of ecosystems. A recent meta-analysis of 143 studies is showing changes in the distribution of species ranging “from molluscs to mammals and from grasses to trees” (Root et al. 2003), as a result of changing climate. It has been recognized, that the rate of this change “*is reaching a level that dwarfs natural rates of change.*” (Hansen, 2006). The rate of projected climate change has also been forecasted to drive to extinction between 15-37% of examined species (Thomas et al. 2004).

Up to now, about half of the carbon we emit remains in the atmosphere. The second half is being absorbed by oceans and by terrestrial ecosystems. The flux of carbon within the terrestrial biosphere is one of the largest components of global carbon cycle (Bolin and Fung, 1992). Going into the future, climate models predict reduced carbon sink capacity of global vegetation, though the beginning and the extent of this process remains unclear (Meir et al. 2006). Some observational evidence suggests that this process may have already started (Canadell et al. 2007). Further, Friedlingstein et al. (2006) determined the range of additional CO<sub>2</sub> emitted from the vegetation to be between 20 to 200 ppm at the end of this century (corresponding to a temperature rise estimate between 0.1 to 1.5°C) by comparison of 11 climate models.

In the face of these early signs of “*global change*” and the uncertain temporal and spatial response of climate-vegetation feedback, there is an urgent need for the better detection and quantification of carbon cycling in terrestrial vegetation. In order to fulfill this complicated task, we need to make the best possible use of remote sensing data inputs into ecosystem process models (Running et al. 1999; Turner et al. 2004).

## 1.2 Research objectives

Based on the recent developments and integration progress (theoretical part) of recently independent scientific methods for observation of plants, namely imaging optical remote sensing (RS) and remote chlorophyll a fluorescence (Chl-F) measurements, in a term emerging as “*physiological remote sensing*”, basic research questions of this work were defined:

- *What is the link between field-based Chl-F measurements and carbon assimilation of plants?*
- *What are the factors influencing the proposed physiologically based optical vegetation indices at the leaf and canopy level?*
- *Is there an intimate link between optical information obtained by remote radiance measurements and the physiological processes occurring in leaves under natural conditions and different types of ecosystems?*
- *Is there a possibility for more accurate estimation of carbon fluxes at canopy level using the optical vegetation indices?*

### 1.3 References

- Bolin B, Fung I (1992) Report: The carbon cycle revisited. In D. Ojima (Ed.), Modelling the earth system. Boulder, Colorado, USA' UCAR/OIES (University Corporation of Atmospheric Research/Office of Inter-Disciplinary Earth Sciences).
- Canadell JG et al. (2007) Contributions to accelerating atmospheric CO<sub>2</sub> growth from economic activity, carbon intensity, and efficiency of natural sinks. Proceedings of the National Academy of Sciences of the United States of America 104:18866-18870
- Crutzen PJ, Steffen W (2003) How long have we been in the Anthropocene era? Comment. Climatic Change 61:251-257
- Friedlingstein P et al. (2006) Climate-carbon cycle feedback analysis: Results from the (CMIP)-M-4 model intercomparison. Journal of Climate 19:3337-3353
- Global Carbon Project (2008) Carbon budget and trends 2007, [www.globalcarbonproject.org, 26 September 2008]
- Hansen J et al. (2005) Earth's energy imbalance: Confirmation and implications. Science 308:1431-1435
- Hansen J (2006) The threat to the planet, The New York Review of Books, July 13 [http://www.nybooks.com/articles/19131]
- Hönisch B, Hemming NG, Archer D, Siddall M, McManus JF (2009) Atmospheric Carbon Dioxide Concentration Across the Mid-Pleistocene Transition. Science 324:1551-1554
- Houghton J (2004) Global Warming - The Complete Briefing, 3rd Edition edn. Cambridge University Press, Cambridge
- IPCC (2007) Climate Change 2007: The Physical Science Basis. Contribution of Working Group I to the Fourth Assessment Report of the Intergovernmental Panel on Climate Change. In: Solomon S, D. Qin, M. Manning, Z. Chen, M. Marquis, K.B. Averyt, M.Tignor and H.L. Miller (ed) Summary for Policymakers. Cambridge University Press, Cambridge, United Kingdom and New York, NY, USA, p 996
- Joos F, Spahni R (2008) Rates of change in natural and anthropogenic radiative forcing over the past 20,000 years. Proceedings of the National Academy of Sciences of the United States of America 105:1425-1430
- Meir P, Cox P, Grace J (2006) The influence of terrestrial ecosystems on climate. Trends in Ecology & Evolution 21:254-260

- Ramanathan V, Feng Y (2008) On avoiding dangerous anthropogenic interference with the climate system: Formidable challenges ahead. *Proceedings of the National Academy of Sciences of the United States of America* 105:14245-14250
- Root TL, Price JT, Hall KR, Schneider SH, Rosenzweig C, Pounds JA (2003) Fingerprints of global warming on wild animals and plants. *Nature* 421:57-60
- Running SW, Baldocchi DD, Turner DP, Gower ST, Bakwin PS, Hibbard KA (1999) A global terrestrial monitoring network integrating tower fluxes, flask sampling, ecosystem modeling and EOS satellite data. *Remote Sensing of Environment* 70:108-127
- Thomas CD et al. (2004) Extinction risk from climate change. *Nature* 427:145-148
- Turner DP, Guzy M, Lefsky MA, Ritts WD, Van Tuyl S, Law BE (2004) Monitoring forest carbon sequestration with remote sensing and carbon cycle modeling. *Environmental Management* 33:457-466

## **CHAPTER 2**

Theory background

## 2.1 Basics of imaging spectroscopy

Imaging spectrometers are instruments that remotely measure a detailed spectrum of reflected solar energy (reflectance,  $R$ ) for each pixel (Ustin et al. 2004). Measured surface  $R$  is predominantly a function  $fR$  defined by spatial, spectral, directional, and temporal scale (Malenovský 2006):

$$R = fR(x, y; \lambda; \Omega_v, \Omega_s; t)$$

where  $x, y$  are spatial coordinates,  $\lambda$  is the wavelength of electromagnetic (EM) spectrum,  $\Omega_v$ ,  $\Omega_s$  describes the angular viewing geometry of the sun-object-sensor system, and  $t$  is the time frequency of the observation.

Based on spectral resolution provided by imaging spectrometers we can basically distinguish the multispectral (several spectral bands) and hyperspectral (several tens to hundreds spectral bands) sensors (e.g. Ustin et al. 2004).

A typical hyperspectral signature of green vegetation results in relatively low  $R$  in the visible part (VIS, 400-700 nm) of the EM spectrum compared to the near-infrared (NIR) region (Fig. 2.1):

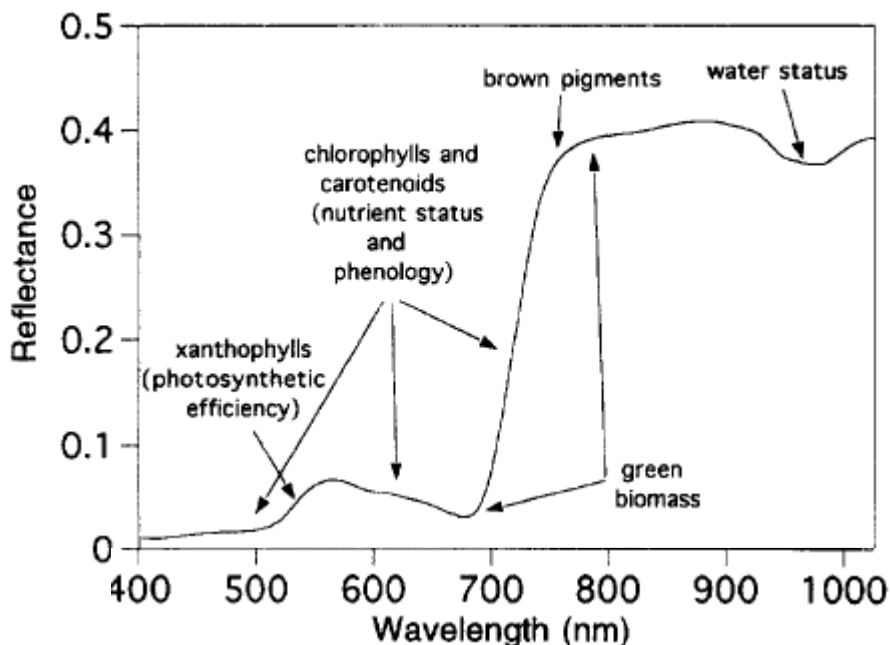


Figure 2.1. Typical spectral signature (y-axis - reflectance, relative signal) for healthy green leaf in a wavelength region from 400 to 1000 nm (x-axis) with a description of areas, where biophysical properties of vegetation can be estimated. (Adapted from Penuelas and Filella 1998, published with permission).

Most direct and simple method for extracting useful information from measured  $R$  signature is the use of vegetation indices (VIs) (Myneni et al. 1995). Each VI is in fact

reduction of information stored within spectral bands into single value, which maximizes the sensitivity to a targeted object property and minimizes the sensitivity to other factors.

Traditional areas of interest in estimation of vegetation biophysical properties are green biomass (Rouse et al. 1973), chlorophyll (le Maire et al. 2004) and carotenoids (Gitelson et al. 2002) leaf pigments content, leaf area index (LAI) (Haboudane et al. 2004), and more recently also the remote estimation of dynamic photosynthetic processes related to the reversible conversion of xanthophyll cycle pigments and Light Use Efficiency (LUE) (Gamon et al. 1992).

## 2.2 Xanthophyll cycle and remote sensing

### 2.2.1 Molecular basis and ecophysiology of xanthophyll cycle

Autotrophic organisms sustain virtually all organic life on Earth. They are able to catch incoming photon flux from the Sun and transform the energy of photons into the energy of chemical compounds, in a process known as photosynthesis. "During this process, the excitation energy is transferred from the site of the absorption of incident light, i.e. from Light Harvesting Complexes (LHCs) of Photosystem I and Photosystem II (PS2) to their Reaction Centers (RCs) (Nield et al. 2000).

During the evolution, two basic processes shaped the optimal functioning of this molecular complex: i) efficient collection of sunlight needed to deliver excitation energy to the photosynthetic reaction centre at a rate sufficient to drive electron transport at the highest sustainable rate and ii) excited states of chlorophyll and the presence of molecular oxygen provide a potentially lethal cocktail that can irreversibly damage the proteins, lipids, and pigments of the photosynthetic membrane (Horton and Ruban 2005). Plants, in order to protect themselves over the effect of photo-oxidative damage (e.g. Osmond 1994), have developed protective pigments (Demmig-Adams and Adams III. 1992; Holt et al. 2005). Under high light conditions, excessive energy is dissipated as a heat through so-called xanthophylls pigment cycle (Fig. 2.2).



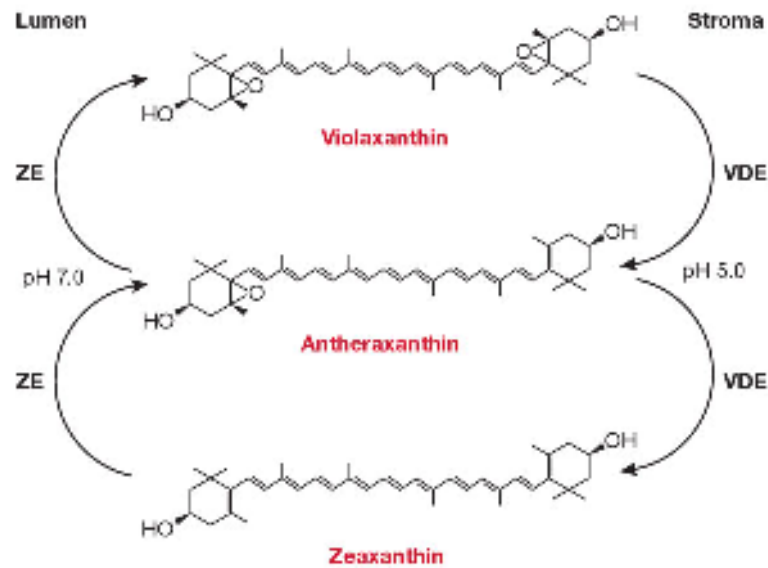


Figure 2.2. Schematic representation of the xanthophyll cycle. Through the action of the enzyme violaxanthin de-epoxidase (VDE), violaxanthin is converted to zeaxanthin in a two-step process, with antheraxanthin as intermediate. The Z can be epoxidized back to violaxanthin by zeaxanthin epoxidase (ZE). (Adapted from Szabo et al. 2005, published with permission).

During the xanthophyll cycle, which is reversible chemical de-epoxidation reaction, violaxanthin (V) is converted to antheraxanthin (A) and finally to zeaxanthin (Z) via pH-dependent enzymes, a process originally described by Briantais et al. (1979). However, this process can be pH-independent (Adams et al. 2004), especially for longer-lived evergreen-species. While now it is recognized and accepted that conversion to Z pigment plays a major part (around 70% according to Li et al. (2000)) in the non-radiative heat dissipation (for a review see Gilmore 1997), the precise mechanisms of specific photoprotective pathways have yet to be elucidated (Demmig-Adams and Adams 2000; Matsubara et al. 2002; Niyogi 1999). Recent studies are showing that light-inducible proteins (Zarter et al. 2006a; 2006b) and/or structural rearrangement of PS2 (Busch et al. 2007) are partly responsible for the photoprotection.

The total amount of xanthophyll cycle pigments (i.e. VAZ) depends on many eco-physiological factors. Sun leaves possess larger pools of VAZ (e.g. Demmig-Adams et al. 1989; Johnson et al. 1993; Thayer and Bjorkman 1990) and a greater capacity for Z formation in the Chl pigment bed in comparison to shade leaves (Demmig-Adams and Adams 1994). In case of evergreen trees, the difference in the VAZ amount between sun- and shade leaves can be up to 5-fold (Demmig-Adams 1998). Relation of larger VAZ with higher integrated Photosynthetic Photon Flux Density (PPFD) is independent of whether VAZ is expressed on the basis of area, mass, chlorophyll or total carotenoids (Adams et al. 1992; Czczuga 1987;

Koniger et al. 1995; Logan et al. 1996; Thayer and Bjorkman 1990). Niinemets et al. (1998) found a positive relation between integrated PPFD, especially for the direct fraction of PPFD, and VAZ during the three days preceding the leaf sampling.

It has been also shown, that Z pigment formation can play a significant role under rapidly fluctuating light conditions. By its ability to quickly optimize both light utilization and photoprotection, it has a critical effect on the plant overall fitness (Kulheim et al. 2002).

Distinct effect of temperature on Z pool has been observed. In case of below-zero temperatures, high amounts of Z can be engaged in the photoprotection (Verhoeven et al. 1998), however the amount can be reduced quickly, when the temperature rises again (Verhoeven et al. 1998).

In relation to temperature, also seasonal pattern in photoprotection was observed, though to different extent for various species, as well as sun vs. shaded adapted leaves. Up-regulation of photoprotection during the winter does not occur in the case of shaded leaves, but to a lesser extent in case of sun leaves (e.g. Adams et al. 2001; Stecher et al. 1999). Similarly, a recent study by Zarter et al. (2006a) on evergreen *Arctostaphylos uva-ursi* found sustained increase in Z content during the winter, which was most significant for shaded leaves. For a full review of photoprotection strategies in over-wintering plants see Adams III et al. (2004).

In an interesting climate change simulation experiment, Busch et al. (2007) separated the effects of temperature and period of year (i.e. day length). Seedlings of conifer Jack Pine (*Pinus banksiana*) in the warm summer treatment dissipated excess energy via Z, while in all other treatments (i.e. cold summer and warm and cold autumn) dissipation of excess energy predominantly via increased aggregation of the light-harvesting complex of PS2 was facilitated (Busch et al. 2007).

There is also relation to photosynthetic performance such that species with higher rates of photosynthesis employ relatively lower level of Z-dependent energy dissipation and species with lower rates of photosynthesis employ higher levels of Z-dependent energy dissipation (Demmig-Adams B. 1999). However, opposite relation was observed for temperate (Niinemets et al. 1998) and tropical (Koniger et al. 1995) tree species.

Studies with leaf nitrogen deficiency have shown that Z pool size increases with decreasing nitrogen in apple (Cheng 2003). Z pool size increases with limited leaf nitrogen also when expressed on a Chl basis in maize and spinach (Khamis et al. 1990; Verhoeven et al. 1997), but no such effect was observed during the midday in case of *Clematis vitalba* (Bungard et al. 1997).

## 2.2.2 Remote sensing of xanthophyll cycle and photosynthetic activity

### 2.2.2.1 Leaf to canopy level

First remote estimation of the xanthophyll cycle conversion was observed by Bilger et al. (1989) in laboratory measurements of individual leaves. Changes in absorbance at the wavelengths of 505-515 nm were associated with conversion of V to Z. The same process showed a reflectance change around 531 nm (first by Gamon et al. 1990). Based on these observations, the so-called “Physiological Reflectance Index” (PRI) (also called Photochemical, or Plant Reflectance Index) was introduced, calculated as  $(R_{531} - R_{REF}) / (R_{531} + R_{REF})$  (Gamon et al. 1992), where R is a reflectance at subscripted wavelength,  $R_{REF}$  is reference wavelength most often at 570 nm. Thus, a very first optical index that was capable to track changes associated with rapid photosynthetic processes has been defined.

Recent study on grape vines (*Vitis vinifera*) by Evain et al. (2004) has demonstrated two different phases of the PRI kinetics. A rapid phase lasting less than 2 seconds after a steep increase in the light intensity and a slow phase of adjustment, after the initial rapid phase that lasts several minutes. At the leaf level, PRI showed a close correlation with epoxidation state (EPS) defined as  $(V + 0.5 \cdot A) / (V + A + Z)$  under non-stressed conditions in diurnal course (Gamon et al. 1992; Peñuelas et al. 1997a) as well as under water-stressed conditions (Tambussi et al. 2002). PRI tracked seasonal changes in the amount of de-epoxidised xanthophyll cycle pigments defined as  $(0.5 \cdot V + Z + A)$  normalized to chl as well as seasonal changes in the CO<sub>2</sub> uptake rate (Stylinski et al. 2002).

PRI was also found to be affected by leaf chlorophyll content (Moran et al. 2000) and by Car/Chl ratio (Guo and Trotter 2004; Sims and Gamon 2002; Stylinski et al. 2002; Zarco-Tejada et al. 2005).

In many studies close correlation between PRI and LUE parameter, which is defined as the amount of assimilated carbon per incoming PPFD, was found (Gamon et al. 1992; Guo and Trotter 2006; Peñuelas et al. 1995a; 1998). Under saturating light conditions, PRI-LUE relationship was linear across different plant functional types and wide range of species (Gamon et al. 1997), and also across different nitrogen (N) levels for the same species (Moran et al. 2000; Peñuelas et al. 1994), as well as for different species (Trotter et al. 2002).

However, PRI-LUE relationship was found to be stronger, when separating for different species (Guo and Trotter 2004), soil water content levels (Inoue and Peñuelas 2006) and CO<sub>2</sub> concentrations (Guo and Trotter 2006).

In a study at the leaf level on *Betula papyrifera*, populations from different altitudes, a close relation between the carbon assimilation under saturating light conditions ( $A_{\max}$ ) and PRI was observed (Richardson and Berlyn 2002), suggesting a potential for detection of plant photosynthetic capacity and performance.

At a small canopy level measurements (Louis et al. 2005) of the Scots pine have shown a good correlation of PRI with carbon assimilation derived from the eddy-covariance (EC) flux towers, during the spring recovery period. On the other hand, a small pot study (Dobrowski et al. 2005) has shown that PRI was only a weak predictor of carbon assimilation under the stress conditions induced by drought and heat.

Investigation of olive tress (*Olea europaea*) using the Airborne Hyperspectral Scanner suggested that PRI can be used for water stress detection (Suarez et al. 2008) through the link of PRI with stem water potential and stomatal conductance ( $G_s$ ).

#### *2.2.2.2 Regional to satellite level*

At the regional level, PRI showed good relationship with EPS in a diurnal cycle, as well as with eddy-covariance flux towers based LUE during the green-up period in the boreal forest (Nichol et al. 2000; 2002). Similar results were obtained also for the barley canopies (Filella et al. 1996) where PRI tracked the diurnal changes in EPS and LUE. Other single species canopy level studies found good relations between PRI and LUE (Gamon et al. 2001; Strachan et al. 2002). In a warming and drought experiment in structurally diverse ecosystem, PRI showed mixed results and the relation with LUE and  $CO_2$  flux was affected by canopy structure and soil background (Filella et al. 2004). However, in evergreen chaparral species the leaf PRI scaled very well with canopy-derived PRI (Stylinski et al. 2002).

Rahman et al. (2001) used Airborne Visible Infrared Imaging Spectrometer (AVIRIS) for successful estimating of the gross  $CO_2$  flux, as estimated from EC flux towers in boreal forest using the PRI and Normalized Difference Vegetation Index NDVI (Rouse et al. 1973).

PRI derived from MODerate Resolution Imaging Spectroradiometer (MODIS) satellite sensor has recently been found to correlate well with daily Net Primary Production (NPP) derived from EC towers (Rahman et al. 2004) and another study using MODIS found significant relation between PRI and EC based LUE only when using back-scattered data (i.e. data with small fraction of shadows within a pixel) (Drolet et al. 2005).

The only modelling study, which investigated the factors complicating the PRI-LUE relationship, found that PRI is sensitive to leaf area index (LAI) and viewing geometry (Barton and North 2001).

## 2.3 Remote sensing of chlorophyll fluorescence

### 2.3.1 Basics of chlorophyll fluorescence

Principle of Chlorophyll Fluorescence (Chl-F) is based on the process associated with light absorption (Maxwell and Johnson 2000). Incoming light which is absorbed by chlorophyll molecules inside green leaf can undergo one of three different fates: i) it can be used to drive photosynthesis (photochemistry); ii) it can be dissipated as heat (chap. 2.1.1.); iii) it can be re-emitted as a light – this process is called chlorophyll fluorescence (Fig. 2.3).

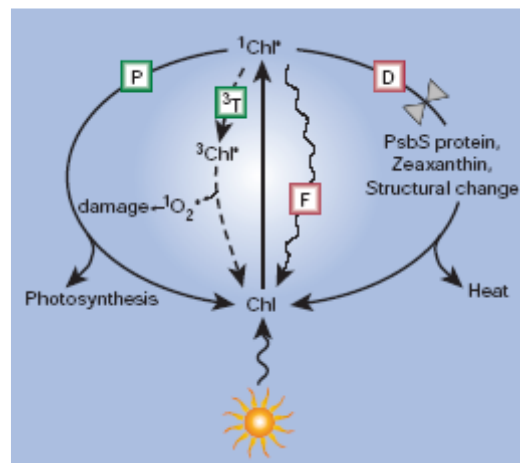


Figure 2.3. Fates of light absorbed in the light-harvesting complexes. Chl, chlorophyll;  $^1\text{Chl}^*$ , excited singlet chlorophyll;  $^3\text{Chl}^*$ , excited triplet chlorophyll; P, photochemistry; D, safe dissipation of excess excitation energy as heat; F, fluorescence;  $^3\text{T}$ , triplet pathway, leading to the formation of singlet oxygen ( $^1\text{O}_2^*$ ) and photo-oxidative damage. (Adapted from Demmig-Adams and Adams 2000, published with permission).

All these three processes are competitive and information about the yield of measured Chl-F at a given time gives us the information about the heat dissipation and photochemical processes. More than 90% of the Chl-F at the room temperature comes from the PS2 (Gitelson et al. 1998), thus reflecting processes in this pigment protein complex.

When the plant is placed into absolute darkness (dark-adapted state, DA) for at least 30 minutes, all RCs are open and an initial value of Chl-F can be measured ( $F_0$ ). After applying the saturating pulse (SP) with very high light intensity ( $>10\,000\ \mu\text{mol m}^{-2}\ \text{s}^{-1}$ ), maximum Chl-

F is obtained ( $F_M$ ). Difference between the minimum and maximum of Chl-F is variable Chl-F ( $F_V$ ). When the plant is exposed to a saturating light continuously a decrease (also called “quenching”) of the Chl-F can be observed until it reaches a steady-state value ( $F_S$ ). This phenomenon was described for the first time by Kautsky and Hirsch (1931) and today it is well-known as “Kautsky effect” (reviewed in Lichtenthaler 1992). After applying a SP to a plant in the light-adapted state, a maximum Chl-F on the light can be detected ( $F_M'$ ). After applying a short pulse of the far-red light a minimum value of chlorophyll fluorescence on the light is measured ( $F_0'$ ).

A large variety of Chl-F parameters have been developed, using special measurement protocols. However, only those with a relevance to our study will be mentioned (for a review see Lichtenthaler et al. 2005; Maxwell and Johnson 2000; Roháček 2002).

### 2.3.2 Basic characteristics of selected chlorophyll fluorescence parameters

In the eco-physiological research the ratio of  $F_V$  to  $F_M$  ( $F_V/F_M$ ) is widely used as the indicator of the potential quantum efficiency of PSII. The values for healthy plants were determined to be around 0.83 (Björkman and Demmig 1987), and lower values can indicate photoinhibition, which is mostly the result of stress.

Non-photochemical quenching (NPQ) is calculated as  $(F_V - F_M')/F_M'$  (Bilger and Bjorkman 1990) and is linearly related to non-radiative heat dissipation. It can reach values from 0 to infinity. For a typical healthy plant under saturating light conditions the values are in the range of 0.5 to 3.5 (Maxwell and Johnson 2000).

Actual quantum yield of PSII ( $\Phi_{II}$ ) is calculated as  $(F_M' - F_S)/F_M'$  and in principle measures the proportion of the light absorbed by chlorophyll associated with PSII that is used in photochemistry. Under laboratory conditions, there is a strong linear relationship between this parameter and the efficiency of carbon fixation but this might be distorted under certain stress conditions, due to changes in the rate of photorespiration or pseudocyclic electron transport (Fryer et al. 1998).

Chl-F decrease ratio ( $R_{Fd}$ ) calculated as  $(F_M - F_S)/F_S$  (Lichtenthaler and Rinderle 1988) quantifies the decrease of Chl-F from the maximum value, i.e.  $F_M$ , to the lowest value under continuous saturating light (e.g. “white light” with the intensity of at least  $2\,000\ \mu\text{mol m}^{-2}\ \text{s}^{-1}$ ). The typical values for shade-adapted leaves are between 1.5 to 2 and for sun-adapted leaves between 3 to 5, reflecting the higher photosynthetic capacity and  $\text{CO}_2$  fixation rates (Lichtenthaler 2004).

### 2.3.3 Measurements of chlorophyll fluorescence emission from reflectance

The first suggestion that Chl-F emission can be measured using the hyperspectral reflectance, was observed by Buschmann and Lichtenthaler (1988) by means of the Visible Infrared Reflectance Absorptance Fluorescence Spectrometer. These early results were further confirmed in a second study on tobacco leaves (*Nicotiana tabacum*) using the same instrument (Buschmann et al. 1994). Further studies have also demonstrated the possible influence of Chl-F on the reflectance (Gamon et al. 1997; Gamon and Surfus 1999; Peñuelas et al. 1995b; Peñuelas et al. 1997b), though only recently these influences were better quantified (Zarco-Tejada et al. 2000a; 2000b; 2002; 2003).

The influence of Chl-F on apparent reflectance was shown by subtracting the reflectance signature of the dark- and light-adapted plant leaves, respectively (Fig. 2.4A):

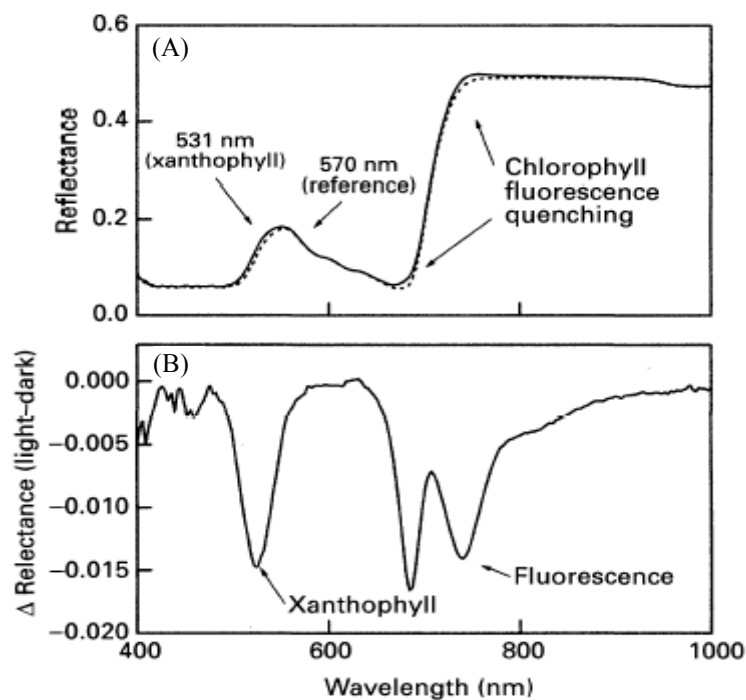


Figure 2.4. A) Reflectance spectrum of a *Helianthus annuus* (sunflower) leaf in the dark state (solid line) and 10 minutes after exposure to the white light (dotted line). B) differential spectrum (reflectance in dark state minus reflectance in light state, i.e.  $\Delta R$ ) derived from the spectra A). (Adapted from Gamon and Surfus 1999, published with permission).

Chl-F can be also measured from reflectance by using the long-pass optical filters (Zarco-Tejada et al. 2000a), or by subtracting the reflectance signature of stressed vs. non-stressed vegetation (Dobrowski et al. 2005).

The peaks in reflectance difference ( $\Delta R$ ) (Fig. 2.4B) associated with Chl-F can be observed at wavelengths of 686 nm (red fluorescence) and 740 nm (far-red fluorescence) (Buschmann et al. 2000).

When one measures the reflectance under natural sun-illumination, so-called Chl-F “*in-filling*” in the oxygen absorption band at 760 nm can be detected (Perez-Priego et al. 2005).

### 2.3.4 Chlorophyll fluorescence vegetation indices and their relation to chlorophyll fluorescence

Several VIs are used to quantify the Chl-F yield from the reflectance either directly or indirectly (Tab. 2.1). In general, these VIs are using combination of two wavelengths; one which is sensitive to Chl-F signal and a second wavelength which is insensitive to Chl-F, used as reference.

Table 2.1. Vegetation indices (VIs) used for quantification of chlorophyll fluorescence (Chl-F). Earlier VIs used for vegetation stress detection are also included as they are using the wavelengths where the effects of Chl-F on the apparent reflectance were later demonstrated.

Index	Algorithm Equation	Measure of	Reference
PRI	$\frac{(R_{531} - R_{570})}{(R_{531} + R_{570})}$	Light-use efficiency (LUE), zeaxanthin content, actual quantum yield ( $\Phi_{II}$ ), non-photochemical quenching (NPQ)	(Gamon et al. 1992)
FRI1	$R_{690}/R_{630}$	$\Phi_{II}$ , steady-state chlorophyll fluorescence ( $F_S$ ); early stress	Zarco-Tejada et al. (1999)
FRI2	$R_{740}/R_{800}$	$F_S$ , early stress	(Dobrowski et al. 2005)
CUR	$R_{683}^2/(R_{675} \cdot R_{691})$	$F_V/F_M$	(Zarco-Tejada et al. 2000a)
---	$R_{760.59}-R_{759.5}$	$F_S$	(Perez-Priego et al. 2005)
---	$R_{695}/R_{760}$	vegetation stress	(Carter 1994)
---	$R_{695}/R_{670}$	vegetation stress	(Carter 1994)
---	$R_{710}/R_{760}$	vegetation stress	(Carter 1994)
---	$R_{740}/R_{720}$	vegetation stress	(Vogelmann et al. 1993)



The already mentioned PRI index is related to Chl-F indirectly, through involvement of the pigments of xanthophyll cycle in the Chl-F quenching mechanisms (e.g. D'Haese et al. 2004). At the leaf level and small canopy level, PRI has been shown to tightly correlate with  $\Phi_{II}$  and NPQ (Evain et al. 2004; Gamon et al. 1997; Guo and Trotter 2004; Nichol et al. 2006; Peñuelas et al. 1995a; Rascher et al. 2007; Tambussi et al. 2002) and weaker, but still significant correlations were maintained when measured using the sensor CHRIS (Compact High Resolution Imaging Spectrometer) (Raddi et al. 2005) onboard satellite PROBA (PRoject for OnBoard Anatomy), both daily and seasonally. However, a recent study by Weng et al. (2006a) investigating plants with different temperature tolerance has shown that  $\Delta$ PRI (which is difference between PRI measured during the night and PRI during the day) is a better predictor of  $\Phi_{II}$  and NPQ, while steady-state values of PRI had weaker relation to these parameters.

Further, a very good relation between DA values of PRI and  $F_V/F_M$  for plant species from different altitudes (Richardson and Berlyn 2002; Richardson et al. 2001), with different temperature tolerance (Weng et al. 2006a) and also during the seasonal course (Weng et al. 2006c) have been reported.

The ratio  $R_{690}/R_{630}$  (FR1) and  $R_{683}^2/(R_{675} \cdot R_{691})$  (CURvature index) in the laboratory canopy level campaign on *Acer saccharum* seedlings (Zarco-Tejada et al. 2000b), have been shown to correlate with diurnal courses of  $F_V/F_M$  and also tracked the changes in  $F_S$  and  $\Phi_{II}$  in stressed, as well as healthy vegetation. In a small grapevine (*Vitis vinifera*) canopy-level study by Dobrowski et al. (2005), the ratios FR1 and  $R_{740}/R_{800}$  (FRI2) tracked the diurnal changes in  $F_S$  of stressed vegetation. Similar results were obtained in crown-level study on water-stressed orchard trees (*Olea europaea*), where the reflectance difference  $R_{760.59}-R_{759.5}$  tracked the changes in  $F_S$  (Perez-Priego et al. 2005).

Similar VIs ( $R_{695}/R_{760}$ ,  $R_{710}/R_{760}$ ,  $R_{740}/R_{720}$ ) have been earlier identified as an early indicators of plant stress (Carter 1994; Vogelmann et al. 1993), though plants in these studies also experienced changes in chlorophyll content and sensitivity of these ratios was not attributed to Chl-F.

## 2.4 References

Adams WW, Demmig-Adams B, Rosenstiel TN, Ebbert V (2001) Dependence of photosynthesis and energy dissipation activity upon growth form and light environment during the winter. *Photosynthesis Research* 67:51-62

- Adams WW, Volk M, Hoehn A, Demmigadams B (1992) Leaf Orientation and the Response of the Xanthophyll Cycle to Incident Light. *Oecologia* 90:404-410
- Adams WW, Zarter CR, Ebbert V, Demmig-Adams B (2004) Photoprotective strategies of overwintering evergreens. *Bioscience* 54:41-49
- Barton CVM, North PRJ (2001) Remote sensing of canopy light use efficiency using the photochemical reflectance index - Model and sensitivity analysis. *Remote Sensing of Environment* 78:264-273
- Bilger W, Bjorkman O (1990) Role of the Xanthophyll Cycle in Photoprotection Elucidated by Measurements of Light-Induced Absorbency Changes, Fluorescence and Photosynthesis in Leaves of *Hedera-Canariensis*. *Photosynthesis Research* 25:173-185
- Bilger W, Bjorkman O, Thayer SS (1989) Light-Induced Spectral Absorbance Changes in Relation to Photosynthesis and the Epoxidation State of Xanthophyll Cycle Components in Cotton Leaves. *Plant Physiology* 91:542-551
- Björkman O, Demmig B (1987) Photon Yield of O<sub>2</sub> Evolution and Chlorophyll Fluorescence Characteristics at 77-K among Vascular Plants of Diverse Origins. *Planta* 170:489-504
- Briantais JM, Vernotte C, Picaud M, Krause GH (1979) Quantitative Study of the Slow Decline of Chlorophyll Alpha-Fluorescence in Isolated-Chloroplasts. *Biochimica Et Biophysica Acta* 548:128-138
- Bungard RA, McNeil D, Morton JD (1997) Effects of nitrogen on the photosynthetic apparatus of *Clematis vitalba* grown at several irradiances. *Australian Journal of Plant Physiology* 24:205-214
- Busch F, Huner NPA, Ensminger I (2007) Increased air temperature during simulated autumn conditions does not increase photosynthetic carbon gain but affects the dissipation of excess energy in seedlings of the evergreen Conifer Jack Pine. *Plant Physiology* 143:1242-1251
- Buschmann C, Langsdorf G, Lichtenthaler HK (2000) Imaging of the blue, green, and red fluorescence emission of plants: An overview. *Photosynthetica* 38:483-491
- Buschmann C, Lichtenthaler, HK (1988) Reflectance and chlorophyll fluorescence signatures in leaves. In *Applications of Chlorophyll Fluorescence*, (HK Lichtenthaler, Ed.), Kluwer Academic, Dordrecht, pp. 325–332.
- Buschmann C, Nagel E, Szabo K, Kocsanyi L (1994) Spectrometer for Fast Measurements of in-Vivo Reflectance, Absorbance, and Fluorescence in the Visible and near-Infrared. *Remote Sensing of Environment* 48:18-24

- Carter GA (1994) Ratios of Leaf Reflectances in Narrow Wavebands as Indicators of Plant Stress. *International Journal of Remote Sensing* 15:697-703
- Czeczuga B (1987) The Effect of Light on the Content of Photosynthetically Active Pigments in Plants .10. Carotenoid Contents in Leaves Grown under Various Light Intensities. *Biochemical Systematics and Ecology* 15:523-527
- D'Haese D, Vandermeiren K, Caubergs RJ, Guisez Y, De Temmerman L, Horemans N (2004) Non-photochemical quenching kinetics during the dark to light transition in relation to the formation of antheraxanthin and zeaxanthin. *Journal of Theoretical Biology* 227:175-186
- Demmig-Adams B (1998) Survey of thermal energy dissipation and pigment composition in sun and shade leaves. In: *Plant cell physiol.*, vol. 39, pp 474-482
- Demmig-Adams B, Adams III. WW (1992) Photoprotection and other responses of plants to high light stress. In: *Annu. Rev. Plant Physiol. Plant Mol. Biol.*, vol. 43, pp 599-626
- Demmig-Adams B, Adams WW (1994) Capacity for Energy-Dissipation in the Pigment Bed in Leaves with Different Xanthophyll Cycle Pools. *Australian Journal of Plant Physiology* 21:575-588
- Demmig-Adams B, Adams WW (2000) Photosynthesis - Harvesting sunlight safely. *Nature* 403:371-+
- Demmig-Adams B, Winter K, Winkelmann E, Kruger A, Czygan FC (1989) Photosynthetic Characteristics and the Ratios of Chlorophyll, Beta-Carotene, and the Components of the Xanthophyll Cycle Upon a Sudden Increase in Growth Light Regime in Several Plant-Species. *Botanica Acta* 102:319-325
- Demmig-Adams B. AWI, Ebbert V., Logan BA (1999) Ecophysiology of the xanthophyll cycle. In: Frank HA YA, Britton G, Cogdell RJ, eds (ed) *The Photochemistry of Carotenoids. Advances in Photosynthesis.* Kluwer Academic, Dordrecht, Netherlands, pp 245-269
- Dobrowski SZ, Pushnik JC, Zarco-Tejada PJ, Ustin SL (2005) Simple reflectance indices track heat and water stress-induced changes in steady-state chlorophyll fluorescence at the canopy scale. *Remote Sensing of Environment* 97:403-414
- Drolet GG et al. (2005) A MODIS-derived photochemical reflectance index to detect inter-annual variations in the photosynthetic light-use efficiency of a boreal deciduous forest. *Remote Sensing of Environment* 98:212-224
- Evain S, Flexas J, Moya I (2004) A new instrument for passive remote sensing: 2. Measurement of leaf and canopy reflectance changes at 531 nm and their relationship

- with photosynthesis and chlorophyll fluorescence. *Remote Sensing of Environment* 91:175-185
- Filella I, Amaro T, Araus JL, Peñuelas J (1996) Relationship between photosynthetic radiation-use efficiency of Barley canopies and the photochemical reflectance index (PRI). *Physiologia Plantarum* 96:211-216
- Filella I, Peñuelas J, Llorens L, Estiarte M (2004) Reflectance assessment of seasonal and annual changes in biomass and CO<sub>2</sub> uptake of a Mediterranean shrubland submitted to experimental warming and drought. *Remote Sensing of Environment* 90:308-318
- Fryer MJ, Andrews JR, Oxborough K, Blowers DA, Baker NR (1998) Relationship between CO<sub>2</sub> assimilation, photosynthetic electron transport, and active O<sub>2</sub> metabolism in leaves of maize in the field during periods of low temperature (vol 116, pg 571, 1998). *Plant Physiology* 117:335-335
- Gamon JA, Field CB, Bilger W, Bjorkman O, Fredeen AL, Peñuelas J (1990) Remote-Sensing of the Xanthophyll Cycle and Chlorophyll Fluorescence in Sunflower Leaves and Canopies. *Oecologia* 85:1-7
- Gamon JA, Field CB, Fredeen AL, Thayer S (2001) Assessing photosynthetic downregulation in sunflower stands with an optically-based model. *Photosynthesis Research* 67:113-125
- Gamon JA, Peñuelas J, Field CB (1992) A Narrow-Waveband Spectral Index That Tracks Diurnal Changes in Photosynthetic Efficiency. *Remote Sensing of Environment* 41:35-44
- Gamon JA, Serrano L, Surfus JS (1997) The photochemical reflectance index: an optical indicator of photosynthetic radiation use efficiency across species, functional types, and nutrient levels. *Oecologia* 112:492-501
- Gamon JA, Surfus JS (1999) Assessing leaf pigment content and activity with a reflectometer. *New Phytologist* 143:105-117
- Gilmore AM (1997) Mechanistic aspects of xanthophyll cycle-dependent photoprotection in higher plant chloroplasts and leaves. *Physiologia Plantarum* 99:197-209
- Gitelson AA, Buschmann C, Lichtenthaler HK (1998) Leaf chlorophyll fluorescence corrected for re-absorption by means of absorption and reflectance measurements. In: *Journal of Plant Physiology*, vol. 152, pp 283-296
- Gitelson AA, Zur Y, Chivkunova OB, Merzlyak MN (2002) Assessing carotenoid content in plant leaves with reflectance spectroscopy. *Photochemistry and Photobiology* 75:272-281

- Guo JM, Trotter CM (2004) Estimating photosynthetic light-use efficiency using the photochemical reflectance index: variations among species. *Functional Plant Biology* 31:255-265
- Guo JM, Trotter CM (2006) Estimating photosynthetic light-use efficiency using the photochemical reflectance index: the effects of short-term exposure to elevated CO<sub>2</sub> and low temperature. *International Journal of Remote Sensing* 27:4677-4684
- Haboudane D, Miller JR, Pattey E, Zarco-Tejada PJ, Strachan IB (2004) Hyperspectral vegetation indices and novel algorithms for predicting green LAI of crop canopies: Modeling and validation in the context of precision agriculture. *Remote Sensing of Environment* 90:337-352
- Holt NE, Zigmantas D, Valkunas L, Li XP, Niyogi KK, Fleming GR (2005) Carotenoid cation formation and the regulation of photosynthetic light harvesting. *Science* 307:433-436
- Horton P, Ruban A (2005) Molecular design of the photosystem II light-harvesting antenna: photosynthesis and photoprotection. *Journal of Experimental Botany* 56:365-373
- Cheng LL (2003) Xanthophyll cycle pool size and composition in relation to the nitrogen content of apple leaves. *Journal of Experimental Botany* 54:385-393
- Inoue Y, Peñuelas J (2006) Relationship between light use efficiency and photochemical reflectance index in soybean leaves as affected by soil water content. *International Journal of Remote Sensing* 27:5109-5114
- Johnson GN, Scholes JD, Horton P, Young AJ (1993) Relationships between Carotenoid Composition and Growth Habit in British Plant-Species. *Plant Cell and Environment* 16:681-686
- Kautsky H, Hirsch A (1931) Neue Versuche zur Kohlensäureassimilation.– *Naturwissenschaften* 19:964
- Khamis S, Lamaze T, Lemoine Y, Foyer C (1990) Adaptation of the Photosynthetic Apparatus in Maize Leaves as a Result of Nitrogen Limitation - Relationships between Electron-Transport and Carbon Assimilation. *Plant Physiology* 94:1436-1443
- Koniger M, Harris GC, Virgo A, Winter K (1995) Xanthophyll-cycle pigments and photosynthetic capacity in tropical forest species: a comparative field study on canopy, gap and understory plants. In: *Oecologia*, vol. 104, pp 280-290
- Kulheim C, Agren J, Jansson S (2002) Rapid regulation of light harvesting and plant fitness in the field. *Science* 297:91-93

- le Maire G, Francois C, Dufrene E (2004) Towards universal broad leaf chlorophyll indices using PROSPECT simulated database and hyperspectral reflectance measurements. *Remote Sensing of Environment* 89:1-28
- Li XP et al. (2000) A pigment-binding protein essential for regulation of photosynthetic light harvesting. *Nature* 403:391-395
- Lichtenthaler H, Babani, F (2004) Light adaptation and senescence of the photosynthetic apparatus: changes in pigment composition, chlorophyll fluorescence parameters and photosynthetic activity. In: Papageorgiou GC, Govindjee (ed) *Chlorophyll Fluorescence: A Signature of Photosynthesis*. Springer, Dordrecht 2004, pp 713-736
- Lichtenthaler HK (1992) The Kautsky Effect - 60 Years of Chlorophyll Fluorescence Induction Kinetics. *Photosynthetica* 27:45-55
- Lichtenthaler HK, Buschmann C, Knapp M (2005) How to correctly determine the different chlorophyll fluorescence parameters and the chlorophyll fluorescence decrease ratio R-Fd of leaves with the PAM fluorometer. *Photosynthetica* 43:379-393
- Lichtenthaler HK, Rinderle U (1988) The Role of Chlorophyll Fluorescence in the Detection of Stress Conditions in Plants. *Crc Critical Reviews in Analytical Chemistry* 19:S29-S85
- Logan BA, Barker DH, DemmigAdams B, Adams WW (1996) Acclimation of leaf carotenoid composition and ascorbate levels to gradients in the light environment within an Australian rainforest. *Plant Cell and Environment* 19:1083-1090
- Louis J et al. (2005) Remote sensing of sunlight-induced chlorophyll fluorescence and reflectance of Scots pine in the boreal forest during spring recovery. *Remote Sensing of Environment* 96:37-48
- Malenovský Z (2006): Quantitative remote sensing of Norway Spruce (*Picea abies* (L.) *Karst.*): Spectroscopy from needles to crowns to canopies. PhD Thesis, Wageningen University, Wageningen, The Netherlands. pp. 141.
- Matsubara S, Gilmore AM, Ball MC, Anderson JM, Osmond CB (2002) Sustained downregulation of photosystem II in mistletoes during winter depression of photosynthesis. *Functional Plant Biology* 29:1157-1169
- Maxwell K, Johnson GN (2000) Chlorophyll fluorescence - a practical guide. *Journal of Experimental Botany* 51:659-668
- Moran JA, Mitchell AK, Goodmanson G, Stockburger KA (2000) Differentiation among effects of nitrogen fertilization treatments on conifer seedlings by foliar reflectance: a comparison of methods. *Tree Physiology* 20:1113-1120

- Myneni RB, Hall FG, Sellers PJ, Marshak AL (1995) The Interpretation of Spectral Vegetation Indexes. *Ieee Transactions on Geoscience and Remote Sensing* 33:481-486
- Nield J, Orlova EV, Morris EP, Gowen B, van Heel M, Barber J (2000) 3D map of the plant photosystem II supercomplex obtained by cryoelectron microscopy and single particle analysis. *Nature Structural Biology* 7:44-47
- Nichol CJ et al. (2000) Remote sensing of photosynthetic-light-use efficiency of boreal forest. *Agricultural and Forest Meteorology* 101:131-142
- Nichol CJ et al. (2002) Remote sensing of photosynthetic-light-use efficiency of a Siberian boreal forest. *Tellus Series B-Chemical and Physical Meteorology* 54:677-687
- Nichol CJ, Rascher U, Matsubara S, Osmond B (2006) Assessing photosynthetic efficiency in an experimental mangrove canopy using remote sensing and chlorophyll fluorescence. *Trees-Structure and Function* 20:9-15
- Niinemets U, Bilger W, Kull O, Tenhunen JD (1998) Acclimation to high irradiance in temperate deciduous trees in the field: changes in xanthophyll cycle pool size and in photosynthetic capacity along a canopy light gradient. In: *Plant Cell and Environment*, vol. 21, pp 1205-1218
- Niyogi KK (1999) Photoprotection revisited: Genetic and molecular approaches. *Annual Review of Plant Physiology and Plant Molecular Biology* 50:333-359
- Osmond CB (1994) What is photoinhibition? Some insights from comparison of shade and sun plants. In: Press MC, Scholes J.D., Barker, M.D. eds (ed) *Photoinhibition of photosynthesis: from molecular mechanisms to the field*. BIOS Scientific, Oxford, pp 1-24
- Peñuelas J, Filella I (1998) Visible and near-infrared reflectance techniques for diagnosing plant physiological status. *Trends in Plant Science* 3:151-156
- Peñuelas J, Filella I, Gamon JA (1995a) Assessment of Photosynthetic Radiation-Use Efficiency with Spectral Reflectance. *New Phytologist* 131:291-296
- Peñuelas J, Filella I, Gamon JA, Field C (1997a) Assessing photosynthetic radiation-use efficiency of emergent aquatic vegetation from spectral reflectance. *Aquatic Botany* 58:307-315
- Peñuelas J, Filella I, Lloret P, Munoz F, Vilajeliu M (1995b) Reflectance Assessment of Mite Effects on Apple-Trees. *International Journal of Remote Sensing* 16:2727-2733
- Peñuelas J, Filella I, Llusia J, Siscart D, Pinol J (1998) Comparative field study of spring and summer leaf gas exchange and photobiology of the Mediterranean trees *Quercus ilex* and *Phillyrea latifolia*. *Journal of Experimental Botany* 49:229-238

- Peñuelas J, Gamon JA, Fredeen AL, Merino J, Field CB (1994) Reflectance Indexes Associated with Physiological-Changes in Nitrogen-Limited and Water-Limited Sunflower Leaves. *Remote Sensing of Environment* 48:135-146
- Peñuelas J, Llusia J, Pinol J, Filella I (1997b) Photochemical reflectance index and leaf photosynthetic radiation-use-efficiency assessment in Mediterranean trees. *International Journal of Remote Sensing* 18:2863-2868
- Perez-Priego O, Zarco-Tejada PJ, Miller JR, Sepulcre-Canto G, Fereres E (2005) Detection of water stress in orchard trees with a high-resolution spectrometer through chlorophyll fluorescence in-filling of the O-2-A band. *Ieee Transactions on Geoscience and Remote Sensing* 43:2860-2869
- Raddi S, Cortes S, Pippi I, Magnani F (2005) Estimation of vegetation photochemical processes: An application of the photochemical reflectance index at the San Rossore test site. In: *Proceedings of the 3<sup>rd</sup> ESA CHRIS/Proba Workshop, 21–23 March, ESRIN, Frascati, Italy.*
- Rahman AF, Cordova VD, Gamon JA, Schmid HP, Sims DA (2004) Potential of MODIS ocean bands for estimating CO<sub>2</sub> flux from terrestrial vegetation: A novel approach. *Geophysical Research Letters* 31
- Rahman AF, Gamon JA, Fuentes DA, Roberts DA, Prentiss D (2001) Modeling spatially distributed ecosystem flux of boreal forest using hyperspectral indices from AVIRIS imagery. *Journal of Geophysical Research-Atmospheres* 106:33579-33591
- Rascher U, Nichol CJ, Small C, Hendricks L (2007) Monitoring spatio-temporal dynamics of photosynthesis with a portable hyperspectral imaging system. *Photogrammetric Engineering and Remote Sensing* 73:45-56
- Richardson AD, Berlyn GP (2002) Spectral reflectance and photosynthetic properties of *Betula papyrifera* (Betulaceae) leaves along an elevational gradient on Mt. Mansfield, Vermont, USA. *American Journal of Botany* 89:88-94
- Richardson AD, Berlyn GP, Gregoire TG (2001) Spectral reflectance of *Picea rubens* (Pinaceae) and *Abies balsamea* (Pinaceae) needles along an elevational gradient, Mt. Moosilauke, New Hampshire, USA. *American Journal of Botany* 88:667-676
- Roháček K (2002) Chlorophyll fluorescence parameters: the definitions, photosynthetic meaning, and mutual relationships. *Photosynthetica* 40:13-29
- Rouse JW, Haas RH, Schell JA, Deering DW (1973) Monitoring vegetation systems in the great plains with ERTS, *Third ERTS Symposium, NASA SP-351 I: 309-317.*



- Sims DA, Gamon JA (2002) Relationships between leaf pigment content and spectral reflectance across a wide range of species, leaf structures and developmental stages. *Remote Sensing of Environment* 81:337-354
- Stecher G, Schwienbacher F, Mayr S, Bauer H (1999) Effects of winter-stress on photosynthesis and antioxidants of exposed and shaded needles of *Picea abies* (L.) Karst. and *Pinus cembra* L. *Phyton-Annales Rei Botanicae* 39:205-211
- Strachan IB, Pattey E, Boisvert JB (2002) Impact of nitrogen and environmental conditions on corn as detected by hyperspectral reflectance. *Remote Sensing of Environment* 80:213-224
- Stylinski CD, Gamon JA, Oechel WC (2002) Seasonal patterns of reflectance indices, carotenoid pigments and photosynthesis of evergreen chaparral species. *Oecologia* 131:366-374
- Suarez L et al. (2008) Assessing canopy PRI for water stress detection with diurnal airborne imagery. *Remote Sensing of Environment* 112:560-575
- Szabo I, Bergantino E, Giacometti GM (2005) Light and oxygenic photosynthesis: energy dissipation as a protection mechanism against photo-oxidation. *Embo Reports* 6:629-634
- Tambussi EA, Casadesus J, Munne-Bosch SM, Araus JL (2002) Photoprotection in water-stressed plants of durum wheat (*Triticum turgidum* var. durum): changes in chlorophyll fluorescence, spectral signature and photosynthetic pigments. *Functional Plant Biology* 29:35-44
- Thayer SS, Bjorkman O (1990) Leaf Xanthophyll content and composition in sun and shade determined by HPLC. In: *Photosynthesis Research*, vol. 23, pp 331-343
- Trotter GM, Whitehead D, Pinkney EJ (2002) The photochemical reflectance index as a measure of photosynthetic light use efficiency for plants with varying foliar nitrogen contents. *International Journal of Remote Sensing* 23:1207-1212
- Ustin SL, Roberts DA, Gamon JA, Asner GP, Green RO (2004) Using imaging spectroscopy to study ecosystem processes and properties. *Bioscience* 54:523-534
- Verhoeven AS, Adams WW, Demmig-Adams B (1998) Two forms of sustained xanthophyll cycle-dependent energy dissipation in overwintering *Euonymus kiautschovicus*. *Plant Cell and Environment* 21:893-903
- Verhoeven AS, Demmig-Adams B, Adams WW (1997) Enhanced employment of the xanthophyll cycle and thermal energy dissipation in spinach exposed to high light and N stress. *Plant Physiology* 113:817-824

- Vogelmann JE, Rock BN, Moss DM (1993) Red Edge Spectral Measurements from Sugar Maple Leaves. *International Journal of Remote Sensing* 14:1563-1575
- Weng JH, Chen YN, Liao TS (2006a) Relationships between chlorophyll fluorescence parameters and photochemical reflectance index of tree species adapted to different temperature regimes. *Functional Plant Biology* 33:241-246
- Weng JH, Liao TS, Hwang MY, Chung CC, Lin CP, Chu CH (2006b) Seasonal variation in photosystem II efficiency and photochemical reflectance index of evergreen trees and perennial grasses growing at low and high elevations in subtropical Taiwan. *Tree Physiology* 26:1097-1104
- Zarco-Tejada PJ et al. (2005) Assessing vineyard condition with hyperspectral indices: Leaf and canopy reflectance simulation in a row-structured discontinuous canopy. *Remote Sensing of Environment* 99:271-287
- Zarco-Tejada PJ, Miller JR, Mohammed GH, Noland TL (2000a) Chlorophyll fluorescence effects on vegetation apparent reflectance: I. Leaf-level measurements and model simulation. *Remote Sensing of Environment* 74:582-595
- Zarco-Tejada PJ, Miller JR, Mohammed GH, Noland TL, Sampson PH (2000b) Chlorophyll fluorescence effects on vegetation apparent reflectance: II. Laboratory and airborne canopy-level measurements with hyperspectral data. *Remote Sensing of Environment* 74:596-608
- Zarco-Tejada PJ, Miller JR, Mohammed GH, Noland TL, Sampson PH (2002) Vegetation stress detection through chlorophyll a+b estimation and fluorescence effects on hyperspectral imagery. *Journal of Environmental Quality* 31:1433-1441
- Zarco-Tejada PJ, Pushnik JC, Dobrowski S, Ustin SL (2003) Steady-state chlorophyll a fluorescence detection from canopy derivative reflectance and double-peak red-edge effects. *Remote Sensing of Environment* 84:283-294
- Zarter CR, Adams WW, Ebbert V, Adamska I, Jansson S, Demmig-Adams B (2006a) Winter acclimation of PsbS and related proteins in the evergreen *Arctostaphylos uva-ursi* as influenced by altitude and light environment. *Plant Cell and Environment* 29:869-878
- Zarter CR, Adams WW, Ebbert V, Cuthbertson DJ, Adamska I, Demmig-Adams B (2006b) Winter down-regulation of intrinsic photosynthetic capacity coupled with up-regulation of Elip-like proteins and persistent energy dissipation in a subalpine forest. *New Phytologist* 172:272-282

## CHAPTER 3

### Differences in pigment composition, photosynthetic rates and chlorophyll fluorescence images of sun and shade leaves of four tree species

*Hartmut K. Lichtenthaler<sup>(1)</sup>, Alexander Ač<sup>(2)</sup>, Michal V. Marek<sup>(1)</sup>, Jiří Kalina<sup>(3)</sup>, Otmar Urban<sup>(1)</sup>,\**

(1) Botanical Institute (Molecular Biology and Biochemistry of Plants), University of Karlsruhe, Kaiserstrasse 12, D-76133 Karlsruhe, Germany

(2) Laboratory of Plants Ecological Physiology, Institute of Systems Biology and Ecology AS CR, Poříčí 3b, CZ-60300 Brno, Czech Republic

(3) Department of Physics, Faculty of Science, Ostrava University, 30. Dubna 22, CZ-701 03 Ostrava, Czech Republic

Published in *Plant Physiology and Biochemistry* 45 (2007) 577-588.

Reprinted with permission

## **Abstract**

The differential pigment composition and photosynthetic activity of sun and shade leaves of deciduous (*Acer pseudoplatanus*, *Fagus sylvatica*, *Tilia cordata*) and coniferous (*Abies alba*) trees was comparatively determined by studying the photosynthetic rates via CO<sub>2</sub> measurements and also by imaging the Chl fluorescence decrease ratio ( $R_{Fd}$ ), which is an in vivo indicator of the net CO<sub>2</sub> assimilation rates. The thicker sun leaves and needles in all tree species were characterized by a lower specific leaf area, lower water content, higher total chlorophyll (Chl)  $a+b$  and total carotenoid (Cars) content per leaf area unit, as well as higher values for the ratio Chl  $a/b$  compared to the much thinner shade leaves and needles that possess a higher Chl  $a+b$  and Cars content on a dry matter basis and higher values for the weight ratio Chls/Cars. Sun leaves and needles exhibited higher rates of maximum net photosynthetic CO<sub>2</sub> assimilation ( $P_{Nmax}$ ) measured at saturating irradiance associated with higher maximum stomatal conductance for water vapor efflux. The differences in photosynthetic activity between sun and shade leaves and needles could also be sensed via imaging the Chl fluorescence decrease ratio  $R_{Fd}$ , since it linearly correlated to the  $P_{Nmax}$  rates at saturating irradiance. Chl fluorescence imaging not only provided the possibility to screen the differences in  $P_N$  rates between sun and shade leaves, but in addition permitted detection and quantification of the large gradients in photosynthetic rates across the leaf area existing in sun and shade leaves.

*Keywords:* Carbon dioxide assimilation; Carotenoid level; Chlorophyll fluorescence decrease ratio; Chlorophyll  $a/b$  ratio; Chlorophyll content; Fluorescence imaging; Stomatal conductance

### 3.1 Introduction

Sun and shade leaves of trees as well as high-light and low-light plants can considerably differ in their relative composition of photosynthetic pigments, electron carriers, their chloroplast ultrastructure and their photosynthetic rates (Anderson et al. 1995; Boardman 1977; Givnish 1988; Meier and Lichtenthaler 1981; Wild et al. 1986)). Leaf and chloroplast adaptation to either high or low irradiance, to direct sun-light or shade proceed during leaf development and comprise special morphological and biochemical adaptations. Sun leaves and high-light plants possess sun-type chloroplasts that are adapted for high rates of photosynthetic quantum conversion, they possess a higher photosynthetic capacity on a leaf area and chlorophyll (Chl) basis, exhibit higher values for the ratio Chl *a/b*, a much lower level of light-harvesting Chl *a/b* proteins (LHCII), and a lower stacking degree of thylakoids than shade leaves and low-light plants with their shade-type chloroplasts (Lichtenthaler et al. 1982; 1984). Major differences in the chloroplast adaptation response to either high- or lowlight quanta fluence rates have recently been summarized (Lichtenthaler and Babani, 2004). This review, giving access to further literature in this field, show that much work has been done with individual herbaceous plants grown at high or low quanta fluence rates or with selected deciduous broad-leaf trees (Anderson et al. 1995; Boardman 1977; Givnish 1988; Hölscher 2004; Nobel 1976). In general, only the net CO<sub>2</sub> assimilation rates  $P_N$  per leaf area unit of sun and shade leaves have been measured, whereas the question if sun and shade leaves differ in their photosynthetic activity, also on a Chl basis, remained open because pigment determinations were not performed. So far the photosynthetic activities of leaves, and especially the differences in CO<sub>2</sub> fixation rates between sun and shade leaves, have primarily been performed by net CO<sub>2</sub> measurements with CO<sub>2</sub>/H<sub>2</sub>O porometer gas-exchange systems. These provide, however, only one integral  $P_N$  rate per measurement of a relatively large leaf area spot or of a certain quantity of needles on a small conifer branch. Whether the photosynthetic activity is evenly distributed over the leaf area or whether inhomogeneities or small local declines in photosynthetic rates exist, cannot be detected using gas exchange measurements. In recent years it has been shown that the chlorophyll fluorescence decrease ratio  $R_{Fd}$  is linearly correlated to the net photosynthetic CO<sub>2</sub> assimilation rate  $P_N$  and is an indicator of the photosynthetic activity of leaves (Lichtenthaler et al. 2005). Moreover, a special imaging technique has been developed (Lichtenthaler and Babani 2000; Lichtenthaler et al. 2000) that allows imaging the  $R_{Fd}$  ratio of whole leaves with at least several tens of thousands, or more than 100,000 pixels per measurement. This should principally be also

possible with the new pulse amplitude fluorescence imaging system (Nedbal et al. 2000) when it is combined with an additional saturating light source. Thus a major objective of this investigation was to prove by means of Chl fluorescence imaging, if the differences in photosynthetic activity of sun and shade leaves would show up in the  $R_{Fd}$  images, and if there were differences between the two leaf types in the distribution of photosynthetic activity across the leaf area. In order to better characterize the leaves, the relative Chl and carotenoid composition, as well as the photosynthetic activity of sun and shade leaves were compared, and we also checked whether the higher  $CO_2$  assimilation rates of sun leaves/needles also exist on a Chl basis. Four common tree species of the temperate zone from the same location and climate with different tolerance to shade conditions (Úradníček et al. 2001) were selected for this study: namely the strongly shade-tolerant linden (*Tilia cordata* Mill.) and fir (*Abies alba* Mill.) as well as the less shade-tolerant beech (*Fagus sylvatica* L.) and maple (*Acer pseudoplatanus* L.).

## 3.2 Materials and methods

### 3.2.1 Site description

Experiments were carried out at the ecological research station in a natural stand of trees in a forest located in the Moravian-Silesian Beskydy Mountains (Bílý Kříž, 49°33'N, 18°32'E, 908 m a.s.l., NE of the Czech Republic) in the middle of the growing season (mid to late July 2005). The climate of the area is characterized by an annual mean temperature of 5.5°C, annual mean relative air humidity of 80%, and a total rainfall of 1000-1400 mm. The geological bedrock is formed by Mesozoic Godula sandstone (flysch type), with ferric podzols. See detailed description in Kratochvílová et al. (1989).

### 3.2.2 Plant material

Fully developed sun and shade adapted leaves of four tree species were sampled: the deciduous species beech (*Fagus sylvatica* L.), maple (*Acer pseudoplatanus* L.), linden tree (*Tilia cordata* Mill.), and shoots of the coniferous fir (*Abies alba* Mill.). Shade leaves at the inner tree crown received up to 100  $\mu\text{mol}(\text{photons})\text{ m}^{-2}\text{ s}^{-1}$  on sunny days, whereas the sun leaves were exposed to a maximum photosynthetic photon flux density of 1200–1500  $\mu\text{mol}(\text{photons})\text{ m}^{-2}\text{ s}^{-1}$ . A branch with the desired leaf or needles was cut from the tree and the cut end was immediately re-cut under water to remove xylem embolisms. This branch end

remained in the water during the measurements. The branches investigated here were derived from three to five trees. The projected leaf area (LAp) of all investigated leaves was estimated using the leaf area meter LI-3000A (LI-COR, Lincoln, NE USA), as well as their fresh (FW) and dry weight (DW) after drying at 80°C for 48 hours. Subsequently, the relative water content (RWC [%];  $RWC = [(FW-DW)/FW]*100$ ) and specific leaf area (SLA [ $\text{cm}^2 \text{g}^{-1}$ ];  $SLA = LAp/DW$ ) were calculated in agreement with Gilmore et al. (1995). In contrast to needles of other coniferous trees, fir needles are flat, their needle area can easily be determined, and thus their SLA can be compared to that of leaves of broadleaf trees. The leaf and needle thickness was determined with a digital micrometer system (Mitutoyo Corp., Japan).

### 3.2.3 Pigment analysis

The photosynthetic plant pigments, Chls and carotenoids, from dark-adapted (30 min) and liquid nitrogen frozen leaves (ca. 100 mg of fresh mass) were extracted with 80% acetone and a small amount of  $\text{MgCO}_3$ . The clear supernatant obtained after centrifugation at 480 g for 3 min was used for spectrophotometric (UV/VIS 550, Unicam, England) estimation of Chl *a*, Chl *b* and total carotenoids in the same extract solution using the extinction coefficients and equations redetermined by Lichtenthaler (1987), and given in more detail in Lichtenthaler and Buschmann (2001). From the pigment levels the weight ratios of pigments, Chl *a/b* and Chls/carotenoids  $(a+b)/(x+c)$  were determined that significantly differ between sun and shade leaves.

### 3.2.4 Gas-exchange measurement

The infra-red gas analyser LI-6400 (LI-COR, Lincoln, NE USA) was used to estimate the maximum  $\text{CO}_2$  assimilation rate ( $P_{N_{\max}}$ ). The values were recorded after ca. 20 min of exposure to saturating irradiance ( $1500 \mu\text{mol}(\text{photons}) \text{m}^{-2} \text{s}^{-1}$ ) when the stomata had fully opened (maximum stomatal conductance;  $G_{S_{\max}}$ ). Leaf temperature, relative air humidity, and  $\text{CO}_2$  concentration inside the leaf chamber were kept constant at 18-21°C, 50-55%, and  $375 \mu\text{mol}(\text{CO}_2) \text{mol}^{-1}$ , respectively.

### 3.2.5 Chlorophyll fluorescence imaging

The Chl-F induction kinetics (Kautsky effect) of pre-darkened leaves (30 min) were measured at the red Chl fluorescence band ( $\lambda = 690 \text{ nm}$ ) using the FluorCam kinetic imaging fluorometer (Photon System Instruments, Ltd., Brno, Czech Republic). The lens of the CCD

camera was ca. 7 cm perpendicular to the leaf surface. At first, the initial fluorescence level,  $F_0$ , was measured in the dark. The measuring flashes were generated in two panels of orange light-emitting diodes (HLMP-EH08, Agilent Technologies, U.S.A.). The measuring flashes, 10  $\mu$ s long, were applied 2 s each and had no detectable actinic effect. Afterwards, the continuous actinic saturating light (ca. 2000  $\mu$ mol(photons)  $m^{-2} s^{-1}$ ), generated by an Oriel 150 W xenon lamp (model 66056) with UV filters, was applied to obtain the maximum fluorescence level,  $F_M$ . The steady state fluorescence level,  $F_S$ , was estimated from the Chl-F induction curve after 5 min of continuous illumination. See Nedbal et al. (2000) for detailed description of the fluorescence system and Lichtenthaler et al. (2005) for details on the measuring protocol. The Chl fluorescence decrease ratio ( $R_{Fd}$ ) was determined from the induction curve according to Lichtenthaler and Babani (2000) and Lichtenthaler et al. (2005):

$$R_{Fd} = F_d/F_S = (F_M - F_S)/F_S$$

where  $F_M$  is the maximum fluorescence level,  $F_S$  is the steady state fluorescence (5 min after onset of saturating irradiance), and  $F_d$  represents the chlorophyll fluorescence decline from  $F_M$  to  $F_S$ . The  $F_M$  and  $F_S$  values were obtained by dividing the sum of the fluorescence counts of all image pixels by the total number of leaf pixels. After the collection of the Chl fluorescence images, the images of the Chl-F intensity distribution and the histograms with the  $R_{Fd}$  frequency distribution were constructed using the FluorCam software package. The histograms on the  $R_{Fd}$  frequency distribution in sun and shade leaves are based on 160 000 leaf pixels (*Fagus*), 90 000 (*Acer*, *Tilia*) and > 40 000 needle pixels for each leaf type. For comparative reasons the  $R_{Fd}$  value distribution is given in relative units (relative frequency distribution, figure 9).

### 3.2.6 Statistical analysis

LSD test (ANOVA) was used to evaluate the statistically significant differences between sun and shade leaves. Differences were tested at levels 0.05 and 0.01. The homogeneity of the variance of the  $R_{Fd}$  frequency distribution was tested using  $F$  test, and subsequently, two sample t-test with uneven variances were used for testing the significant differences between sun and shaded  $R_{Fd}$  histograms of the tree species. All statistical tests were performed using STATISTICA software.

## 3.3 Results



### 3.3.1 General leaf characteristics

The sun-exposed leaves from end-branches of the three broadleaf trees investigated showed the typical, larger thickness of sun leaves (by ca. 40% to 65%) as compared to shade leaves. Since this had not been clearly investigated in the case of sun and shade fir needles, we have measured the thickness of several needle age classes and found that sun needles were 62% to 76% thicker than shade needles depending on the needle age (Fig. 3.1). Sun leaves and needles had a smaller projected leaf and needle area as compared to the thinner shade leaves and needles that possess a higher relative water content. Thus, the relative water content (RWC) in sun leaves was significantly ( $p < 0.01$ ) lower (by 8-22%) as compared to shade leaves in all tree species (Fig. 3.2A). In addition, there also existed the expected statistically significant differences ( $p < 0.01$ ) in the specific leaf area (SLA) with higher values for shade leaves and needles as compared to sun leaves and sun needles (Fig. 3.2B).

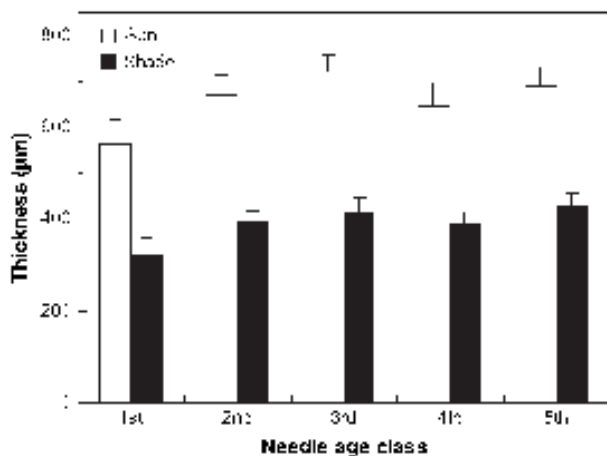


Figure 3.1 Differences in needle thickness ( $\mu\text{m}$ ) between sun and shade needles of fir (*Abies alba*) of different needle years. The values are given for 1<sup>st</sup>, 2<sup>nd</sup>, 3<sup>rd</sup>, 4<sup>th</sup> and 5<sup>th</sup> year needles. Needles from three branches of two trees ( $n = 18$  for each needle year and condition). Columns represent mean values and bars standard deviations. The differences are highly significant ( $p < 0.001$ ).

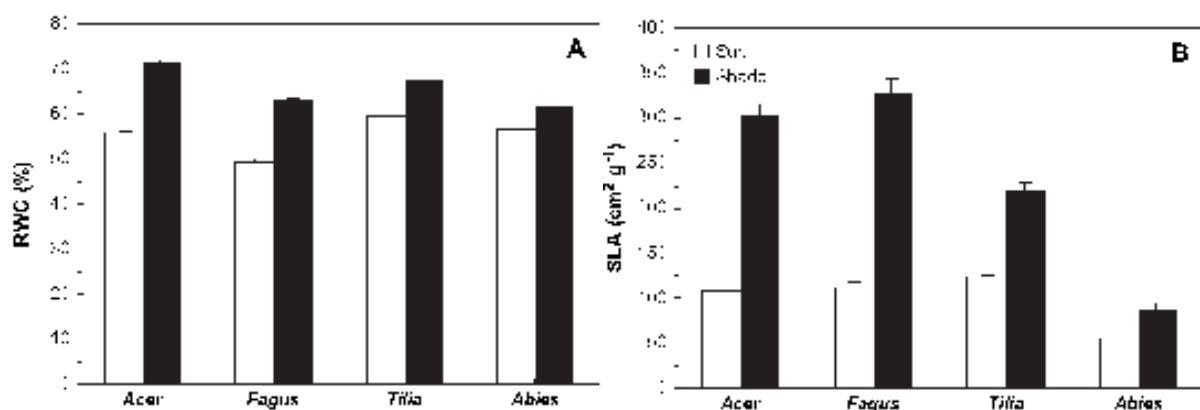


Figure 3.2. A,B. Relative water content (RWC; A) and specific leaf area (SLA; B) in sun (white columns) and shade leaves (black columns) of deciduous *Acer pseudoplatanus*, *Fagus sylvatica*, *Tilia cordata* and coniferous *Abies alba*. All differences between sun and shade leaves are statistically highly significant ( $p < 0.01$ ). Columns represent mean values and bars standard deviations.  $n = 8$ .

### 3.3.2 Chlorophyll and carotenoid levels

The differences in chlorophyll (Chls) and total karotenoid (Cars) contents between sun and shade leaves are summarized in Fig. 3.3. One has to differentiate between two reference systems, the levels per leaf area unit and the levels per leaf dry weight, which yield contrasting results. Regarding photosynthetic processes that are controlled by incident light, it is more appropriate to use the leaf area as a reference system; however, the dry weight often indicated in the literature is given here for comparative reasons as well. On a leaf area basis the Chl ( $a+b$ ) amounts were significantly higher in sun leaves of *A. pseudoplatanus* and *T. cordata* (Fig. 3.3A) as compared to shade leaves, but the differences were not statistically significant ( $p > 0.05$ ) in *F. sylvatica* and *A. alba*. In contrast, on a dry matter basis the shade leaves and needles had a significantly ( $p < 0.01$ ) higher Chl ( $a+b$ ) content, up to 147% for all four tree species (Fig. 3.3B). The content of total Cars on a leaf area basis was significantly lower ( $p < 0.01$ ) in shade leaves compared to sun leaves (Fig. 3.3C), except for *A. alba* where the difference was not significant ( $p > 0.05$ ). On a dry matter basis, however, the shade leaves and needles had a significantly higher total Cars content (Fig. 3.3D).

### 3.3.3 Pigment ratios

The typical differences between sun and shade leaves in the pigment ratios Chl  $a/b$  and Chls/Cars were found to be as expected (Fig. 3.4). The sun leaves of all investigated tree species had significantly higher values for the ratio Chl  $a/b$  (Fig. 3.4A) and lower values for the ratio of Chls/Cars (Fig. 3.4B), which is also known as ratio  $(a+b)/(x+c)$  (Babani and Lichtenthaler 1996).

### 3.3.4 Measurements of photosynthetic rates $P_N$

Maximum CO<sub>2</sub> assimilation rates ( $P_{Nmax}$ ) per leaf area unit (Fig. 3.5A) at saturating photosynthetic photon flux density (PPFD  $\approx 1500 \mu\text{mol m}^{-2} \text{s}^{-1}$ ) were significantly ( $p < 0.01$ ) higher in sun leaves and needles (range: from 97% to 168%) than in shade leaves. Even on a Chl ( $a+b$ ) basis the sun leaves and needles exhibited a higher  $P_{Nmax}$  rate than shade leaves and needles (Fig. 3.5B). However, the differences in  $P_{Nmax}$  rates on a Chl basis were not as high (range: from 76% to 128%) as on a leaf area basis. There was an additional difference when the  $P_{Nmax}$  rate on a leaf dry weight basis, reflecting the influence of the leaves' morphological

structure, was taken as a reference system (Fig. 3.5C). As compared to sun leaves, higher  $P_{Nmax}$  rates on a leaf dry weight basis were detected in the shade leaves of *A. pseudoplatanus* (19%) and *F. sylvatica* (48%), whereas the  $P_{Nmax}$  rates were lower in the shade leaves of *T. cordata* (34%) and *A. alba* (32%). These differences were statistically significant ( $p < 0.01$ ) except for *A. pseudoplatanus*. At saturating PPFD,  $P_{Nmax}$  linearly correlated ( $P_{Nmax} = 0.0631 G_{Smax}$ ;  $R^2 = 0.78$ ) with maximum stomatal conductance ( $G_{Smax}$ ) as shown in Fig. 3.6. The  $G_{Smax}$  values of sun leaves and needles were always significantly higher as compared to those of shade leaves. In all cases the latter remained below values of  $100 \text{ mmol m}^{-2} \text{ s}^{-1}$ , whereas sun leaves and needles exhibited  $G_{Smax}$  values of above  $100 \text{ mmol m}^{-2} \text{ s}^{-1}$  as indicated in Fig. 3.6 by a broken line.

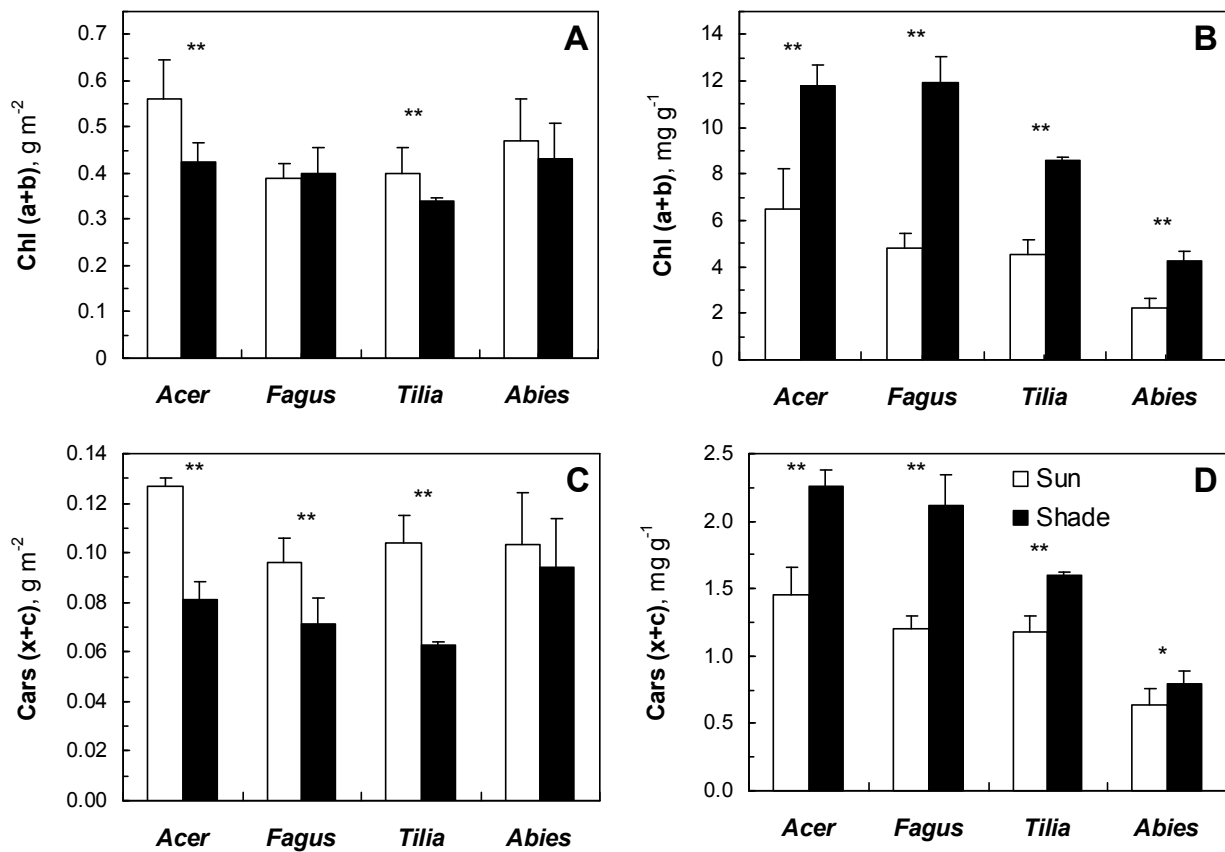


Figure 3.3. A-D. Total chlorophyll (Chl (a+b); A, B), and carotenoid content (Cars (x/c); C, D) expressed per leaf area unit (A, C) and dry weight unit (B, D). Sun (white columns) and shade leaves (black columns) of deciduous *Acer pseudoplatanus*, *Fagus sylvatica*, *Tilia cordata* and coniferous *Abies alba* are presented. Columns represent mean values and bars standard deviations. \*\* and \* represent the statistically significant differences at  $p < 0.01$  and  $p < 0.05$  level, respectively.  $n = 8$ .

### 3.3.5 Chlorophyll fluorescence imaging

The chlorophyll (Chl) fluorescence images (Fig. 3.7A,B) demonstrate that the red Chl-F signal (band near 690 nm) is unevenly distributed across the leaf area at both the maximum

Chl-F at a saturating pulse ( $F_M$ ), and at the steady state Chl-F at a saturating photosynthetic photon flux density ( $F_S$ ). These images may subsequently be applied to deduce the distribution of the  $R_{Fd}$  values in leaves (Fig. 3.8C,D). The  $R_{Fd}$  images indicate significantly higher  $R_{Fd}$  values in sun leaves in comparison to shade leaves, e.g. of the broadleaf *F. sylvatica* (Fig. 3.7C,D) and even in the needles of the coniferous *A. alba* (Fig. 3.8). The normalized frequency distribution of the  $R_{Fd}$  values of all tree species studied demonstrated highly significant ( $p < 0.001$ ) differences in the distribution of the  $R_{Fd}$  values between sun and shade leaves (Fig. 3.9A-D). The  $R_{Fd}$  value distributions, shown here for better comparison as percentage distribution, are based on more than 90,000 leaf pixels and on more than 40,000 needle pixels per  $R_{Fd}$  image evaluated. In fact, the average  $R_{Fd}$  values of sun leaves were several times higher than those in shade leaves (*Acer* 2.0×, *Fagus* 1.7×, *Tilia* 2.7×, and *Abies* 3.7×). The Chl-F images and the  $R_{Fd}$  frequency distributions, shown in Fig. 3.9, are of one leaf and one needle shoot sample. Parallel images were taken of additional leaves and needle shoots of all tree species, and the differences in images and  $R_{Fd}$  value distribution (data not shown) were very similar and practically almost identical to those shown. When  $R_{Fd}$  values and  $P_{Nmax}$  rates, both measured at saturating PPFD, were compared, a close linear correlation ( $R_{Fd} = 0.27 P_{Nmax} + 1.33$ ;  $R^2 = 0.91$ ) between both parameters showed up (Fig. 3.10). The same linear relationship applies to both sun and shade leaves and needles. Correspondingly, at zero net  $CO_2$  assimilation rate ( $P_{Nmax} = 0 \mu\text{mol m}^{-2} \text{s}^{-1}$ ) an  $R_{Fd}$  value of ca. 1.33 is found.

### 3.4 Discussion

In this study all four common tree species of the temperate zone exhibited major differences between sun and shade leaves that had developed at either sun exposed or fully shaded conditions. The lower RWC (Fig. 3.2A) and a lower SLA (Fig. 3.2B) in sun leaves and sun needles of the four tree species investigated as compared to shade leaves and needles, is in accordance with previous studies showing a lower water content (51%), a lower SLA ( $116 \text{ cm}^2 \text{ g}^{-1}$ ) in beech sun leaves as compared to beech shade leaves (SLA:  $335 \text{ cm}^2 \text{ g}^{-1}$ , water content 64%) (Lichtenthaler 1981). This was confirmed in an independent investigation indicating that sun leaves of *F. sylvatica* had a significantly lower SLA ( $118 \text{ cm}^2 \text{ g}^{-1}$ ) and water content (42%) than shade leaves (SLA:  $282 \text{ cm}^2 \text{ g}^{-1}$ ; water content: 53%) (Pilegaard et al. 2003). Significantly lower SLA values were also described for the sunlit leaves of the upper canopy level as compared to leaves of the lower canopy level in ash, hornbeam, maple

and linden trees (Hölscher et al. 2004). SLA values are considered a measurement of leaf structure, thickness, the amount of mechanical tissues in leaves, and a measurement of the morphological difference between sun and shade leaves and needles (Gilmore et al. 1995). In fact, beech sun leaves are thicker (144 to 185  $\mu\text{m}$ ) than shade leaves (88-93  $\mu\text{m}$ ) (Lichtenthaler 1981; Lichtenthaler et al. 1981), which was confirmed in the present investigation and extended for the other trees. Practically the same observations were made using the inverse SLA ratio, the leaf dry mass per area LMA, which, in several hundred broad-leaf trees and woody species, linearly increased with increasing irradiance together with leaf thickness (Niinemets 1997; 2001). Moreover, a close relationship between SLA and RWC was reported in groundnut (*Arachis hypogaea*) leaves (Nautiyal et al. 2002), whereby the rate of reduction in leaf RWC during a progressive moisture deficit was directly related to SLA and, as a consequence, affected the leaf carbon exchange. Differences in  $P_{\text{Nmax}}$  on a leaf area unit between sun and shade leaves (Fig. 3.5A) were similar to those previously described for beech (Lichtenthaler 1981; Lichtenthaler et al. 1981), several other broadleaf (Kubiske and Pregitzer 1997; Lichtenthaler et al. 2000; Pandey et al. 2003) and coniferous tree species (Priwitzer et al. 1998; Spunda et al. 1998), as well as various other

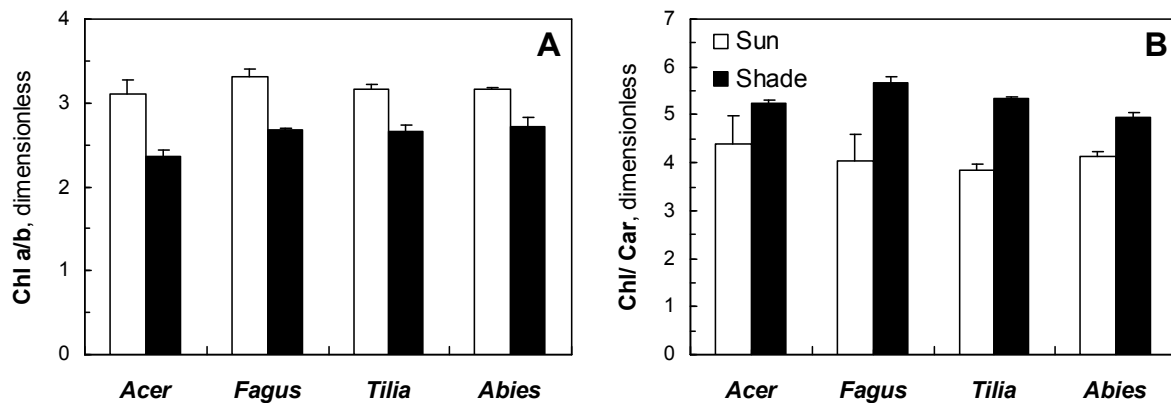
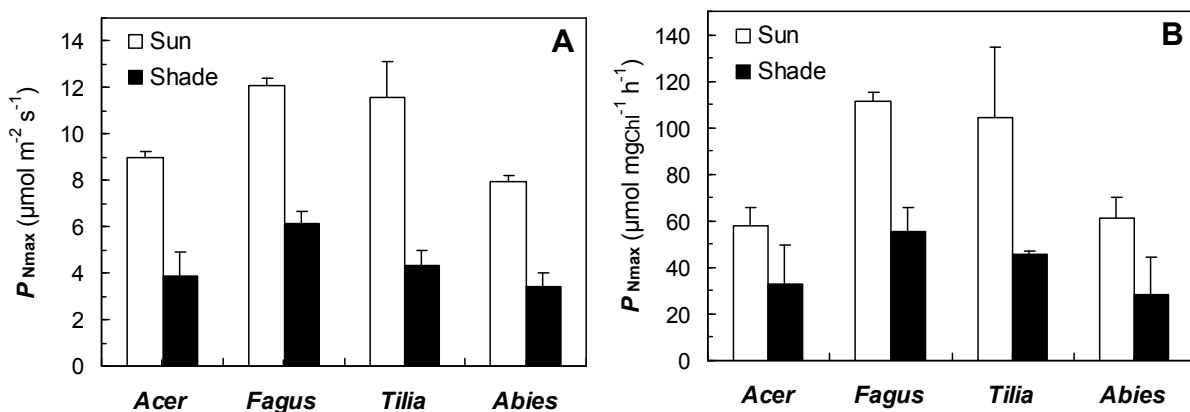


Figure 3.4. A,B. Ratio of Chl a to Chl b (Chl a/b; A) and weight ratio of total chlorophylls to total carotenoids (Chls/Cars; B) in sun (white columns) and shade leaves (black columns) of deciduous *Acer pseudoplatanus*, *Fagus sylvatica*, *Tilia cordata* and coniferous *Abies alba* are presented. All differences between sun and shade leaves are statistically highly significant ( $p < 0.01$ ). Columns represent mean values and bars the standard deviations.  $n = 8$ .



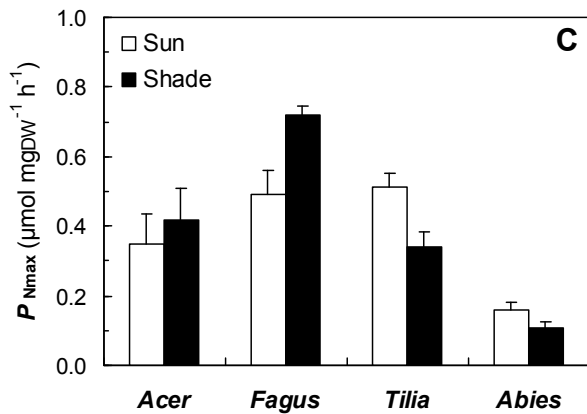


Figure 3.5. A-C. Maximum of light-saturated  $\text{CO}_2$  assimilation rate ( $P_{N\max}$ ) expressed on a projected leaf area basis (A), on a chlorophyll ( $a+b$ ) basis (B), and on a leaf dry weight basis (C). Mean values (columns) and standard deviations (bars) of sun (white columns) and shade leaves and needles (black columns) of *Acer pseudoplatanus*, *Fagus sylvatica*, *Tilia cordata*, and *Abies alba* are presented. All differences between sun and shade leaves are statistically highly significant ( $p < 0.01$ ), except  $P_{N\max}$  expressed on a leaf dry weight basis (C) in *A. pseudoplatanus*.  $n = 8$ .

plants (Boardman 1977; Lichtenthaler and Babani 2000; Nobel 1976). Also, in sunlit leaves of the upper canopy level of four tree species higher photosynthetic rates per leaf area unit were found as compared to leaves of the lower canopy level (Hölscher 2004), whereby tree specific differences showed up. Higher light saturated rates of photosynthesis in sun leaves are mainly associated with a greater amount of

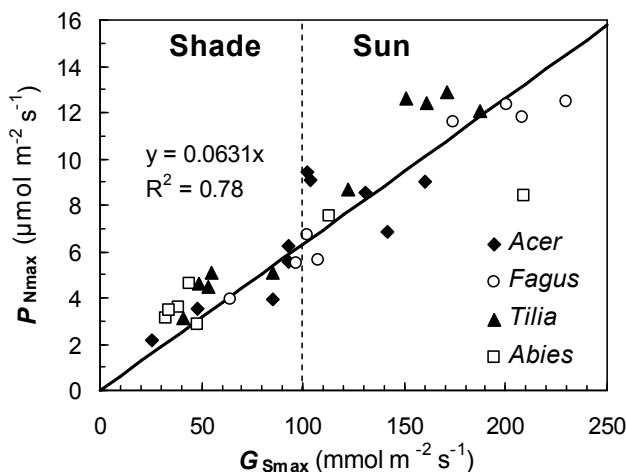


Figure 3.6. Relationship between maximum  $\text{CO}_2$  assimilation rate ( $P_{N\max}$ ) and maximum stomatal conductance for water vapor ( $G_{S\max}$ ) at saturating photosynthetic photon flux density (PPFD $\approx 1500 \mu\text{mol m}^{-2} \text{s}^{-1}$ ). Symbols represent the mean of five measurements of sun and shade leaves of *A. pseudoplatanus*, *F. sylvatica*, *T. cordata*, and shoots of *A. alba*. All data were fitted using linear regression. The perpendicular broken line was drawn to indicate the values of sun leaves (upper right part) and shade leaves (lower left part).

nitrogen per leaf area unit in sun leaves as compared to shade leaves (Herrick and Thomas 1999; Hölscher 2004; Kubiske and Pregitzer 1997), and they usually have a higher level of Chls per leaf area unit (cf. Fig. 3.3A) as shown before for ginkgo, beech, hornbeam, and poplar (Sarijeva et al. 2007; Sun et al. 2003). Moreover, the higher nitrogen levels per leaf area unit also result in a higher content of Rubisco enzyme and subsequently in the stimulation of  $\text{CO}_2$  uptake at high irradiances (Kubiske and Pregitzer 1997). The level range of total Chls per leaf area unit can partially overlap in sun and shade leaves. However, on a dry matter basis shade leaves always contain significantly higher amounts of total Chls as compared to sun leaves (Fig. 3.3B). This has been shown before for horse chestnut, oak, hornbeam and ginkgo (Sarijeva et al. 2007) and other plants (Nobel 1976). Our observation

that sun leaves and sun needles possess much higher values for the maximum stomatal conductance for water vapor ( $G_{S_{max}}$ ) (Fig. 3.6) as compared to shade leaves and shade needles may indicate that they are able to open their stomata much wider than shade leaves and shade needles. This certainly appears to be an essential prerequisite for their higher photosynthetic rates. However, also a higher stomata density per leaf area unit of sun leaves and upper canopy leaves as compared to shade leaves and lower canopy leaves must be taken into consideration in this respect (Hölscher 2004). The organization of the pigment apparatus and the relative levels of Chl *a* and Chl *b* as well as the ratio of total Chls to total Cars is also an essential difference between sun and shade leaves and needles. Sun leaves/needles possess sun-type chloroplasts with higher values for the ratio Chl *a/b* and lower values for the weight ratio Chls/Cars (Fig. 3.4A,B) than the shade-type chloroplasts of shade leaves and leaves of low light plants (Babani and Lichtenthaler 1996; Demmig-Adams 1998). The values for the ratio Chl *a/b* in sun (range: from 3.0 to 3.4) and shade leaves (range: from 2.4 to 2.7) as well as the values for the ratio Chls/Cars (sun leaves 3.8 to 4.4, shade leaves 4.8 to 5.7) were found in the normal range of physiologically active leaves (Lichtenthaler and Babani 2004; Sarijeva et al. 2007). Such differential pigment ratios are characteristic for sun-type and shade-type chloroplasts (Lichtenthaler and Babani 2004; Sarijeva et al. 2007). Significantly higher values for the ratio Chl *a/b* were also found in the sunlit leaves of the upper canopy level of four broadleaf tree species as compared to leaves of the lower canopy level (Hölscher 2004). The considerably higher level of carotenoids on a Chl reference basis in sun leaves versus shade leaves, and hence lower values for the ratio Chls/Cars, is primarily caused by their higher level of the xanthophyll cycle carotenoids (Demmig-Adams 1998; Hölscher 2004; Tausz et al. 2004; Thayer and Bjorkman 1990). In addition, these differences in the pigment ratios are also a result of the high irradiance adaptation response of the photosynthetic pigment apparatus of sun leaves (sun chloroplasts) with fewer light-harvesting Chl *a/b* proteins (LHCII) and a larger number of reaction center pigment proteins (e.g. CPa, CPI) on a total Chl basis as compared to shade chloroplasts (Lichtenthaler et al. 1982), as well as a greater number of electron transport chains (Lichtenthaler and Babani 1984; Lichtenthaler and Buschmann 1981; Wild et al. 1986). At the same time shade leaves and shade-type chloroplasts exhibit higher and broader grana thylakoid stacks and primarily invest into the pigment antenna (Lichtenthaler et al. 1982). As a consequence of the adaptation response of their chloroplasts to high irradiance, sun leaves of trees with their sun-type chloroplasts possess considerably higher  $P_N$  rates on a leaf area basis than shade leaves. One reason for the higher  $P_{N_{max}}$  rates of sun leaves and needles as compared to shade leaves is their generally

higher Chl content per leaf area unit, but the major reason is the possession of sun-type chloroplasts with their different ultrastructure, biochemical organization and a special arrangement of their Chls and Cars in the thylakoids. The possession of sun-type chloroplasts is also the major reason why sun leaves and needles exhibit higher net CO<sub>2</sub> assimilation rates  $P_{Nmax}$ , not only on a leaf area basis but also on a Chl basis (Fig. 3.5B). The lower differences in  $P_N$  rates on a Chl basis between sun and shade leaves (Fig. 3.5B) indicate that one possible reason for the higher PN rates in sun leaves/needles is their generally higher Chl content per leaf area unit (Fig. 3.2A), as also found in the fan-shaped gymnosperm leaves of *Ginkgo* (Sarijeva et al. 2007). The higher  $P_{Nmax}$  rates of sun leaves/needles are also well reflected in the higher values of the Chl-F decrease ratio  $R_{Fd}$  (Fig. 3.10) that represents a non-destructive indicator of the in vivo photosynthetic rates of leaves and is measured from near distance without any direct contact with the leaf (Lichtenthaler and Babani; Lichtenthaler et al. 2000; Sarijeva et al. 2007). Light-saturated rates of photosynthesis on leaf area basis ( $P_{Nmax}$ ) depend not only on photosynthetic biochemistry but also on the mesophyll structure of leaves. Since resistance to CO<sub>2</sub> diffusion from the substomatal cavity to the stroma is substantial, it is likely that the mesophyll structure affects  $P_{Nmax}$  by affecting the diffusion of CO<sub>2</sub> (Terashima et al. 2001) and the penetration of light (Vogelmann and Martin 1993) in the leaf. In addition, the photosynthetic rate per leaf area unit represents the sum of assimilation rates of individual cells; however, the thicker sun leaves contain significantly more cells as compared to the thinner shade leaves (Lichtenthaler 1981; 1984; Pearcy and Sims 1994). Therefore, the  $P_{Nmax}$  rates per unit leaf weight (Fig. 3.5C) reflect the influence of the morphological leaf structure on CO<sub>2</sub> uptake. We found significantly higher  $P_{Nmax}$  per leaf weight unit in shade leaves of *A. pseudoplatanus* and *F. sylvatica* as compared to sun leaves, whereas  $P_{Nmax}$  per leaf weight unit of shade leaves was lower in the highly shade-tolerant species *A. alba* and *T. cordata* as compared to sun leaves (Fig. 3.5C). Kubiske and Pregitzer (1997) concluded that the shade leaves of shade-intolerant species respond to shade primarily by altering SLA, whereas shade-tolerant species respond largely via biochemical acclimation of the photosynthetic apparatus.



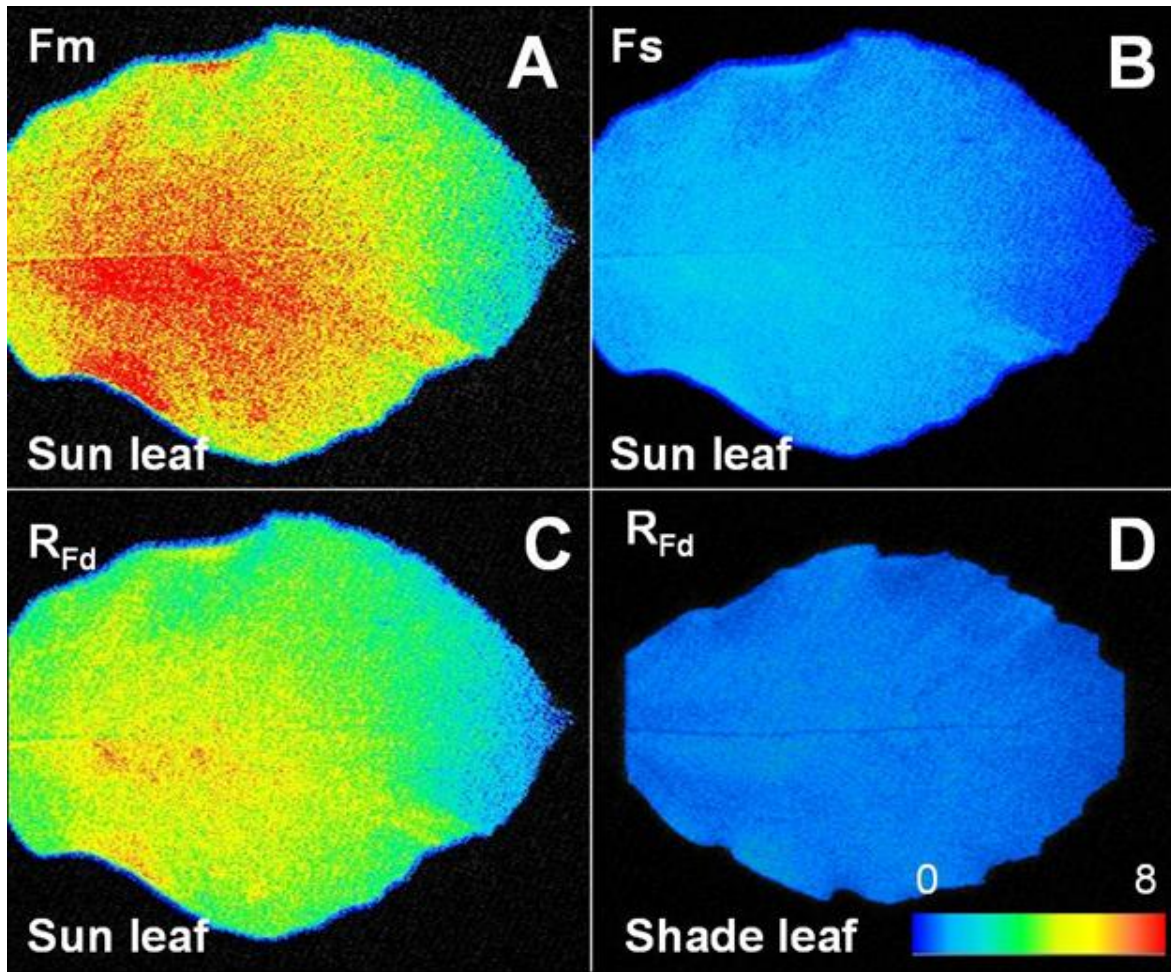


Figure 3.7. A-D. Images of the maximum Chl-F at a saturating light pulse ( $F_m$ ; A), and at steady state Chl-F after 5 min of continuous saturating light ( $F_s$ ; B), and the Chl-F decrease ratio ( $R_{Fd}$ ) in sun (C) and shade leaves (B) of *Fagus sylvatica*. The differences in the relative Chl-F yield of the different leaf parts are indicated by false colors with red for high and blue for low Chl-F. In case of the  $R_{Fd}$  ratio images (C, D) the colors indicate the absolute values of the ratio. See scale in (D).

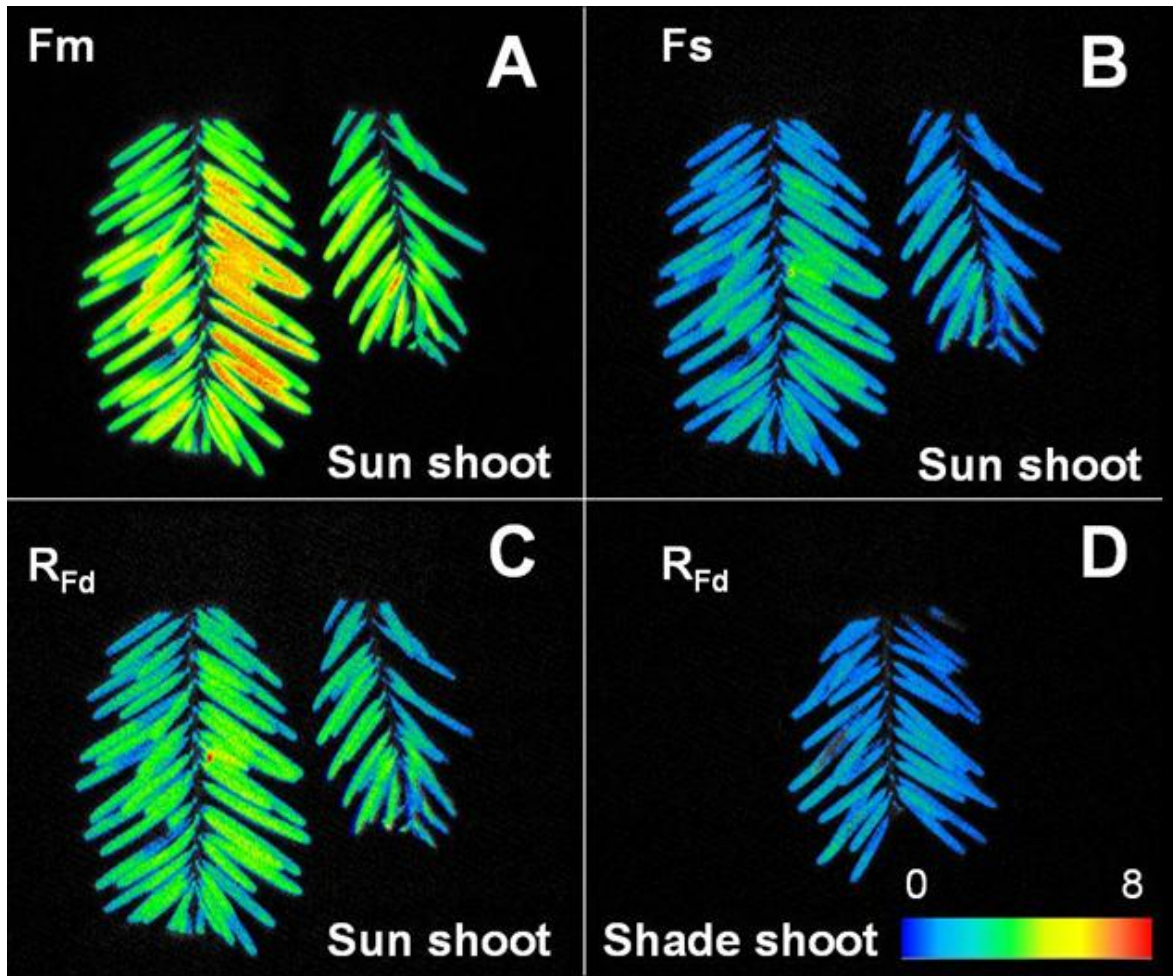
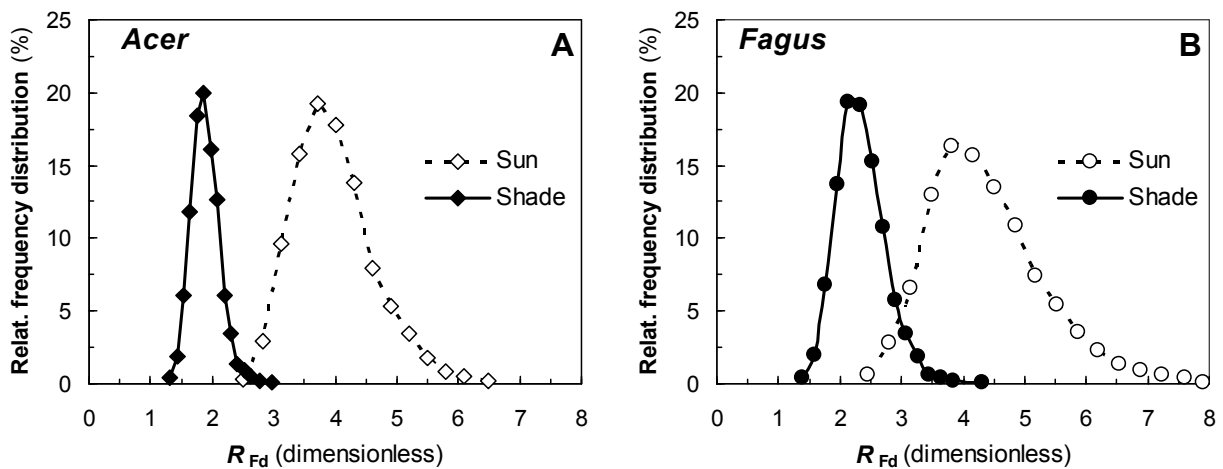


Figure 3.8. A-D. Images of the maximum Chl-F (red band near 690 nm) at a saturating pulse ( $F_M$ ; A), the steady state Chl-F after 5 min of continuous saturating light ( $F_S$ ; B), and the Chl-F decrease ratio ( $R_{Fd}$ ) in first-year sun (C) and shade needles (B) of *Abies alba*. The differences in the relative Chl fluorescence yield of the different needle parts are indicated by false colors with red for high and blue for low Chl-F. The fluorescence images of the  $R_{Fd}$  ratio are given in false colors that state the absolute values of the ratio. See scale in (D).



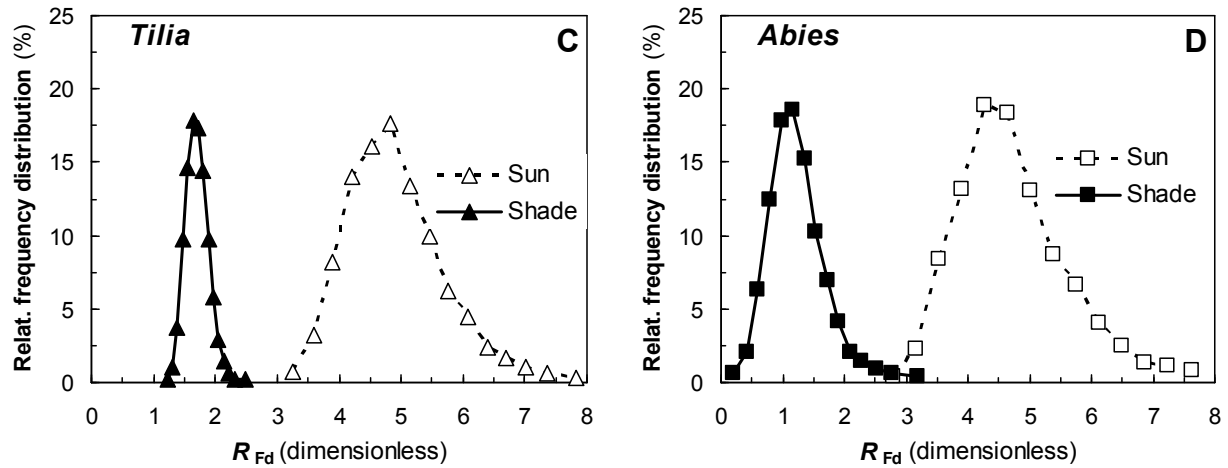


Figure 3.9. A-D. Histograms of the relative frequency distribution of the Chl-F decrease ratio ( $R_{Fd}$ ) measured in sun (empty symbols) and shade leaves and needles (filled symbols) of *Acer pseudoplatanus* (A), *Fagus sylvatica* (B), *Tilia cordata* (C), and *Abies alba* (D). The  $R_{Fd}$  value distributions are based on several ten thousand leaf and needle pixels as indicated in Section 2. The relative frequency is indicated here as percentage, which allows to better compare the results of the four trees, since the absolute pixel numbers were not the same for all leaves.

Sun leaves and sun adapted plants are known to have small stomata, however, a higher stomatal density as compared to shade leaves (Zhang et al. 1995), and this also applies to the leaves of high irradiance in comparison to low irradiance plants (Wild and Wolf, 1980). Hence, higher light saturated stomatal conductance ( $G_{Smax}$ ) is usually found in sun leaves (Fig. 3.6). The much higher stomata opening in sun leaves ( $G_{Smax}$  range 100 up to 300  $\text{mmol m}^{-2} \text{s}^{-1}$ ; in shade leaves clearly below 100  $\text{mmol m}^{-2} \text{s}^{-1}$ ) contributes to the higher intercellular  $\text{CO}_2$  concentrations, and thus to the higher  $\text{CO}_2$  assimilation rates. Moreover, Fig. 3.6 shows that  $P_{Nmax}$  at saturating PPFD linearly correlates with maximum stomatal conductance ( $G_{Smax}$ ). Similar relationships were found for Southern Beech (*Nothofagus cunninghamii*) (Hovenden and Brodribb 2000), African savanna tree species (Midgley et al. 2004) and for temperate grassland species (Urban et al. 2007). The relationship between  $P_{Nmax}$  and  $G_{Smax}$  indicates that stomatal control of  $\text{CO}_2$  uptake at  $G_{Smax}$  is smaller than about 200  $\text{mmol m}^{-2} \text{s}^{-1}$ . However, the response curves level off at high stomatal conductance above 300  $\text{mmol m}^{-2} \text{s}^{-1}$  (Midgley et al. 2004). Non-uniform opening of stomata was observed in leaves of *F. sylvatica* (Kuppers et al. 1999), needles of *A. alba* (Beyschlag et al. 1994) and other plants (reviewed in (Pospíšilová and Šantrůček 1994). The stomatal patchiness is a consequence of the heterogeneous water status in different parts of the leaf and can be induced by all ambient factors causing such heterogeneities (Beyschlag and Eckstein 2001). It leads to a non-uniform distribution of intercellular  $\text{CO}_2$  concentration within the leaf and subsequently to a non-

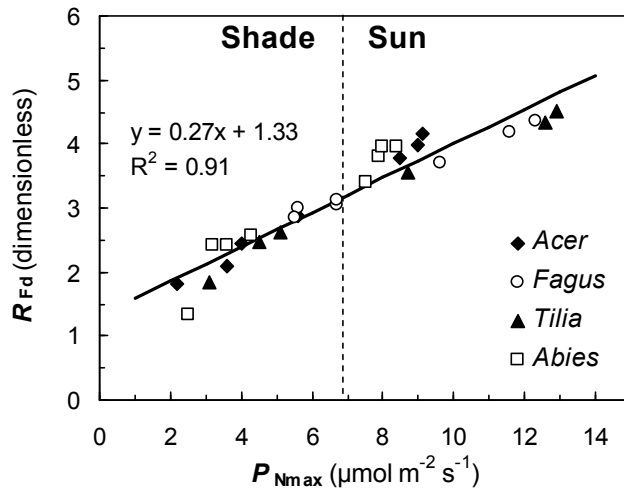


Figure 3.10. Correlation between the red (band near 690 nm) chlorophyll fluorescence decrease ratio ( $R_{Fd}$ ) and the maximum  $CO_2$  assimilation rate ( $P_{Nmax}$ ) at saturating photosynthetic photon flux density ( $PPFD \approx 1500 \mu mol m^{-2} s^{-1}$ ) of sun and shade leaves/needles of *Acer pseudoplatanus*, *Fagus sylvatica*, *Tilia cordata*, and *Abies alba*. All data were fitted using linear regression. The perpendicular broken line was drawn to indicate the values of the sun leaves (upper right part) and the shade leaves (lower left part).

uniform distribution of photosynthetic activity across the whole leaf area. However, the  $P_{Nmax}$  rate estimated via the gas-exchange technique (Fig. 3.6) at the whole leaf level represents the sum of assimilation rates of individual cells. The calculation of some photosynthetic characteristics (e.g. carboxylation efficiency) from such gas-exchange measurements is markedly affected by the patchy distribution of stomatal apertures on the leaf/needle surface (Beyschlag et al. 1994). The close linear correlation between  $P_{Nmax}$  and Chl-F decrease ratio  $R_{Fd}$  at saturating PPFD (Fig. 3.10) proves the usefulness of  $R_{Fd}$  values as indicators of photosynthetic activity. Although the Chl-F is primarily a trait of photosystem II, which in principle also applies to the ratio  $R_{Fd}$ , the latter is a good indicator of the photosynthetic rates, because high  $R_{Fd}$  values are only obtained when not only photosystem II photochemistry works but the whole photosynthetic process including  $CO_2$  fixation. The relationship between  $R_{Fd}$  values and  $CO_2$  assimilation is not only restricted to sun and shade plants but also exists in non-stomatal cryptogamic plants, such as mosses (Tuba et al. 1997). It has been underlined by our observation that at fully closed stomata, when no net  $CO_2$  exchange is measurable between the leaf and the atmosphere, the leaf photosynthetic activity persists, making use of the intercellular leaf  $CO_2$  available from respiratory processes. The ratio  $R_{Fd}$  still exhibited a value of ca. 1.33 indicating photosynthetic quantum conversion. The uneven  $R_{Fd}$  distribution over the leaf (Fig. 3.7C,D) and shoot area (Fig. 3.8C,D) indicates the existence of a considerable variability in photosynthetic activity within sun leaves/needles and also within shade leaves/needles (Fig. 3.9A-D), as defined by significantly lower values of variance ( $p < 0.05$ ) in shade leaves as compared to sun leaves. This had also been observed (Lichtenthaler and Babani 2004; Lichtenthaler et al. 2000) using a different Chl-F imaging method. Although we found gradients in the  $R_{Fd}$  values over the leaf and needle area, we did not detect such small local areas or dots within the leaf or the leaf rim, which were virtually free of

photochemical activity (i.e. very low  $R_{Fd}$  values and no Chl-F induction kinetics), that can show up under stress conditions (Lang et al. 1996). This, as well as the normal  $P_N$  rates, indicated that the leaves investigated were physiologically active and without any recognizable stress constraints. Thus, the Chl-F image technique represents a very useful approach in the study of stomatal and photosynthetic heterogeneity across the leaf area. We observed the distribution of the photosynthetic activity at saturating PPFD to be more uniform in shade leaves (Fig. 3.6C,D) and needles (Fig. 3.7C,D) as compared to sun leaves/needles. These findings support the conclusion of Kupperts et al. (1999) that the presence of stomatal patchiness does not necessarily affect the intercellular  $CO_2$  concentrations in shade and halfshade leaves. The hypothesis explaining the lower gradient of photosynthetic activity in shade leaves is that shade leaves are exposed to a more homogeneous environment during most of their existence, therefore enabling more homogeneous leaf properties.

### 3.5 Conclusions

The results of this investigation show that Chl-F imaging of  $R_{Fd}$  values of leaves, together with the  $R_{Fd}$  frequency distribution (Fig. 3.9), permits an extremely accurate and highly statistically significant differentiation between the higher photosynthetic activity of sun versus shade leaves and needles. This method has also successfully been applied to detect a decrease in photosynthetic activity due to water stress in bean leaves (Lichtenthaler and Babani 2000), and it can be used to find out the effect of other stress constraints on the photosynthetic performance of leaves as well. Chl-F imaging has the great advantage of the detection and location of smaller and larger gradients in photosynthetic quantum conversion across the leaf and needle areas as shown here for sun and shade leaves. Such gradients as well as small local disturbances and/or dots with a full decline of photosynthetic activity, e.g. on the leaf rim or at various isolated points across the leaf area, representing early or very early stress symptoms, can be detected only via Chl-F imaging, which simultaneously screens the physiological information of many ten thousands leaf pixels. Such dots or gradients cannot be detected by the classical  $P_N$  measurements using gas-exchange systems that provide only one integrated value of a larger leaf area, usually of several  $cm^2$ , per measurement. This emphasizes the importance of the new technique of Chl-F imaging for screening differences in the physiological function of the photosynthetic apparatus, not only between leaves and plants of different age and canopy light exposition, but also in the detection of early stress symptoms and long before damage becomes visually evident.

### 3.6 Acknowledgments

The authors wish to thank Mr. Michal Popík for his excellent assistance with the Chl-F imaging system in the Beskydy Mountains and for collecting the appropriate leaf branches of the trees investigated. This project is part of the research supported by grant no. 522/05/P515 (Grant Agency of the Czech Republic), by CzechCarbo project VaV 640/18/03 (Ministry of Environmental Protection), and by the ISBE research intention AV0Z60870520.

### 3.7 References

- Anderson JM, Chow WS, Park YI (1995) The grand design of photosynthesis: Acclimation of the photosynthetic apparatus to environmental cues. *Photosynthesis Research* 46:129-139
- Babani F, Lichtenthaler HK (1996) Light-induced and age-dependent development of chloroplasts in etiolated barley leaves as visualized by determination of photosynthetic pigments, CO<sub>2</sub> assimilation rates and different kinds of chlorophyll fluorescence ratios. *Journal of Plant Physiology* 148:555-566
- Beyschlag W, Eckstein J (2001) Towards a causal analysis of stomatal patchiness: the role of stomatal size variability and hydrological heterogeneity. *Acta Oecologica-International Journal of Ecology* 22:161-173
- Beyschlag W, Kresse F, Ryel RJ, Pfanz H (1994) Stomatal patchiness in conifers-experiments with *Picea abies* (L.) Karst and *Abies alba* Mill. *Trees-Structure and Function* 8:132-138
- Boardman NK (1977) Comparative photosynthesis of sun and shade plants. *Annual Review of Plant Physiology and Plant Molecular Biology* 28:355-377
- Demmig-Adams B (1998) Survey of thermal energy dissipation and pigment composition in sun and shade leaves. In: *Plant cell physiol.*, vol. 39, pp 474-482
- Gilmore DW, Seymour RS, Halteman WA, Greenwood MS (1995) Canopy dynamics and the morphological development of *Abies balsamea*: effects of foliage age on specific leaf area and secondary vascular development. In: *Tree Physiology*, vol. 15, pp 47-55
- Givnish TJ (1988) Adaptation to sun and shade - a whole plant perspective. *Australian Journal of Plant Physiology* 15:63-92

- Herrick JD, Thomas RB (1999) Effects of CO<sub>2</sub> enrichment on the photosynthetic light response of sun and shade leaves of canopy sweetgum trees (*Liquidambar styraciflua*) in a forest ecosystem. *Tree Physiology* 19:779-786
- Hölscher D (2004) Leaf traits and photosynthetic parameters of saplings and adult trees of co-existing species in a temperate broad-leaved forest. *Basic and Applied Ecology* 5:163-172
- Hovenden MJ, Brodribb T (2000) Altitude of origin influences stomatal conductance and therefore maximum assimilation rate in Southern Beech, *Nothofagus cunninghamii*. *Australian Journal of Plant Physiology* 27:451-456
- Kratochvilová I, Janouš D, Marek M, Barták M, Říha L (1989) Production activity of mountain cultivated Norway spruce stands under the impact of air pollution. In: *Ekologia*, vol. 8, pp 407-419
- Kubiske ME, Pregitzer KS (1997) Ecophysiological responses to simulated canopy gaps of two tree species of contrasting shade tolerance in elevated CO<sub>2</sub>. In: *Functional Ecology*, vol. 11, pp 24-32
- Kuppers M, Heiland I, Schneider H, Neugebauer PJ (1999) Light-flecks cause non-uniform stomatal opening - studies with special emphasis on *Fagus sylvatica* L. *Trees-Structure and Function* 14:130-144
- Lang M, Lichtenthaler HK, Sowinska M, Heisel F, Miehe JA (1996) Fluorescence imaging of water and temperature stress in plant leaves. *Journal of Plant Physiology* 148:613-621
- Lange OL, Schulze E-U (1971) Measurement of CO<sub>2</sub> gas exchange and transpiration in the beech (*Fagus sylvatica*, L.), in: H. Ellenberg (Ed.), *Ecological Studies, Analysis and Synthesis*, Vol. 2, Springer, Berlin
- Lichtenthaler HK (1981) Adaptation of leaves and chloroplasts to high quanta fluence rates, in: G. Akoyunoglou (Ed.), *Photosynthesis VI*, Balaban International Science Service, Philadelphia
- Lichtenthaler HK (1984) Differences in morphology and chemical composition of leaves grown at different light intensities and qualities, in: Baker NR, Davies WJ, Ong CK (Eds.), *Control of Leaf Growth*, S.E.B. Seminar Series, vol. 27. Cambridge University Press, Cambridge
- Lichtenthaler HK (1987) Chlorophylls and carotenoids: pigments of photosynthetic biomembranes. In: *Methods in enzymology*, vol. 148, pp 350-382



- Lichtenthaler HK, Babani F (2000) Detection of photosynthetic activity and water stress by imaging the red chlorophyll fluorescence. *Plant Physiology and Biochemistry* 38:889-895
- Lichtenthaler HK, Babani F (2004) Light adaptation and senescence of the photosynthetic apparatus. Changes in pigment composition, chlorophyll fluorescence parameters and photosynthetic activity, in: G.C. Papageorgiou, Govindjee (Eds.), *Chlorophyll Fluorescence: A Signature of Photosynthesis*, Springer, Dordrecht
- Lichtenthaler HK, Buschmann C (2001) Chlorophylls and carotenoids: Measurement and characterisation by UV-VIS, *Current Protocols in Food Analytical Chemistry (CPFA)*, John Wiley, New York
- Lichtenthaler HK, Buschmann C, Doll M, Fietz HJ, Bach T, Kozel U, Meier D, Rahmsdorf U (1981) Photosynthetic activity, chloroplast ultrastructure, and leaf characteristics of high-light and low-light plants and of sun and shade leaves. *Photosynthesis Research* 2:115-141.
- Lichtenthaler HK, Kuhn G, Prenzel U, Meier D (1982) Chlorophyll-protein levels and stacking degree of thylakoids in radish chloroplasts from highlight, low-light and bentazon-treated plants. *Physiologia Plantarum* 56:183-188
- Lichtenthaler HK, Meier D, Buschmann C (1984) Development of chloroplasts at high and low light quanta fluence rates. *Israel Journal of Botany* 33:185-194
- Lichtenthaler HK, Babani F, Langsdorf G, Buschmann C (2000) Measurement of differences in red chlorophyll fluorescence and photosynthetic activity between sun and shade leaves by fluorescence imaging. *Photosynthetica* 38:521-529
- Lichtenthaler HK, Buschmann C, Knapp M (2005) How to correctly determine the different chlorophyll fluorescence parameters and the chlorophyll fluorescence decrease ratio R-Fd of leaves with the PAM fluorometer. *Photosynthetica* 43:379-393
- Marek M, Masarovičová E, Kratochvířová I, Eliáš, P, Janouš D (1989) Stand microclimate and physiological activity of tree leaves in an oak-hornbeam forest. II. Leaf photosynthetic activity. *Trees Structure and Function* 4:234-240.
- Meier D, Lichtenthaler HK (1981) Ultrastructural development of chloroplasts in radish seedlings grown at high and low light conditions and in the presence of the herbicide bentazon. *Protoplasma* 107:195-207
- Midgley GF, Aranibar JN, Mantlana KB, Macko S (2004) Photosynthetic and gas exchange characteristics of dominant woody plants on a moisture gradient in an African savanna. *Global Change Biology* 10:309-317



- Nautiyal PC, Rachaputi NR, Joshi YC (2002) Moisture-deficit-induced changes in leaf-water content, leaf carbon exchange rate and biomass production in groundnut cultivars differing in specific leaf area. *Field Crops Research* 74:67-79
- Nedbal L, Soukupova J, Kaftan D, Whitmarsh J, Trtilek M (2000) Kinetic imaging of chlorophyll fluorescence using modulated light. *Photosynthesis Research* 66:3-12
- Niinemets U (1997) Role of foliar nitrogen in light harvesting and shade tolerance of four temperate deciduous woody species. *Functional Ecology* 11:518-531
- Niinemets U (2001) Global-scale climatic controls of leaf dry mass per area, density, and thickness in trees and shrubs. *Ecology* 82:453-469
- Nobel PS (1976) Photosynthetic rates of sun versus shade leaves of *Hyptis emoryi*. *Plant Physiology* 58:218-223
- Pandey S, Kumar S, Nagar PK (2003) Photosynthetic performance of *Ginkgo biloba* L. grown under high and low irradiance. *Photosynthetica* 41:505-511
- Pearcy RW, Sims DA (1994) Photosynthetic acclimation to changing light environments: scaling from the leaf to the whole plant, in: Caldwell MM, Pearcy RW (Eds.), *Exploitation of Environmental Heterogeneity by Plants*. Academic Press, San Diego, pp. 145-174.
- Pilegaard K, Mikkelsen TN, Beier C, Jensen NO, Ambus P, Ro-Poulsen H (2003) Field measurements of atmosphere-biosphere interactions in a Danish beech forest. *Boreal Environment Research* 8:315-333
- Pospíšilová J, Šantrůček J (1994) Stomatal patchiness. In: *Biologia plantarum*, vol. 36, pp 481-510
- Priwitzer T, Urban O, Šprtová M, Marek MV (1998) Chloroplastic carbon dioxide concentration in Norway spruce (*Picea abies* [L.] Karst.) needles relates to the position within the crown. In: *Photosynthetica*, vol. 35, pp 561-571
- Sarijeva G, Knapp M, Lichtenthater HK (2007) Differences in photosynthetic activity, chlorophyll and carotenoid levels, and in chlorophyll fluorescence parameters in green sun and shade leaves of *Ginkgo* and *Fagus*. *Journal of Plant Physiology* 164:950-955
- Seybold A, Egle K (1937) Lichtfeld und Blattfarbstoffe I, *Planta* 26:491-515.
- Spunda V, Cajanek M, Kalina J, Lachetova I, Sprtova M, Marek MV (1998) Mechanistic differences in utilization of absorbed excitation energy within photosynthetic apparatus of Norway spruce induced by the vertical distribution of photosynthetically active radiation through the tree crown. *Plant Science* 133:155-165

- Sun BN, Dilcher DL, Beerling DJ, Zhang CJ, Yan DF, Kowalski E (2003) Variation in *Ginkgo biloba* L. leaf characters across a climatic gradient in China. Proceedings of the National Academy of Sciences of the United States of America 100:7141-7146
- Tausz M et al. (2004) Photostress, photoprotection, and water soluble antioxidants in the canopies of five Canarian laurel forest tree species during a diurnal course in the field. Flora 199:110-119
- Terashima I, Miyazawa SI, Hanba YT (2001) Why are sun leaves thicker than shade leaves? Consideration based on analyses of CO<sub>2</sub> diffusion in the leaf. Journal of Plant Research 114:93-105
- Thayer SS, Bjorkman O (1990) Leaf Xanthophyll content and composition in sun and shade determined by HPLC. In: Photosynthesis Research, vol. 23, pp 331-343
- Tuba Z, Csintalan Z, Badacsonyi A, Proctor MCF (1997) Chlorophyll fluorescence as an exploratory tool for ecophysiological studies on mosses and other small poikilohydric plants. Journal of Bryology 19:401-407
- Úřadníček L, Maděra P, Kolibáčová S, Koblížek J, Šefl J (2001) Woody Species in the Czech Republic, Matice Lesnická, Písek.
- Urban O et al. (2007) Temperature dependences of carbon assimilation processes in four dominant species from mountain grassland ecosystem. Photosynthetica 45:392-399
- Vogelmann TC, Martin G (1993) The functional significance of palisade tissue: penetration of directional versus diffuse light. In: Plant, Cell and Environment, vol. 16, pp 65-72
- Wild A, Wolf G (1980) The effect of light intensities on the frequency and size of stomata and on the number, size and the control of chloroplasts in the mesophyll and guard cells during the development of the primary leaves of *Sinapis alba*, Z. Pflanzenphysik 97:325-342.
- Wild A, Hopfner M, Ruhle W, Richter M (1986) Changes in the stoichiometry of photosystem II components as an adaptive response to high-light and low-light conditions during growth. Zeitschrift Fur Naturforschung C-a Journal of Biosciences 41:597-603
- Willstätter R, Stoll A (1913) Untersuchungen über Chlorophyll, Springer, Berlin.
- Zhang HH, Sharifi MR, Nobel PS (1995) Photosynthetic characteristics of sun versus shade plants of *Encelia farinosa* as affected by photosynthetic photon flux density, intercellular CO<sub>2</sub> concentration, leaf water potential, and leaf temperature. In: Aust J Plant Physiol, vol. 22, pp 833-841

## CHAPTER 4

### Near distance imaging spectroscopy investigating chlorophyll fluorescence and photosynthetic activity of grassland in the daily course

*Alexander Ac<sup>1,2</sup>, Zbyněk Malenovsky<sup>3</sup>, Jan Hanuš<sup>1</sup>, Ivana Tomášková<sup>1</sup>, Otmar Urban<sup>1</sup> and Michal V. Marek<sup>1,4</sup>*

<sup>1</sup>Laboratory of Plants Ecological Physiology, Division of Ecosystem Processes, Institute of Systems Biology and Ecology, Poříčí 3b, CZ-60300 Brno, Czech Republic

<sup>2</sup>Agricultural Faculty, University of South Bohemia, Studentská 13, CZ-370 05 České Budějovice, Czech Republic

<sup>3</sup>Remote Sensing Laboratories, Department of Geography, University of Zürich, Winterthurerstrasse 190, CH-8057 Zürich, Switzerland

<sup>4</sup>Mendel University, Zemědělská 1, CZ-613 00 Brno, Czech Republic

*Accepted to *Functional Plant Biology**

## Abstract

Detection of grassland canopy chlorophyll fluorescence (Chl-F), conducted with an imaging spectroradiometer, provided solid evidence of potential remote sensing estimation of steady-state Chl-F ( $F_S$ ). Daily near-nadir views of extremely high spatial resolution hyperspectral images were acquired from a distance of 4 meters at a temperate montane grassland in the Czech Republic. Simultaneously, the ground single leaf measurements of Chl-F and total chlorophyll content (Chl  $a+b$ ) were collected. A specifically designed “shade removal” experiment revealed the influence of dynamic plant physiological processes on hyperspectral reflectance of three wavelengths: 532, 686, and 740 nm. Based in this information the vegetation indexes  $R_{686}/R_{630}$ ,  $R_{740}/R_{800}$  and PRI calculated as  $(R_{532}-R_{570})/(R_{532}+R_{570})$  were tested for statistical significance with directly measured Chl-F parameters (maximum fluorescence yield –  $F_V/F_M$ , steady-state chlorophyll fluorescence –  $F_S$ , and actual quantum yield –  $\Phi_{II}$ ). The grassland species under investigation were: *Festuca rubra* agg. (L.), *Hieracium* sp., *Plantago* sp., *Nardus stricta* (L.), and *Jacea pseudophrygia* (C.A. MEYER). The coefficients of determination ( $R^2$ ) for best-fit relationships between PRI- $\Phi_{II}$  and PRI- $F_S$ , measured in the daily course, show quite a high variability of 0.23-0.78 and 0.20-0.65, respectively.  $R^2$  for the  $R_{686}/R_{630}$ - $\Phi_{II}$  and  $R_{686}/R_{630}$ - $F_S$  relationships varied between 0.20-0.73 and 0.41-0.70, respectively. The highest average  $R^2$  values were found between PRI and Chl  $a+b$  (0.63) and  $R_{686}/R_{630}$  and Chl  $a+b$  (0.72). The ratio  $R_{740}/R_{800}$  did not yield a statistically significant result.

**Keywords:** Chlorophyll fluorescence, vegetation indexes, hyperspectral remote sensing, actual fluorescence yield, grassland ecosystem

## 4.1 Introduction

One of the most fundamental key players in ongoing global climate change (IPCC, 2007) is the global productivity of the terrestrial ecosystem (Running *et al.* 1999). Recent evidence suggests decreasing carbon sink capacity of the biosphere at a local to global scale (Canadell *et al.* 2007). For these reasons, the remote sensing scientific community reinforced their efforts to capture spatial and temporal dynamics in photosynthetic processes of the terrestrial vegetation and, consequently, in the carbon-cycling, using air- and space-borne image data (e.g. Grace *et al.* 2007). For example, the remotely sensed estimation of the Light Use Efficiency (LUE, calculated as CO<sub>2</sub> assimilation rate per incident photosynthetic photon flux density), regarded as an important parameter for the estimation of global carbon assimilation (Monteith 1977), is expected to greatly improve the accuracy of the global productivity estimation (Ahl *et al.* 2004; Turner *et al.* 2003).

The significant relations between remotely measured reflectance signals and rapid physiological processes in plants have been found at spectral regions of three wavelengths: 530, 690, and 740 (Gamon *et al.* 1990; Zarco-Tejada *et al.* 2000a; 2000b). The reflectance changes in the region around 531 nm were attributed to the photo-protective reaction forming the zeaxanthin pigment and affecting the LUE (Gamon *et al.* 1992), but lately also to the chlorophyll fluorescence (Chl-F) parameters, such as Non-Photochemical Quenching (NPQ) and actual quantum yield ( $\Phi_{II}$ ) of PSII (Evain *et al.* 2004). The reflectance changes at the wavelengths of 690 nm and 740 nm were related mainly to Chl-F emissions originating from PSII (Buschmann *et al.* 2000; Zarco-Tejada *et al.* 2000a).

The changes in zeaxanthin concentration were related to the reflectance intensity at 531 nm by means of the physiological (also referred to as plant or photochemical) reflectance index (PRI), calculated as  $(R_{531}-R_{REF})/(R_{531}+R_{REF})$ , where  $R_{REF}$  is the reflectance at 570 or 550 nm (Gamon *et al.* 1992; Gamon and Surfus 1999). The use of this vegetation index has been verified by strong leaf level experimental evidence. It is possible to estimate the vegetation LUE from spectrometric leaf and to some extent also from canopy measurements in daily and seasonal courses, when applied to several plant species growing in various environmental conditions (Grace *et al.* 2007; Suarez *et al.* 2008). Nevertheless, as shown in scenarios modeled by Barton and North (2001) for canopy level radiative transfer models and in further experimental studies (Filella *et al.* 2004), the application of remotely sensed PRI as an actual measure of photosynthesis or LUE (Drolet *et al.* 2005; Rahman *et al.* 2004) is far from being operational due to high sensitivity to the non-physiological factors and features commonly

associated with the remote sensing acquisitions (e.g. angular anisotropy of the vegetation canopy reflectance, sun-target-sensor geometry, spectral mixing with a non-photosynthetic biomass, atmospheric effects, etc.). Lately, it has been shown as well that PRI is a robust proxy of LUE only when photochemical and carbon assimilation efficiency of PSII are well co-ordinated (Guo and Trotter 2004; 2006; Inoue and Penuelas 2006).

Numerous studies provided evidence for a possible detection of the Chl-F signal at 690 and 740 nm wavelengths from the leaf (e.g. Buschmann et al. 1994) as well as at canopy reflectance measurements (Dobrowski et al. 2005; Gamon and Surfus 1999; Zarco-Tejada et al. 2000a; 2000b; 2002; 2003). For instance, the ratio of reflectance at 690 nm and at 630 nm ( $R_{690}/R_{630}$ ), designed to track changes in steady-state Chl-F ( $F_S$ ), was identified as a useful indicator of early stress reactions of plants (Zarco-Tejada et al. 2000b). Similarly, the vegetation indexes (VIs), such as  $R_{695}/R_{420}$  and  $R_{695}/R_{760}$  have been found to be statistically linked to early vegetation stress (Carter 1994), however, without any causal physiological explanation for these relations. Recently, a small canopy experiment described by Dobrowski et al. (2005) investigated a non-invasive detection of early heat-stress reactions of plants. It revealed a statistically significant correlation between  $F_S$  and VIs  $R_{740}/R_{800}$  and  $R_{690}/R_{600}$ , whereas a correlation of low significance was found in the case of PRI.

It has been suggested that the  $F_S$  signal is capable of tracking changes in the photosynthesis performance induced by actual heat and water stress influences (Dobrowski et al. 2005; Flexas et al. 2000; 2002; Freedman et al. 2002). A recent seasonal study by Soukupova et al. (2008) showed that  $F_S$  can potentially be an accurate indicator of the beginning and end of a photosynthetically active period of overwintering temperate plants. Further, Moya et al. (2004) found that relative Chl-F yield measured passively at 760 nm by Fraunhofer Line Discriminator Principle method might be an useful indicator of stress in maize plants. Still, the plant physiologists consider  $F_S$  as being rather a general non-specific signal integrating information on several photosynthetic processes (Papageorgiou GC 2004).

The 'process-related' remote sensing techniques focuses on monitoring physiological plant processes using aircraft and/or satellite sensors. Several airborne/ground experimental campaigns, e.g., the European Space Agency SEN2FLEX campaign in 2005, have been aiming their estimation of LUE and  $F_S$  at vegetation reflectance (Grace et al. 2007; Zarco-Tejada et al. 2000b). In spite of this, canopy measurements carried out in the daily course at very high spatial resolution are necessary to reveal the complexity of the  $F_S$  signal detection under the natural environmental conditions. In this respect, the performance of VIs proposed for remote estimation of LUE (i.e., PRI) and  $F_S$  (i.e.,  $R_{686}/R_{REF}$  and  $R_{740}/R_{800}$ ) is also of

interest. Thus the first objective of this study was to investigate the relationships between Chl-F and reflectance signals of vegetation measured at the level of single leaves. Within the second objective we attempted the detection of a natural grassland sun-induced Chl-F signal using a commonly available imaging spectroradiometer. Finally, in daily course performance we compared selected vegetation indexes proposed for the quantification of photosynthesis related processes.

## 4.2 Materials and Methods

### 4.2.1 Study site description

The study site of the natural montane grassland is located at the permanent experimental study site Bílý Kříž (Beskydy Mts., the Czech Republic, 18.54°E, 49.49°N, 898 m a.s.l.). The experimental plot is characterized by a cool (annual mean temperature of 5.5°C) and humid (annual mean relative air humidity of about 80%) climate, with an annual precipitation of about 1000 – 1400 mm. The leaf area index of the grass canopy, as measured by the Plant Canopy Analyser (LAI-2000, Li-Cor, Lincoln, NE USA) in 2006, was equal to  $3.5 \pm 0.5$  m<sup>2</sup> m<sup>-2</sup> (mean  $\pm$  standard deviation). Plant species richness of the present *Nardo-Callunetea* association (class *Nardo-Agrostion tenuis*) accounted for about 25 herbaceous species. The most abundant herbaceous species recorded at the experimental plot were: *Festuca rubra* agg. (L.), *Hieracium* sp., *Plantago* sp., *Nardus stricta* (L.), and *Jacea pseudophrygia* (C.A. Meyer). Further details about dominant plant species of the experimental grassland are available in Urban et al. (2007).

### 4.2.2 Measurement of leaf chlorophyll fluorescence

During the field campaigns twenty intact leaves of *Jacea pseudophrygia*, *Festuca rubra* agg., *Hieracium* sp., *Plantago lanceolata* (L.), and *Alchemilla mollis* (L.) in different states of seasonal ontogeny were measured by the pulse modulation fluorometer (PAM-2000, H. Walz, Effeltrich, Germany). Those leaves were marked with white flags for a later identification on hyperspectral images obtained across the experimental plot. Prior to sunrise, the maximal Chl-F yield (i.e.,  $F_V/F_M$ ) of these leaves adapted over night for dark was measured. The Chl-F signal, integrated from an area of ca. 80 mm<sup>2</sup> in the center of each leaf fixed in a leaf-clip was

measured at an irradiance level above  $400 \mu\text{mol m}^{-2} \text{s}^{-1}$ . Saturating pulses of above  $1200 \mu\text{mol m}^{-2} \text{s}^{-1}$  were used to calculate the fluorescence quantum yield ( $\Phi_{\text{II}}$ ). The maximal Chl-F yield, quantifying the highest efficiency of photon capture by open reaction centers (Kitajima and Butler 1975), was calculated as  $(F_M - F_0)/F_M$  where  $F_M$  is the maximal Chl-F of a dark adapted leaf with fully closed reaction centers and  $F_0$  is the minimal Chl-F of a dark adapted leaf with fully open reaction centers. Subsequently, the actual  $\Phi_{\text{II}}$ , denoting the actual efficiency of the PSII photon capture at an actual irradiance level, was calculated as  $(F_M' - F_S)/F_M'$  (Genty et al. 1989), where  $F_M'$  represents maximum Chl-F and  $F_S$  is the steady-state Chl-F of a light adapted leaf. Daily courses of Chl-F parameters were measured at 7:00, 12:30 and 15:00 on July 4<sup>th</sup>, and at a one-hour interval between 8:00 and 16:00 on July 19<sup>th</sup>, 2006. The total chlorophyll content ( $\text{Chl}_{a+b}$ ) of intact leaves was measured during both days with a chlorophyllmeter (SPAD-502, Konica Minolta Sensing, Osaka, Japan) calibrated previously in laboratory to deliver  $\text{Chl}_{a+b}$  *per leaf area* measurements.

#### 4.2.3 Ground-based imaging spectroscopy

Daily near-nadir views of hyperspectral images, covering the experimental plot area of about  $1.5 \times 4.0$  m, were acquired from a distance of 4 m above canopy using a visible and near-infrared Airborne Imaging Spectroradiometer for Applications (AISA-Eagle Specim, Oulu, Finland) (see Fig. 4.1).

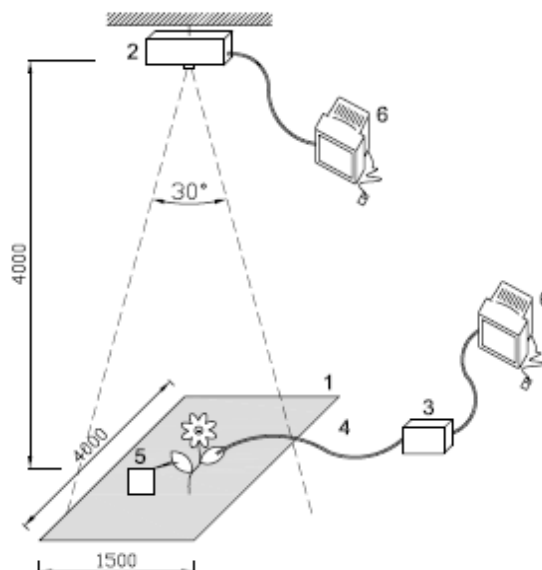




Figure 4.1. Experimental set-up of daily hyperspectral measurements performed with the visible and near-infrared AISA Eagle imaging spectroradiometer. The extent of the experimental plot was approximately 1.5 x 4.0 m; a black blanket was covering part of the experimental grassland plot (referred to as “mantled plot” in the text). Legend: 1 – extent of sensed experimental plot; 2 – AISA hyperspectral sensor head, 3 – PAM Chlorophyll Fluorometer; 4 – PAM optical cable with a leaf clip; 5 – SPAD Chlorophyllmeter, 6 – AISA Eagle acquisition unit.

Images of 260 spectral bands between 400-940 nm with full-width-half-maximum of 2.2 nm were recorded at a pixel-size of about 2 mm on July 4<sup>th</sup> at 7:00, 12:30, and 15:30 and on July 19<sup>th</sup> in 1-hour intervals from 10:00 to 16:00 local time. The leaf Chl-F measurements were performed simultaneously with each image acquisition.

The acquired hyperspectral images were converted into radiance values using sensor specific calibration files. Subsequently, radiance images were transformed into at-sensor reflectance data via vicarious empirical line calibration, using five near-Lambertian calibration panels of known flat reflectance signatures. An automatically supervised Maximum Likelihood classification (Lillesand and Kiefer, 2000) was applied to distinguish the sun-lit and shaded grass pixels. Finally, an appropriate threshold filter was applied on the images of green Normalized Difference Vegetation Index ( $\text{green NDVI} = (R_{554} - R_{677}) / (R_{554} + R_{677})$ ) (modified according to Smith et al. 1995) to separate the photosynthetically active (green) leaves from a dry litter. Only image pixels of sun-lit green vegetation were used in the subsequent analysis. The processing of hyperspectral images was carried out using special software (ENVI, Research Systems Inc., Boulder, CO USA).

#### 4.2.3.1 Leaf and canopy observational levels

The hyperspectral image processing was carried out at two observational levels: i) *leaf*, and ii) *canopy*. In our study the *leaf* level experiments were performed on a reflectance integrated from 8-20 pixels of the ground monitored leaves. VIs of these leaves computed per pixel were averaged and correlated to the PAM-2000 leaf Chl-F and SPAD-502 chlorophyll content measurements. At the *canopy* level, experiments refer to an average of more than 400 000 sun-lit green vegetation pixels classified within the acquired hyperspectral images. VIs of these pixels computed per image were averaged and correlated to the averaged Chl-F of all monitored ground leaves ( $n = 20$ ), located on hyperspectral images.

#### 4.2.3.2 “Shade-removal” experiment

In order to create an artificially dark-adapted grass canopy, part of the experimental plot (subplot of 0.5 x 4 m referred to as *mantled plot* in the text) was covered by a black non-transparent blanket for 30 min prior to each spectral measurement. The way of darkening enabled a lateral air convection, which prevented the changes being induced by a higher than ambient air temperature. The second part of the experimental plot, i.e., the *control plot*, was exposed to a natural daily radiation regime. Three subsequent AISA Eagle images of both plots were always acquired at the 5<sup>th</sup>, 90<sup>th</sup>, and 200<sup>th</sup> second after blanket removal. The subtraction of successive reflectance scans of the mantled plot after blanket removal was expected to detect reflectance differences of sun-lit photosynthetically active grassland pixels. The Savitzky-Golay method (Savitzky and Golay, 1964) was applied to filter noise out of the reflectance difference ( $\Delta R$ ) spectra.

#### 4.2.3.3 Optical vegetation indexes

Based on the results of the shade-removal experiment that revealed a dynamic response of vegetation reflectance at three wavelength regions (see Fig. 4.2A,B and Tab. 4.1), a performance of three photosynthetic process related optical vegetation indexes (VIs) was proposed to be tested. These VIs (i.e., PRI,  $R_{686}/R_{630}$  and  $R_{740}/R_{800}$ ) were derived from the AISA Eagle reflectance x;images. No other VIs (e.g., VIs for chlorophyll content estimation) were included.

#### 4.2.4 Statistical analysis

A curve-fitting software (TableCurve 2D, SYSTAT Inc., Evanston, IL USA) was used to find the best fitting regression relationship between variables tested. The significance of each statistical model was tested at three probability levels:  $p < 0.01$  (\*),  $p < 0.001$  (\*\*) and  $< 0.0001$  (\*\*\*), using the analysis of variance (ANOVA). The determination coefficient ( $R^2$ ) was computed to express the variation percentage of a dependent variable explained by an established regression to the independent variable. The statistical tests were conducted in statistical software (Statistica 7.0, StatSoft Inc., Tulsa, OK USA).

### 4.3 Results

## 4.3.1 Chlorophyll fluorescence detection from image data

The apparent fluorescence emission with peaks at 532, 686 and 740 nm was observed from a reflectance intensity acquired from the mantled plot, measured at the 5<sup>th</sup> and 90<sup>th</sup> s after uncovering (Fig. 4.2A, grey dots). In contrast to this result, the reflectance subtraction of the same image pixels acquired at the 90<sup>th</sup> and 200<sup>th</sup> s after uncovering did no longer reveal any significant reflectance changes (Fig. 4.2A, black dots). The daily course of  $\Delta R$  with peaks at 532 and 740 nm appeared to be less distinct than the daily course of Chl-F at 686 nm (Fig. 4.2B). Specifically spectral features associated with a xanthophyll pigment transformation ranged from 490 to 570 nm (Fig. 4.2B). Nevertheless, in the daily course that peak was less pronounced during the morning and afternoon.  $\Delta R$  for wavelengths greater than 700 nm appeared to vary more as a result of radiometric corrections per image combined with high vegetation absorption (Fig. 4.2B).

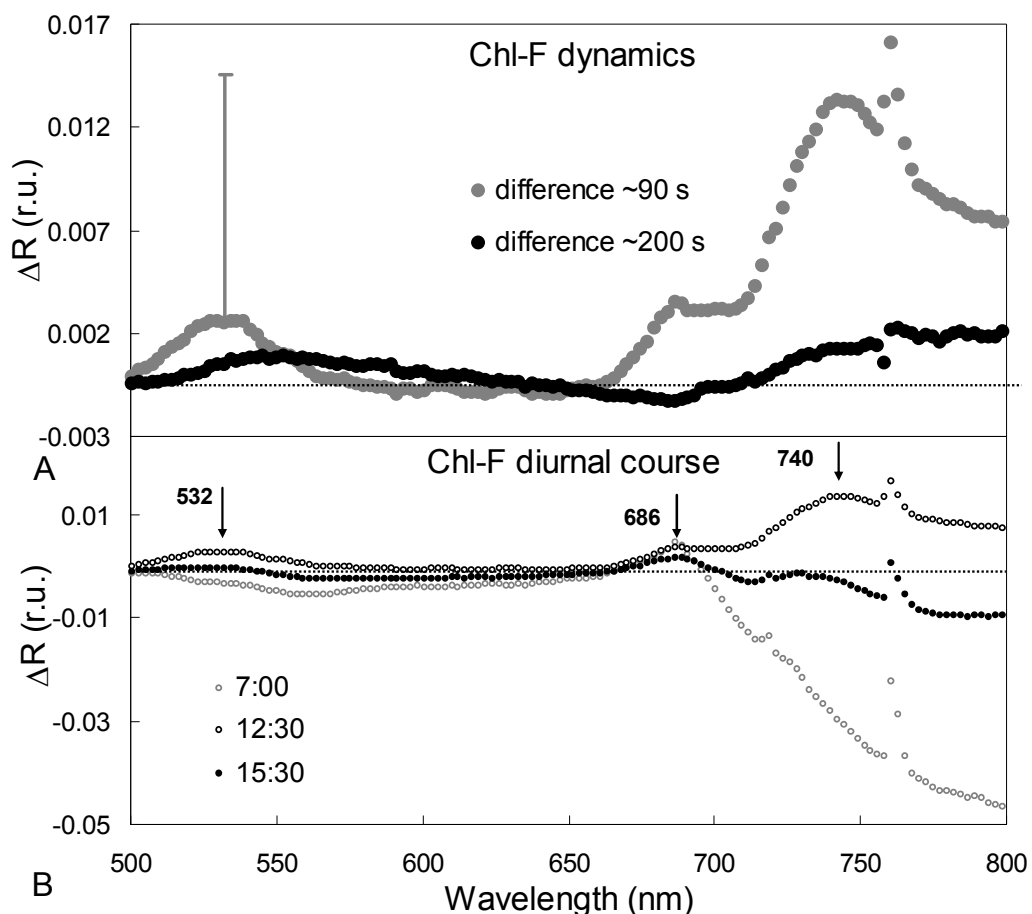


Figure 4.2. Reflectance difference ( $\Delta R$ ) spectra observed when subtracting the reflectance of green sun exposed pixels of the mantled plot acquired at the 5<sup>th</sup> and 90<sup>th</sup> s (●) and at the 90<sup>th</sup> and 200<sup>th</sup> s (●) after removal of a non-transparent blanket inducing the dark-adapted state of the canopy within 480-800 nm (A) intervals; vertical lines indicate SD ( $n > 400,000$ ). The results of July 4<sup>th</sup> are presented; nevertheless, similar results were also obtained on July 19<sup>th</sup>. The intensity of zeaxanthin and

chlorophyll fluorescence signals (numbers indicate peak wavelengths) in the daily course acquired on July 4<sup>th</sup> is indicated (B).

### 4.3.2 Interpretation of hyperspectral images at leaf level

Process-related VIs were correlated in the daily course with selected biochemical and physiological leaf parameters (Fig. 4.3A–C). The regression analysis showed best fits (quantified by  $R^2$ ) for PRI and  $R_{686}/R_{630}$  VIs. No significant relationships were observed in the case of  $R_{740}/R_{800}$  with any of the examined parameters. The highest daily average  $R^2$  values were found between ratio  $R_{686}/R_{630}$  and the total chlorophyll content (Chl  $a+b$ ) and a potential quantum yield of Chl-F ( $F_V/F_M$ ), lower for  $F_S$ , and lowest for the actual quantum yield of Chl-F ( $\Phi_{II}$ ) (Fig. 4.3A–C).

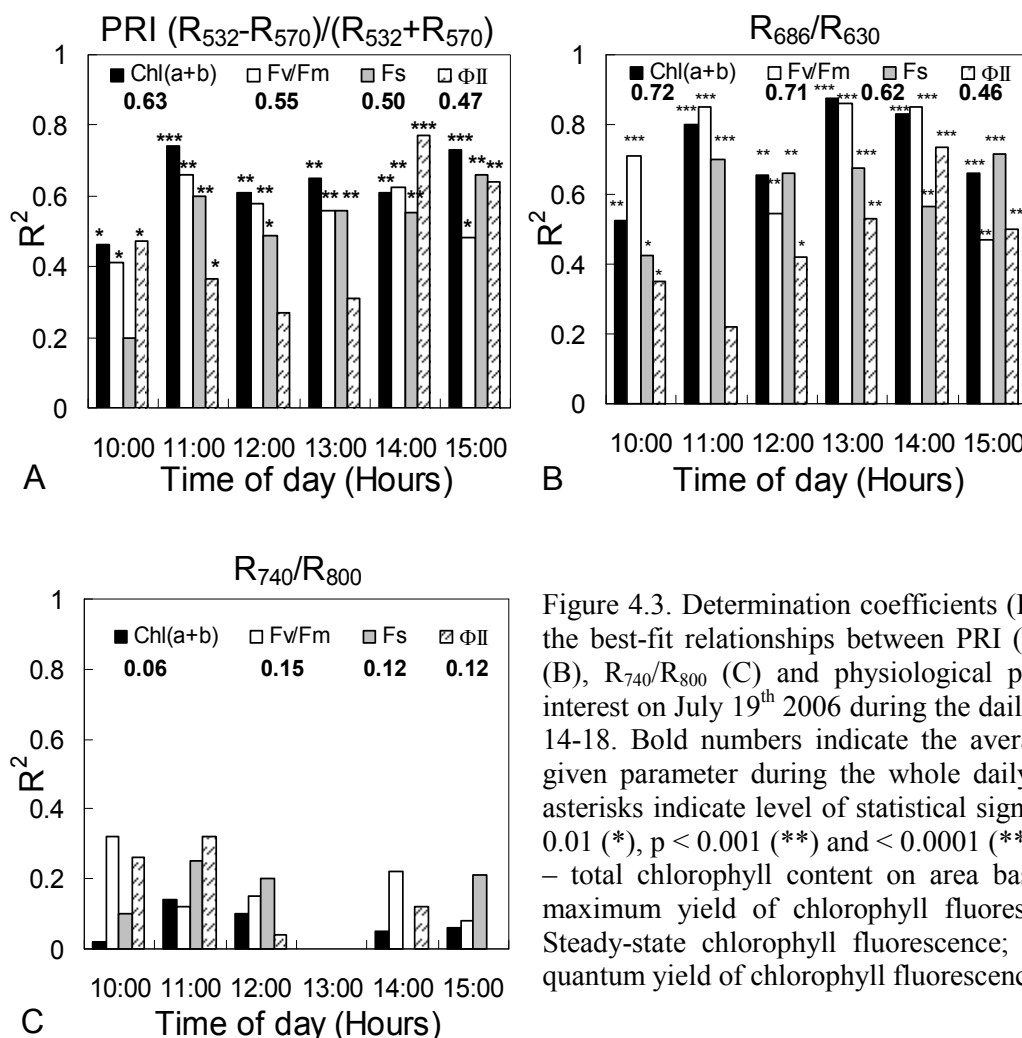
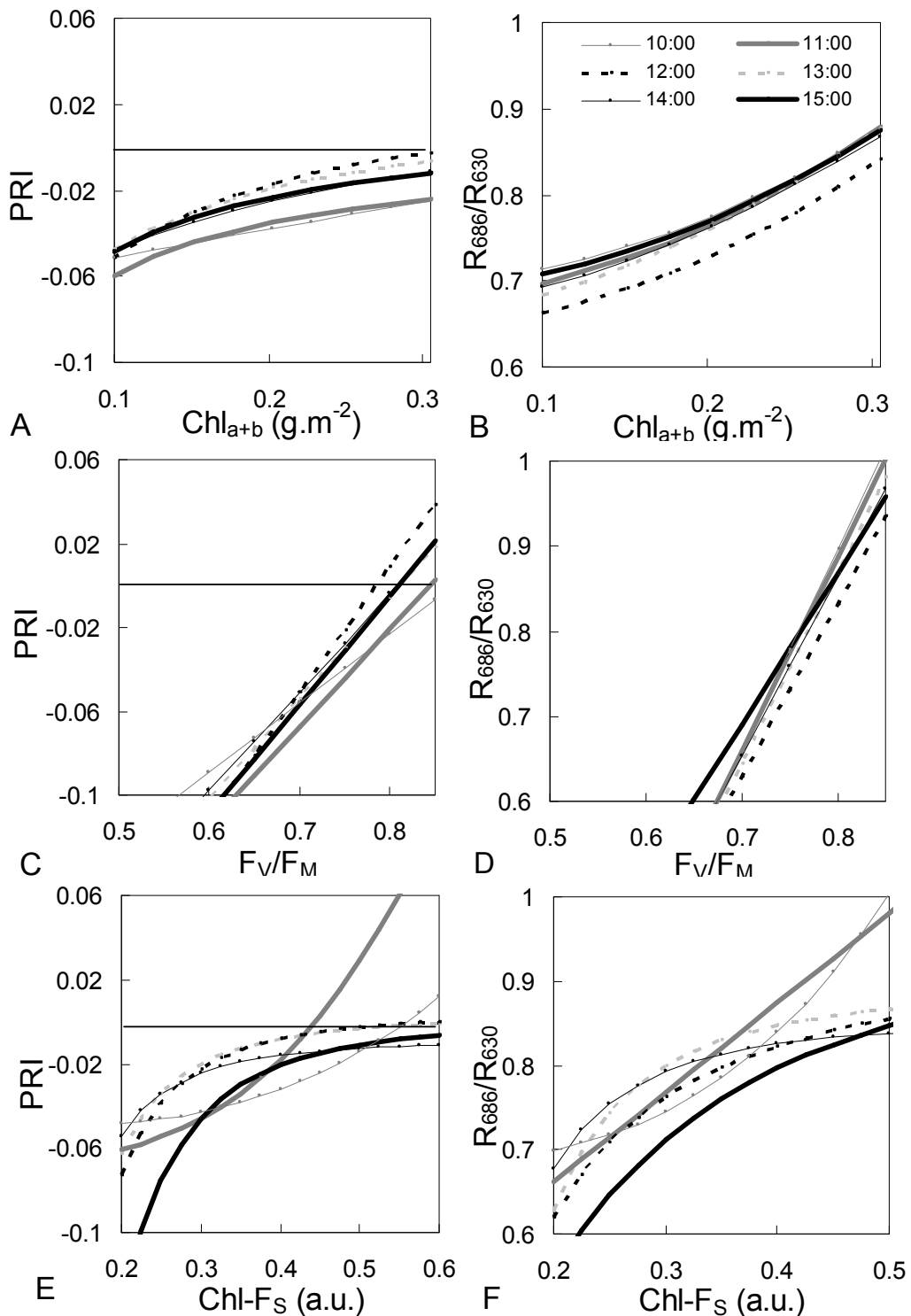


Figure 4.3. Determination coefficients ( $R^2$ ) found for the best-fit relationships between PRI (A),  $R_{686}/R_{630}$  (B),  $R_{740}/R_{800}$  (C) and physiological parameters of interest on July 19<sup>th</sup> 2006 during the daily course,  $n = 14-18$ . Bold numbers indicate the average  $R^2$  for a given parameter during the whole daily course and asterisks indicate level of statistical significance:  $p < 0.01$  (\*),  $p < 0.001$  (\*\*) and  $< 0.0001$  (\*\*\*). (Chl  $a+b$  – total chlorophyll content on area basis;  $F_V/F_M$  – maximum yield of chlorophyll fluorescence;  $F_S$  – Steady-state chlorophyll fluorescence;  $\Phi_{II}$  – actual quantum yield of chlorophyll fluorescence.)

In the daily course PRI was significantly correlated with Chl  $a+b$  (daily average  $R^2 = 0.63$ ; logarithmic function) except at 10:00 (linear function) (Fig. 4.4A; Table 1.). The exponential

relationships plotted between  $R_{686}/R_{630}$  and Chl  $a+b$  were more consistent and stable compared to PRI. The relation between  $R_{686}/R_{630}$  and Chl  $a+b$  showed the lowest daily values at 12:00 (Fig. 4.4B). In the case of  $F_V/F_M$ , both indexes showed best fits via linear regressions (Figs. 4.4C,D; Table 1.). The relationship between  $F_S$  and PRI was exponential at 10:00 and 11:00, and logarithmic for the rest of the day (Fig. 4.4E, Table 1.). Similar relationships were found also between Chl- $F_S$  and  $R_{686}/R_{630}$ , except at 10:00 the function was linear (Fig. 4.4F). Relationships with the actual quantum yield of Chl-F ( $\Phi_{II}$ ) were all found to be linear or logarithmic, with the lowest  $\Phi_{II}$  values at 12:00 (Figs. 4.4G,H; Table 1.).



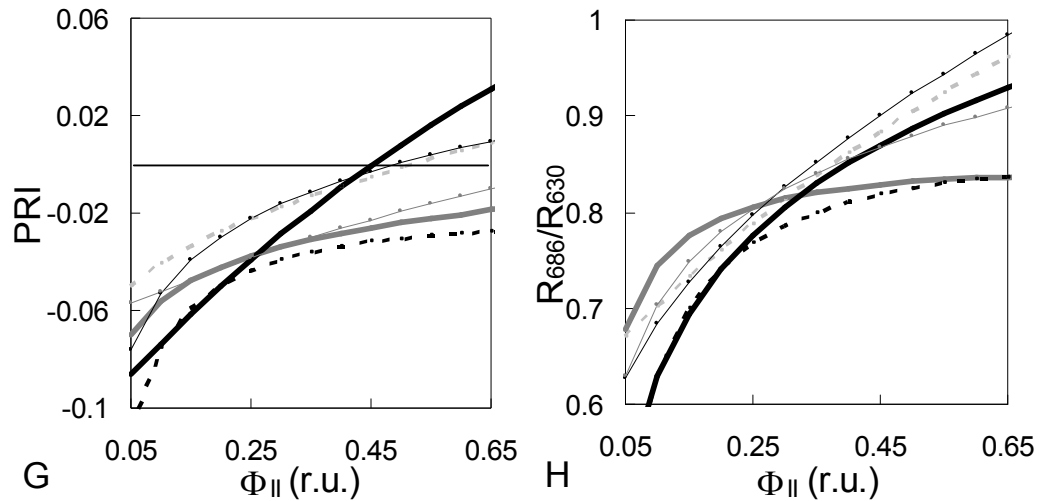


Figure 4.4. Best fit regressions between the physiological parameters [total chlorophyll content ( $Chl\ a+b$ ), maximum yield of chlorophyll fluorescence ( $F_v/F_M$ ), steady-state chlorophyll fluorescence ( $F_s$ ) and actual quantum yield of chlorophyll fluorescence ( $\Phi_{II}$ )] and vegetation indexes (PRI and  $R_{686}/R_{630}$ ) (A–H). The numbers indicate local time of the fit during the daily course. The respective determination coefficients ( $R^2$ ) of the regressions are summarized in figure 3.  $N = 14-18$ . See Table 1 for best fit equations.

<b>Photochemical Reflectance Index (y)</b>				
<b>Hours</b>	<b>Chl <math>a+b</math> (x)</b>	<b><math>F_v/F_M</math> (x)</b>	<b>Chl-<math>F_s</math> (x)</b>	<b><math>\Phi_{II}</math> (x)</b>
10:00	$-0.07+0.001*x$	$-0.29+0.33*x$	$-0.05+0.29*x^3$	$0.047-0.1096*\exp(-x)$
11:00	$-0.005-4.87/x^{1.5}$	$-0.39+0.47*x$	$-0.07+0.76*x^3$	$-0.01+0.02*\ln(x)$
12:00	$0.02-6.7/x^{1.5}$	$-0.47+0.6*x$	$0.0025+0.0019*\ln(x)/x^2$	$-0.026-0.009*\ln(x)^2$
13:00	$0.01-5.6/x^{1.5}$	$-0.39+0.48*x$	$0.001+0.0016*\ln(x)/x^2$	$-0.073+0.101*x^{0.5}$
14:00	$0.07-0.57/x^{1.5}$	$-0.38+0.47*x$	$0.0096+0.0011*\ln(x)/x^2$	$0.024+0.0335*\ln(x)$
15:00	$0.007-5.0/x^{1.5}$	$-0.42+0.52*x$	$-0.0016+0.0033*\ln(x)/x^2$	$0.174-0.273*\exp(-x)$
<b>Ratio <math>R_{686}/R_{630}</math> (y)</b>				
10:00	$0.68+x^{2.5}$	$0.26-0.15/\ln(x)$	$(0.83+1.42*x^3)^2$	$0.955+0.109*\ln(x)$
11:00	$0.66+x^{2.5}$	$-0.94+2.29*x$	$y = 0.45+1.06*x$	$0.84-0.018*\ln(x)^2$
12:00	$0.62+x^{2.5}$	$-0.8+2.04*x$	$0.9+0.0354*\ln(x)/x$	$0.844-0.04*\ln(x)^2$
13:00	$0.4+x^{2.5}$	$-0.93+2.25*x$	$0.884+0.0064*\ln(x)/x^2$	$-1.315-0.677*\exp(-x)$
14:00	$0.42+x^{2.5}$	$-0.82+2.1*x$	$0.85+0.0043*\ln(x)/x^2$	$0.491+0.611*x^{0.5}$
15:00	$0.67+x^{2.5}$	$-0.56+1.78*x$	$0.914-0.14*\ln(x)^2$	$0.998+0.16*\ln(x)$

Table 4.1 Best-fit regressions between vegetation indexes and tested physiological parameters. Legend: Total chlorophyll content – Chl  $a+b$ , Potential yield of chlorophyll fluorescence –  $F_v/F_M$ ; Steady-state chlorophyll fluorescence – Chl-Fs; Actual quantum yield of chlorophyll fluorescence –  $\Phi_{II}$ .

#### 4.3.3 Interpretation of hyperspectral images at canopy level

The error assessment of the maximum likelihood classification, used for the selection of vegetation exposed to the sun revealed accuracy between 83.1–87.8%, with the kappa coefficient between 0.78–0.83. The fraction of non-photosynthetic vegetation was about 6–7% and the fraction of directly sun illuminated vegetation varied from 5% (morning) to 32% (midday) of the total experimental plot area.

The comparison of the VI daily courses of selected regions of interest (ROI), i.e. average values of VIs of all sample leaves (total number of pixels between 150-180) and of all sun-exposed leaves in the image (total number of pixels > 400 000) showed quite a different pattern (Fig. 4.5A–C). For instance, in the case of PRI the areas had their lowest values at 11:00, whereas the whole image showed the highest values at the same time (Fig. 4.5A). The absolute values of PRI derived from ROI were, in general, lower than values derived from the whole image. Similarly, the ratio  $R_{686}/R_{630}$  calculated from ROI was lowest at 12:00 whereas highest when calculated from the whole image.  $R_{686}/R_{630}$  calculated from ROI was lower than the ratio calculated from the image except at 15:00 (Fig. 4.5B). The ratio  $R_{740}/R_{800}$  derived from ROI had higher absolute values than values derived from the whole image (Fig. 4.5C). Finally, a close linear relation was observed between  $F_S$  and  $\Phi_{II}$  ( $R^2=0.92$ ) measured on sample leaves when both parameters showed a decrease around midday, from 11:00 to 14:00 (Fig. 4.5D).

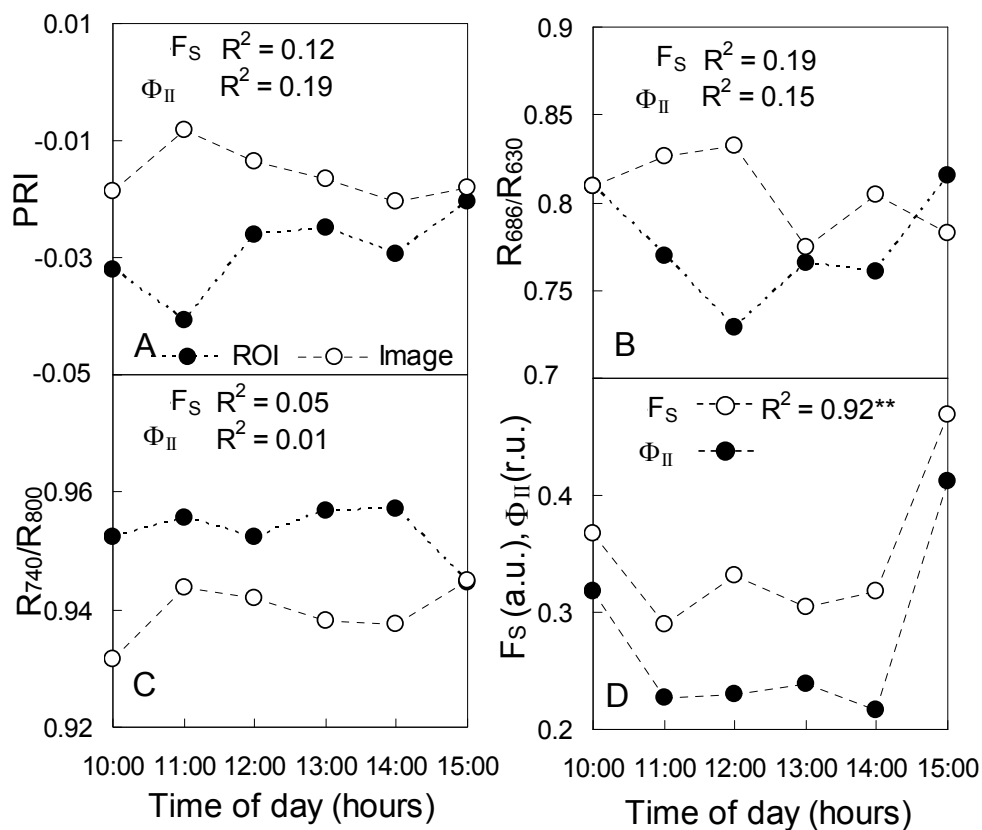


Figure 4.5. Daily courses of vegetations indexes derived from the region of interest (ROI) (●) and from sun-exposed pixels of the whole image (○) for: (A) PRI, (B)  $R_{686}/R_{630}$ , and  $R_{740}/R_{800}$  (C). ROI represents the average of all measured leaves (N=150-180), and the image represents the average of all green sun-exposed pixels ( $n > 400\ 000$ ).  $R^2$  coefficients of determination between the given vegetation index derived from the whole image and steady-state chlorophyll fluorescence ( $F_S$ ). Actual quantum yields of  $F_S$  ( $\Phi_{II}$ ) are indicated. Graph (D) shows the daily course of  $F_S$  (○) and the actual quantum yield of Chl-F (●) measured on sample leaves (ROI). Asterisks denote the significance at the probability level  $p < 0.001$ (\*\*).

## 4.4 Discussion

### 4.4.1 Remote detection of chlorophyll fluorescence signals

Chl-F effects on the apparent reflectance were observed when using dark to light transition of grassland canopy exposed to natural light conditions (Fig. 4.2A–C). These results are in agreement with the previous laboratory studies of Chl-F detection in single leaves (Buschmann et al. 1994; Gamon et al. 1990; Gamon and Surfus 1999; Zarco-Tejada et al. 2000a) and also at the canopy level (Zarco-Tejada et al. 2000b; 2002; 2003), which supports the applicability of remote sensing techniques for monitoring the Chl-F daily cycle under natural irradiation (Fig. 4.2C). Observed rapid reflectance changes followed by steady-state in ~90 s after uncovering the dark-adapted plot are also in agreement with the kinetic previously



observed in reflectance (Zarco-Tejada et al. 2000a) and Chl-F induction (Kautsky and Hirsch, 1933) at the leaf level.

The reflectance change at 531 nm associated mostly with zeaxanthin formation has been reported by Gamon et al. (1992). Our results showed that the peak of this spectral feature is quite flat and broad (Fig. 4.2A), with a wavelength interval ranging from 490 nm up to 570 nm (Fig. 4.2B). Such a broad spectral interval suggests that much more processes apart from the dynamic zeaxanthin conversion are mirrored in the reflectance change around 531 nm. These processes, such as energization (Ruban *et al.* 1993) and acidification (e.g. Schreiber and Klughammer 2008) of the thylakoid membrane, water fluxes increasing light scattering (e.g. Heber *et al.* 1986) and changes in pigment-binding protein (Li *et al.* 2000), are limiting the use of PRI only as a specific indicator of photosynthetic rate not only for remote sensing applications (Grace *et al.* 2007). At the same time this broad reflectance interval provides the possibility to apply an alternative approach integrating the reflectance signal of all these wavelengths instead of the PRI index, which is computed from only two narrow wavelengths. Similarly, the peak of reflectance change around 686 nm, as observed in our study, was previously published in studies conducted on sunflower leaves (Gamon and Surfus 1999). Contrary to this result, two peaks at wavelengths of 695 and at 700 nm were reported in a study on *Acer saccharum* leaves and canopy (Zarco-Tejada et al. 2001). This difference can be explained by the fact that Zarco-Tejada et al. (2001) subtracted the canopy reflectance scans acquired at 8:00 and 12:30. In such a time period, one can expect changes in atmospheric conditions, and also a different shadow fraction distribution with a different influence of vegetation structure causing appearance of these two peaks.

Finally, the earlier reported reflectance change at 740 nm (far-red Chl-F) (Dobrowski et al. 2005; Gamon and Surfus 1999) has also been observed (Fig. 4.2A–C). All these outcomes supports a previously established hypothesis that the  $F_S$  intensity retrieved correctly from hyperspectral reflectance could potentially be used for the estimation of vegetation carbon assimilation (Dobrowski et al. 2005; Flexas et al. 2002; Freedman et al. 2002; Garbulsky et al. 2008; Grace et al. 2007).

#### 4.4.2 Fluorescence vegetation indexes – leaf image observations

Positive curvilinear relations fitted between PRI and Chl  $a+b$  (Fig. 3A;4A) are in line with results of other leaf (Moran et al. 2000) and canopy level studies (Sims et al. 2006), showing that higher leaf Chl  $a+b$  content may lead to higher LUE. However, the relationship between

PRI and Chl  $a+b$  was relatively unstable in the daily course (Fig. 4.4A), suggesting that the PRI index might be sensitive to non-physiological factors (Barton and North 2001; Filella et al. 2004). More consistent relationships were observed between  $R_{686}/R_{630}$  and Chl  $a+b$ , reaching the lowest  $R_{686}/R_{630}$  values at 12:00 (Fig. 4.4B). This  $R_{686}/R_{630}$  decrease could be related to the daily variation of  $F_S$  (Fig. 4.5D), which is typically lower during midday (Dobrowski et al. 2005).

Compared to PRI the reflectance ratio  $R_{686}/R_{630}$  also yielded a slightly higher average  $R^2$  when related to  $F_S$  and  $F_V/F_M$  parameters. However, correlations with  $\Phi_{II}$  were of similar statistical significance (Fig. 4.3A,B). While other leaf level studies demonstrated a close correlation between  $\Phi_{II}$  and PRI (Evain et al. 2004; Guo and Trotter 2006) (Rascher et al. 2007), and also a significant relationship between  $\Phi_{II}$  and  $R_{685}/R_{655}$  computed from reflectance airborne data (Zarco-Tejada et al. 2000b), the daily  $R^2$  values for PRI- $\Phi_{II}$  and  $R_{686}/R_{630}$ - $\Phi_{II}$  in our study strongly varied between 0.27-0.78 and 0.20-0.70, respectively. This might be related to the high heterogeneity of leaf angle distribution presented due to the extremely high spatial resolution of all analyzed pixels (Rascher et al. 2005). In general, no specific pixel size can be pronounced as ‘optimal’ for the retrievals of different geobiophysical properties of vegetation (Rahman et al. 2003). The optimal spatial resolution undoubtedly depends on the user required scale of observation (biomes vs. ecosystem), but also on type of the parameter to be estimated.

The positive relationships, observed between PRI and pre-dawn  $F_V/F_M$  values (Fig. 4.3A) in the daily course ( $R^2=0.40-0.65$ ), agree with studies recently conducted in forest ecosystems (Richardson et al. 2001; Weng et al. 2006a; 2006b). These results are suggesting the potential capability of PRI to estimate the photosynthetic leaf capacity. However, even stronger statistical daily relationships were obtained between  $R_{686}/R_{630}$  and  $F_V/F_M$  ( $R^2=0.45-0.83$ , Fig. 4.3B), which correspond to the daily relationship discovered between the measured  $F_V/F_M$  and VI ratios designed around  $R_{690}$  (i.e.  $R_{685}^2/(R_{675}\times R_{690})$ ,  $R_{685}/R_{630}$ ,  $R_{690}/R_{630}$ ,  $R_{680}/R_{630}$  and  $R_{687}/R_{630}$ ) (Zarco-Tejada et al. 2000b). These findings support a conclusion that the ratio  $R_{686}/R_{630}$  is less sensitive to non-physiological (e.g., structural) canopy effects than PRI.

Similar to our results (Fig. 4.3A, 4.4C), a positive relation between PRI and  $F_S$  has been observed in water stressed canopies of olive trees (*Olea europea*) (Suarez et al. 2008) and grapevines (Dobrowski et al. 2005). In consistence with our results in Fig. 4.3B, Dobrowski et al. (2005) observed a stronger relationship between  $F_S$  and  $R_{690}/R_{600}$  than between  $F_S$  and PRI. Nevertheless, one has to keep in mind that the experimental design of Dobrowski et al. (2005) used heat to induce plant water stress observed by a non-imaging sensor, which is

potentially decreasing comparability of fitted statistical models. Also, in contrast to the study of Dobrowski et al. (2005) our ratio  $R_{740}/R_{800}$  showed only a weak relation with the examined Chl-F parameters, reflecting the fact that the NIR wavelengths are affected by the angular reflectance anisotropy of vegetation foliage (especially at such a high spatial resolution).

#### 4.4.3 Fluorescence vegetation indexes – canopy level

Compared to the studies presenting a strong relationship between  $\Phi_{II}$  or  $F_S$  and PRI retrieved from the ground (Nichol et al. 2006), aircraft (Suarez et al. 2008) and satellite (e.g. Chris-PROBA) canopy observations (Raddi et al. 2005), our relation between PRI and  $\Phi_{II}$  or  $F_S$  (Fig. 4.5A) was rather weak. It was observed that the PRI of selected leaves did not correspond well to the canopy level PRI (Fig. 4.5A). Whereas the daily course of PRI derived from selected ROI of individual leaves supports the PRI applicability for the LUE estimation (Gamon et al. 1992; Nichol et al. 2000; 2002), the PRI derived from sun-exposed pixels of whole image suggests the opposite trend (Fig. 4.5A). These results revealed that a PRI response measured on single leaves could not resemble the PRI response whole canopy, most probably due to a biological and structural diversity of the natural grassland canopy. Similar behavior was observed in case of the  $R_{690}/R_{630}$  reflectance ratio. Zarco-Tejada et al. (2000b) retrieved from a 20 m spatial resolution image data of *Acer Saccharum* daily courses of the  $R_{690}/R_{630}$  ratio that varied by 17% while tracking the midday decrease in  $F_V/F_M$ . In spite of the fact that our  $R_{686}/R_{630}$  ratio derived from ROI was following a daily trend of  $\Phi_{II}$  and  $F_S$ , reaching low values during the midday (Fig. 4.5D), the canopy derived  $R_{686}/R_{630}$  ratio showed the opposite daily course (Fig. 4.5B).

Many canopy level studies (Grace et al. 2007; Hall et al. 2008; Hilker et al. 2008; Suarez et al. 2008) had been using non-imaging sensors integrating the sunlit and shaded canopy parts in one reflectance. Recently Hall et al. (2008) provided evidence that the daily PRI variation of forest canopy can be attributed solely to biological processes (changes in zeaxanthin) when accounting for the shadow fraction of vegetation estimated with airborne laser scanning. Although in our study we directly excluded shadow fraction and non-green portions of vegetation from the reflectance signal, the daily course of the whole image PRI still did not correspond to the expected daily course of LUE (i.e. lower values during midday). Potential explanation can be the extent of the scanned plot (1.5 x 4 m) that might not be able to capture typical daily LUE course of the whole grassland ecosystem measured within a larger spatial footprint by the eddy-covariance system. Still, when considering the use of remotely sensed

PRI at larger spatial scales, we strongly recommend a minimization of angular and shading effects as well as an exclusion of non-green vegetation surfaces (Drolet et al. 2005) within the scanned canopy (Filella et al. 2004; Gamon et al. 1995).

## 4.5 Conclusions

This study employed a new experimental design to provide further evidence of the ground based remote sensing Chl-F detection. The spectrometric measurements performed with a common imaging spectroradiometer over mountain grassland in the daily course of natural light conditions revealed all the previously known vegetation fluorescence spectral features.

At the leaf level, selected VIs sensitive to Chl-F (especially PRI and  $R_{686}/R_{630}$ ) were found to be usable for tracking the spatial variation of the Chl-F parameters (i.e.  $F_v/F_M$ ,  $F_S$ , and  $\Phi_{II}$ ). The ratio  $R_{686}/R_{630}$  performed slightly better than PRI in explaining the daily course variability of Chl-F. In our study the  $R_{740}/R_{800}$  ratio was only weakly related to Chl-F parameters.

At the canopy level, a strong angular anisotropy of grassland canopy reflectance (especially at NIR wavelengths) possibly reduced the positive performance of indices found at the leaf level. Therefore, more detailed studies investigating temporal canopy reflectance changes induced by the vegetation structural features are necessary to establish techniques able to retrieve accurately the vegetation Chl-F signal from a high spatial resolution imaging spectroscopy data.

## 4.6 Acknowledgements

This work is part of the research supported by the National Research Grant Programme No. 2B06068 (ISBE ASCR), and by the grants AV0Z60870520 (ISBE ASCR), ForChange (SP/2d1/70/08, Ministry of Environment of the Czech Republic) and 6007665808 (IPB). Language correction by Mrs. Gabrielle Johnson is gratefully acknowledged.

## 4.7 References

Ahl DE, Gower ST, Mackay DS, Burrows SN, Norman JM, Diak GR (2004) Heterogeneity of light use efficiency in a northern Wisconsin forest: implications for modeling net primary production with remote sensing. *Remote Sensing of Environment* 93:168-178

- Barton CVM, North PRJ (2001) Remote sensing of canopy light use efficiency using the photochemical reflectance index - Model and sensitivity analysis. *Remote Sensing of Environment* 78:264-273
- Buschmann C, Langsdorf G, Lichtenthaler HK (2000) Imaging of the blue, green, and red fluorescence emission of plants: An overview. *Photosynthetica* 38:483-491
- Buschmann C, Nagel E, Szabo K, Kocsanyi L (1994) Spectrometer for Fast Measurements of in-Vivo Reflectance, Absorptance, and Fluorescence in the Visible and near-Infrared. *Remote Sensing of Environment* 48:18-24
- Canadell JG Le Queré C, Raupach MR, Field CB, Buitenhuis ET, Ciais P, Conway TJ, Gillet NP, Houghton RA, Marland G (2007) Contributions to accelerating atmospheric CO<sub>2</sub> growth from economic activity, carbon intensity, and efficiency of natural sinks. *Proceedings of the National Academy of Sciences of the United States of America* 104:18866-18870
- Carter GA (1994) Ratios of Leaf Reflectances in Narrow Wavebands as Indicators of Plant Stress. *International Journal of Remote Sensing* 15:697-703
- Dobrowski SZ, Pushnik JC, Zarco-Tejada PJ, Ustin SL (2005) Simple reflectance indices track heat and water stress-induced changes in steady-state chlorophyll fluorescence at the canopy scale. *Remote Sensing of Environment* 97:403-414
- Drolet GG et al. (2005) A MODIS-derived photochemical reflectance index to detect inter-annual variations in the photosynthetic light-use efficiency of a boreal deciduous forest. *Remote Sensing of Environment* 98:212-224
- Evain S, Flexas J, Moya I (2004) A new instrument for passive remote sensing: 2. Measurement of leaf and canopy reflectance changes at 531 nm and their relationship with photosynthesis and chlorophyll fluorescence. *Remote Sensing of Environment* 91:175-185
- Filella I, Amaro T, Araus JL, Penuelas J (1996) Relationship between photosynthetic radiation-use efficiency of Barley canopies and the photochemical reflectance index (PRI). *Physiologia Plantarum* 96:211-216
- Filella I, Penuelas J, Llorens L, Estiarte M (2004) Reflectance assessment of seasonal and annual changes in biomass and CO<sub>2</sub> uptake of a Mediterranean shrubland submitted to experimental warming and drought. *Remote Sensing of Environment* 90:308-318
- Flexas J, Briantais JM, Cerovic Z, Medrano H, Moya I (2000) Steady-state and maximum chlorophyll fluorescence responses to water stress in grapevine leaves: A new remote sensing system. *Remote Sensing of Environment* 73:283-297

- Flexas J et al. (2002) Steady-state chlorophyll fluorescence (Fs) measurements as a tool to follow variations of net CO<sub>2</sub> assimilation and stomatal conductance during water-stress in C-3 plants. *Physiologia Plantarum* 114:231-240
- Freedman A, Cavender-Bares J, Keabian PL, Bhaskar R, Scott H, Bazzaz FA (2002) Remote sensing of solar-excited plant fluorescence as a measure of photosynthetic rate. *Photosynthetica* 40:127-132
- Gamon JA, Field CB, Bilger W, Bjorkman O, Fredeen AL, Penuelas J (1990) Remote-Sensing of the Xanthophyll Cycle and Chlorophyll Fluorescence in Sunflower Leaves and Canopies. *Oecologia* 85:1-7
- Gamon JA et al. (1995) Relationships between NDVI, Canopy Structure, and Photosynthesis in 3 Californian Vegetation Types. *Ecological Applications* 5:28-41
- Gamon JA, Penuelas J, Field CB (1992) A Narrow-Waveband Spectral Index That Tracks Diurnal Changes in Photosynthetic Efficiency. *Remote Sensing of Environment* 41:35-44
- Gamon JA, Surfus JS (1999) Assessing leaf pigment content and activity with a reflectometer. *New Phytologist* 143:105-117
- Garbulsky MF, Penuelas J, Papale D, Filella I (2008) Remote estimation of carbon dioxide uptake by a Mediterranean forest. *Global Change Biology* 14:2860-2867
- Genty B, Briantais JM, Baker NR (1989) The relationship between the quantum yield of photosynthetic electron transport and quenching of chlorophyll fluorescence. *Biochimica Et Biophysica Acta* 990:87-92
- Grace J, Nichol C, Disney M, Lewis P, Quaife T, Bowyer P (2007) Can we measure terrestrial photosynthesis from space directly, using spectral reflectance and fluorescence? *Global Change Biology* 13:1484-1497
- Guo JM, Trotter CM (2004) Estimating photosynthetic light-use efficiency using the photochemical reflectance index: variations among species. *Functional Plant Biology* 31:255-265
- Guo JM, Trotter CM (2006) Estimating photosynthetic light-use efficiency using the photochemical reflectance index: the effects of short-term exposure to elevated CO<sub>2</sub> and low temperature. *International Journal of Remote Sensing* 27:4677-4684
- Hall FG Hilker T, Coops NC, Lyapustin A, Huemmrich KF, Middleton E, Margolis H, Drolet G, Black TA (2008) Multi-angle remote sensing of forest light use efficiency by observing PRI variation with canopy shadow fraction. *Remote Sensing of Environment* 112:3201-3211

- Heber U, Neimanis S, Lange OL (1986) Stomatal aperture, photosynthesis and water fluxes in mesophyll cells as affected by the abscission of leaves. Simultaneous measurements of gas exchange, light scattering and chlorophyll fluorescence. *Planta* 167:554–562.
- Hilker T et al. (2008) Separating physiologically and directionally induced changes in PRI using BRDF models. *Remote Sensing of Environment* 112:2777-2788
- Inoue Y, Penuelas J (2006) Relationship between light use efficiency and photochemical reflectance index in soybean leaves as affected by soil water content. *International Journal of Remote Sensing* 27:5109-5114
- IPCC (2007) *Climate Change 2007: The Physical Science Basis. Contribution of Working Group I to the Fourth Assessment Report of the Intergovernmental Panel on Climate Change.* In: Solomon S, D. Qin, M. Manning, Z. Chen, M. Marquis, K.B. Averyt, M.Tignor and H.L. Miller (ed) Summary for Policymakers. Cambridge University Press, Cambridge, United Kingdom and New York, NY, USA, p 996
- Kautsky H, Hirsch A. (1931) Neue Versuche zur Kohlensäureassimilation. *Naturwissenschaften* 19:964.
- Kitajima M, Butler WL (1975) Quenching of chlorophyll fluorescence and primary photochemistry in chloroplasts by dibromothymoquinone. *Biochimica Et Biophysica Acta* 376:105-115
- Li XP, Bjorkman O, Shih C, Grossman AR, Rosenquist M, Jansson S, Niyogi KK (2000) A pigment-binding protein essential for regulation of photosynthetic light harvesting. *Nature* 403:391-395.
- Lillesand TM, Kiefer RW (2000) 'Remote sensing and image interpretation, 4th edition.' (John Wiley & Sons: New York, USA)
- Monteith JL (1977) Climate and Efficiency of Crop Production in Britain. *Philosophical Transactions of the Royal Society of London Series B-Biological Sciences* 281:277-294
- Moran JA, Mitchell AK, Goodmanson G, Stockburger KA (2000) Differentiation among effects of nitrogen fertilization treatments on conifer seedlings by foliar reflectance: a comparison of methods. *Tree Physiology* 20:1113-1120
- Moya I, Camenen L, Evain S, Goulas Y, Cerovic ZG, Latouche G, Flexas J, Ounis A (2004) A new instrument for passive remote sensing 1. Measurements of sunlight-induced chlorophyll fluorescence. *Remote Sensing of Environment* 91:186-197.
- Nichol CJ et al. (2000) Remote sensing of photosynthetic-light-use efficiency of boreal forest. *Agricultural and Forest Meteorology* 101:131-142

- Nichol CJ et al. (2002) Remote sensing of photosynthetic-light-use efficiency of a Siberian boreal forest. *Tellus Series B-Chemical and Physical Meteorology* 54:677-687
- Nichol CJ, Rascher U, Matsubara S, Osmond B (2006) Assessing photosynthetic efficiency in an experimental mangrove canopy using remote sensing and chlorophyll fluorescence. *Trees-Structure and Function* 20:9-15
- Papageorgiou GC, Govindjee (2004) Chlorophyll a fluorescence: a signature of photosynthesis. *Advances in photosynthesis and respiration*. Springer, Dordrecht, Netherlands
- Rahman AF, Cordova VD, Gamon JA, Schmid HP, Sims DA (2004) Potential of MODIS ocean bands for estimating CO<sub>2</sub> flux from terrestrial vegetation: A novel approach. *Geophysical Research Letters* 31
- Rahman AF, Gamon JA, Sims DA, Schmidts M (2003) Optimum pixel size for hyperspectral studies of ecosystem function in southern California chaparral and grassland. *Remote Sensing of Environment* 84:192-207
- Rascher U, Nichol CJ, Small C (2005) Hyperspectral imaging of photosynthesis from the single leaf to the complex canopy- understanding the spatio-temporal variations of photosynthesis within a drought stressed tropical canopy. *Proceedings of the 4<sup>th</sup> EARSeL Workshop on Imaging Spectroscopy*. New Quality in Environmental Studies. Warsaw University, Poland.
- Ruban AV, Young AJ, Horton P (1993) Induction on non-photochemical energy dissipation and absorbance changes in leaves. Evidence for changes in the state of the light harvesting system of photosystem II in vivo. *Plant Physiology* 102:741-750.
- Running SW, Baldocchi DD, Turner DP, Gower ST, Bakwin PS, Hibbard KA (1999) A global terrestrial monitoring network integrating tower fluxes, flask sampling, ecosystem modeling and EOS satellite data. *Remote Sensing of Environment* 70:108-127.
- Savitzky A, Golay, MJE (1964) Smoothing and differentiation of data by simplified least squares procedures. *Anal. Chem* 36:1627-1639.
- Schreiber U, Klughammer C (2008) Non-photochemical fluorescence quenching and quantum yields in PS I and PS II: Analysis of heat-induced limitations using Maxi-Imaging-PAM and Dual-PAM-100. *PAM Application Notes* 1:15-18.
- Sims DA, Luo HY, Hastings S, Oechel WC, Rahman AF, Gamon JA (2006) Parallel adjustments in vegetation greenness and ecosystem CO<sub>2</sub> exchange in response to



- drought in a Southern California chaparral ecosystem. *Remote Sensing of Environment* 103:289-303
- Smith RCG, Adams J, Stephens DJ, Hick PT (1995) Forecasting wheat yield in a Mediterranean-type environment from the NOAA satellite. *Australian Journal of Agricultural Research*:46, 113-125.
- Soukupova J et al. (2008) Annual variation of the steady-state chlorophyll fluorescence emission of evergreen plants in temperate zone. *Functional Plant Biology* 35:63-76
- Suarez L et al. (2008) Assessing canopy PRI for water stress detection with diurnal airborne imagery. *Remote Sensing of Environment* 112:560-575
- Urban O et al. (2007) Temperature dependences of carbon assimilation processes in four dominant species from mountain grassland ecosystem. *Photosynthetica* 45:392-399
- Weng JH, Chen YN, Liao TS (2006a) Relationships between chlorophyll fluorescence parameters and photochemical reflectance index of tree species adapted to different temperature regimes. *Functional Plant Biology* 33:241-246
- Weng JH, Jhaung LH, Jiang JY, Lai GM, Liao TS (2006b) Down-regulation of photosystem 2 efficiency and spectral reflectance in mango leaves under very low irradiance and varied chilling treatments. *Photosynthetica* 44:248-254
- Zarco-Tejada PJ, Miller JR, Mohammed GH, Noland TL (2000a) Chlorophyll fluorescence effects on vegetation apparent reflectance: I. Leaf-level measurements and model simulation. *Remote Sensing of Environment* 74:582-595
- Zarco-Tejada PJ, Miller JR, Mohammed GH, Noland TL, Sampson PH (2000b) Chlorophyll fluorescence effects on vegetation apparent reflectance: II. Laboratory and airborne canopy-level measurements with hyperspectral data. *Remote Sensing of Environment* 74:596-608
- Zarco-Tejada PJ, Miller JR, Mohammed GH, Noland TL, Sampson PH (2002) Vegetation stress detection through chlorophyll a+b estimation and fluorescence effects on hyperspectral imagery. *Journal of Environmental Quality* 31:1433-1441
- Zarco-Tejada PJ, Pushnik JC, Dobrowski S, Ustin SL (2003) Steady-state chlorophyll a fluorescence detection from canopy derivative reflectance and double-peak red-edge effects. *Remote Sensing of Environment* 84:283-294

## CHAPTER 5

Are simple reflectance ratios related to chlorophyll fluorescence able to track changes in carbon fluxes of grassland and forest ecosystems?

*Alexander Ač<sup>1,2</sup>, Zbyněk Malenovský<sup>4</sup>, Otmar Urban<sup>1</sup>, Jan Hanuš<sup>1</sup>, Martina Košvancová<sup>1,3</sup>,  
Martin Navrátil<sup>5</sup>, Martina Vašková<sup>5</sup>, Julie Olejníčková<sup>6</sup>, Michal Marek<sup>1,3</sup>*

<sup>1</sup>Laboratory of Plants Ecological Physiology, Institute of Systems Biology and Ecology, Academy of Sciences CR, Poříčí 3b, CZ-603 00 Brno, Czech Republic

<sup>2</sup>Agricultural Faculty, University of South Bohemia, Studentská 13, CZ-370 05 České Budějovice, Czech Republic

<sup>3</sup>Mendel University, Zemědělská 1, CZ-613 00 Brno, Czech Republic

<sup>4</sup>Remote Sensing Laboratories, Department of Geography, University of Zürich, Winterthurerstrasse 190, CH-8057 Zürich, Switzerland

<sup>5</sup>Department of Physics, Faculty of Science, University of Ostrava, 30. dubna 22, CZ-701 03 Ostrava, Czech Republic.

<sup>6</sup>Laboratory of Physiology and Ecology, Department of Biological Dynamics, Institute of Systems Biology and Ecology, Academy of Sciences CR, Zámek 136, CZ-37333 Nové Hrady, Czech Republic

Intended for publication to *Oecologia*

**Abstract**

In this study, we explored the potential of simple optical vegetation indexes (VIs) related to chlorophyll fluorescence emission ( $R_{686}/R_{630}$ ,  $R_{740}/R_{800}$ ) and de-epoxidation state of xanthophyll cycle pigments (PRI) to track changes in CO<sub>2</sub> assimilation rate and Light Use Efficiency (LUE) in montane grassland and coniferous Norway spruce forest ecosystems, both at leaf and canopy level. VIs were measured by ground-based high spatial/spectral resolution imaging spectroscopy, a technique used also in remote sensing. Under steady-state conditions during measurement conducted only in grassland, no correlation between VIs and light-saturated CO<sub>2</sub> assimilation ( $A_{\max}$ ) measured at the leaf level, was detected. However, once the temporal dimension was included into the experimental setup, statistically significant changes in VIs related to tested physiological parameters were revealed.  $\Delta$ PRI and  $\Delta(R_{686}/R_{630})$  were significantly correlated with  $A_{\max}$ , when measured during dark-to-light transition in minutes. During daily variations of VIs and physiological parameters during the day in both, grassland and forest ecosystems, In general, daily variation of reflectance ratios using the chlorophyll fluorescence wavelengths ( $R_{686}/R_{630}$ ,  $R_{740}/R_{800}$ ) correlate better with variation of physiological parameters than that of PRI. We conclude that the simple reflectance ratios related to chlorophyll fluorescence can track variations in carbon fluxes on the level of grassland and forest ecosystems.

*Keywords:* Imaging spectroscopy, Hyperspectral remote sensing, Eddy-covariance, PRI, Chlorophyll fluorescence, CO<sub>2</sub> assimilation

## 5.1 Introduction

Ongoing global climate change (IPCC 2007) might turn ecosystems over large areas from carbon sink to carbon source (Kurz et al. 2008), therefore accurate assessment of global carbon balance is of increasing importance. Remote sensing (RS) provides the only cost effective and large scale tool to monitor spatio-temporal properties of CO<sub>2</sub> assimilation in various plant ecosystems (Rahman et al. 2004; Schaepman 2007). One of the traditional approaches to quantify RS information is transformation of reflectance spectra into vegetation indexes (VIs). VIs are mathematical transformations of reflectance at specifically selected spectral bands that maximize sensitivity to target biophysical variable and minimize confounding environmental factors (e.g. Myneni et al. 1995). Since the advent of the satellite era several VIs have been developed for remote quantification of leaf chlorophyll content (Chl *a+b*) (le Maire et al. 2004), leaf area index (LAI) (Haboudane et al. 2004) and/or other biophysical variables (Ustin et al. 2004) that are important for assessment of health status and functioning of terrestrial ecosystems. However, most of these derived variables and VIs are rather insensitive to actual changes in ecosystem carbon fluxes (but see Boelman et al. 2003). Recent advances in RS opened a possibility to estimate physiological parameters related to the dynamic processes of CO<sub>2</sub> fixation by photosynthesis (Grace et al. 2007). One of directly related processes is the chlorophyll fluorescence emission (reviewed by Govindjee and Papageorgiou 2004), indirectly related are changes in xanthophyll cycle pigments (Demmig-Adams and Adams 2000). The xanthophyll cycle pigments protect photosynthetic apparatus from overexcitation. Under high light conditions, plants activate a photo-protective pathway via de-epoxidative reactions of xanthophyll pigments, resulting in zeaxanthin as the final product (e.g. Morosinotto et al. 2003). This process enables dissipation of excessive energy in the form of heat (e.g. Baroli and Niyogi 2000) and is associated, along with other processes, with reduction in photochemical efficiency of Photosystem II (PSII) (Demmig-Adams and Adams 2000). In spectral characteristics of plants were these these rapid and light intensity dependent changes firstly detected remotely as changes in absorbance around 515 nm (Bilger et al. 1989) and later as changes in reflectance around 530 nm (Gamon et al. 1990). Subsequently, Gamon et al. (1992) proposed Photochemical Reflectance Index (or Physiological Reflectance Index, PRI), calculated as  $(R_{531}-R_{570})/(R_{531}+R_{570})$ , where  $R_{XXX}$  is an reflectance intensity at subscripted wavelength. This index has been related to zeaxanthin pigment content (Filella et al. 1996; Gamon et al. 1992; Gamon et al. 1997), light use efficiency (LUE) parameter (defined as the amount of assimilated carbon per unit of incoming

light) measured at leaf (Gamon et al. 1997) and later also at canopy (Nakaji et al. 2008; Nichol et al. 2000; 2002) level. Several studies linked carbon sink capacity measured by eddy-covariance flux towers PRI in grassland (Black and Guo 2008) and forest ecosystems (Louis et al. 2005).

Changes in zeaxanthin are also closely related to commonly used chlorophyll fluorescence (Chl-F) parameter - Non Photochemical Quenching (NPQ) (Muller et al. 2001). Chl-F is another plant optical signal used in photosynthesis research (e.g. Maxwell and Johnson 2000). Chl-F is produced by plant photosynthetically active tissues with maximum intensity at 690 and 740 nm (Buschmann et al. 2000). Chl-F is a competitive process to the photosynthetic energy conversion, together with a heat loss (see Govindjee 1995; Maxwell and Johnson 2000, Papageorgiou and Govindjee 2004). Thus, the competition between Chl-F and photosynthetic processes is responsible for the intimate link between the Chl-F and photosynthesis yields.

When a healthy dark adapted plant is exposed to actinic irradiance, its Chl-F increases first to a high peak value and then decreases to a steady state level ( $F_S$ ) (Papageorgiou et al. 2007). When saturating light is used, the Chl-F reaches its maximum level ( $F_M$ ). The relative Chl-F decrease ( $R_{Fd}$ ) from dark-to-light adapted state, quantified as  $R_{Fd} = (F_M - F_S) / F_S$ , was shown to be linearly correlated with light-saturated photosynthetic rate (e.g. Lichtenthaler et al. 2007). The only solar-induced Chl-F signal that can be tracked by passive RS sensors is  $F_S$  (Gamon and Surfus 1999; Zarco-Tejada et al. 2000a; Zarco-Tejada et al. 2000b). Results of several studies suggested that solar-induced  $F_S$  (Carter et al. 1996; Flexas et al. 2000; Flexas et al. 2002; Freedman et al. 2002; Soukupova et al. 2008; Theisen et al. 1994) is linked to CO<sub>2</sub> assimilation. Consequently several VIs, such as reflectance ratios  $R_{686}/R_{630}$ ,  $R_{690}/R_{630}$ ,  $R_{740}/R_{800}$  and  $R_{760.59}/R_{759.5}$  have been proposed to quantify  $F_S$  (Dobrowski et al. 2005; Perez-Priego et al. 2005; Zarco-Tejada et al. 2000b), where the first wavelength corresponds to maximum intensity of  $F_S$ , and second wavelength is unaffected by Chl-F thus serving as a normalization factor. Another method used for  $F_S$  signal extraction from reflectance measurements is Fraunhofer Line Discriminator principle (Louis et al. 2005). Nevertheless, most of the studies using reflectance and Chl-F were done either in laboratory conditions or with non-imaging sensors. Only limited number of studies mapping the spatial distribution of carbon fluxes was carried out from airborne (Fuentes et al. 2006; Rahman et al. 2001) or spaceborne (Drolet et al. 2005; Rahman et al. 2004) imaging sensors. Moreover, air- and spaceborne sensors have in general relatively low spatial resolution resulting in spectrally mixed information of several surface objects. To our knowledge, no study has evaluated the

potential of various VIs for estimation of LUE or CO<sub>2</sub> assimilation using very high spatial resolution imaging spectroscopy data.

In this study, we explored the ability of reflectance VIs related to  $F_S$  signal, as  $R_{686}/R_{630}$ ,  $R_{740}/R_{800}$  and PRI, to estimate the CO<sub>2</sub> assimilation at canopy level in grassland and forest ecosystems. First, we evaluated whether the heterogeneity of VIs over measured grassland plot can reveal heterogeneity in light saturated CO<sub>2</sub> assimilation rate ( $A_{max}$ ) under steady state conditions. Second, we followed VIs change in scale in minutes and in days and searched correlations between VIs variations and variations of physiological parameters, particularly LUE, gLUE (gross LUE) net ecosystem exchange (NEE) and gross primary production (GPP), measured by the eddy-covariance systems at the scale of grassland and forest ecosystem. We propose that this study was to explore potentials and limitations of scaling the carbon cycle related physiological processes, observable by RS methods, from leaf to canopy level. This way the feasibility of larger scale RS observation of vegetation processes at ecosystem level can be advanced.

## 5.2 Materials and methods

### 5.2.1 Study site

Montane grassland and forest research plots are located at the experimental study site Bílý Kříž (Beskydy Mts., the Czech Republic, 18.54°E, 49.49°N, 855 m and 908 m a.s.l., respectively), which is part of CARBOEUROPE network ([www.carboeurope.org](http://www.carboeurope.org)). This site is characterized by cool (annual mean temperature of 5.5°C) and humid (annual mean relative air humidity about 80%) climate with high annual precipitation (ca 1000 – 1400 mm). The geological bedrock is formed by Mesozoic Godula sandstone (flysch type), with ferric podzols.

#### 5.2.1.1 Grassland ecosystem

The grassland (association *Nardo-Callunetea*, class *Nardo-Agrostion tenuis*) is characterized by high plant species biodiversity. The most abundant species occurring at the experimental plot were: *Festuca rubra* agg. (L.), *Hieracium* sp., *Plantago* sp., *Nardus stricta* (L.), and *Jacea pseudophrygia* (C.A. Meyer). Further details about the experimental stand and physiological properties of dominant plant species are presented in Urban et al. (2007a).

### 5.2.1.2 Forest ecosystem

The forest stand has been planted since 1981 with 4-years-old seedlings of *Picea abies* (L.) Karst. (99%) and *Abies alba* (Mill). (1%) on the slope (11–16°) with south-southwest orientation over an area of 6.2 ha (Urban et al. 2007b). Presently, the stand density is 2600 trees ha<sup>-1</sup> (hemi-surface leaf area index of about 11 m<sup>2</sup>m<sup>-2</sup>), with mean ( $\pm$  standard deviation) tree height of 8.5 ( $\pm$  0.1 m) and stand diameter at 1.3 m of 10.1  $\pm$  (0.1 cm).

### 5.2.2 Hyperspectral images

The acquisition of nadir viewing canopy reflectance was performed using a visible-near infrared hyperspectral imaging system AISA Eagle during sky clear, sunny days. 260 spectral bands with 2.2 nm full width at half maximum were collected within wavelength range of 400-940 nm. In the forest ecosystem the Airborne Imaging Spectrometer for Applications (AISA, Specim, FI) sensor was mounted to the tower at the height of 20 meters (i.e. approximately 10 m above the top of canopy). The covered area of about 50 m<sup>2</sup> was within a footprint of an eddy-covariance tower system and is characterized with a pixel resolution of 1cm.

In the case of the grassland ecosystem, the sensor was attached to a ladder at the height of 4 meters above top of canopy, sensing a total image area of about 4 m<sup>2</sup> within a footprint of an eddy-covariance tower system. The resulting pixel resolution is about 0.3 cm.

#### 5.2.2.1 Image data processing

The acquired hyperspectral images were transformed into the radiance values using the AISA Eagle calibration files, and afterward converted into at-sensor reflectance by means of the empirical line calibration method, using five near Lambertian calibration panels of known flat reflectance. A method of automatic supervised Maximum Likelihood classification (Lillesand and Kiefer, 2000) was used to distinguish and to mask shaded pixels at AISA Eagle images. Only photosynthetically active pixels with strong reflectance signal can be considered for the analysis. Therefore, an appropriate threshold of the green normalized difference VI (green NDVI=  $(R_{554}-R_{677})/(R_{554}+R_{677})$ ) was applied to separate the green sunlit grass leaves from a dry litter. Three VIs (PRI,  $R_{686}/R_{630}$ ,  $R_{740}/R_{800}$ ) related to photosynthetic processes were

derived out of the AISA Eagle reflectance scans per pixel and thereafter averaged (Tab. 5.1). No other optical VIs, for instance chlorophyll content estimating VIs, were analyzed.

Vegetation Index	Designed as indicator of	Reference
$PRI = \frac{(R_{532.2} - R_{570.8})}{(R_{532.2} + R_{570.8})}$	LUE, Zeaxanthin content,	Gamon et al. 1992
$R_{686.7}/R_{630.0}$	$F_s$ , Early stress	Zarco-Tejada et al. 2000b
$R_{740.0}/R_{800.0}$	$F_s$ , Early stress	Dobrowski et al. 2005

Table 5.1. Vegetation indices (VIs) used in this study. Legend:  $R_\lambda$  is reflectance at a wavelength  $\lambda$  in nm, Light use efficiency - LUE; *Steady-state* chlorophyll fluorescence -  $F_s$ .

### 5.2.3 Measured parameters

#### 5.2.3.1 Gas exchange measurements

Intact leaves of following grassland species were measured for with gas-exchange rate: *Festuca rubra* agg., *Hieracium* sp., *Jacea Pseudophrygia*, *Plantago lanceolata*, *Tarraxacum* spp., and *Veronica chamaedris* (L.). were investigated. All *in situ* CO<sub>2</sub> assimilation rate measurements were conducted with an open gasometrical system with infra-red gas analyser Li-6400 (Li-Cor, USA) at saturating light intensities (Photosynthetic Photons Flux Density (PPFD)  $\approx 1300 \pm 10 \mu\text{mol}(\text{photons}) \text{m}^{-2} \text{s}^{-1}$ ). All environmental conditions inside the assimilation chamber remained unchanged and referred to field conditions: leaf temperature (34–37°C), relative humidity (35–45%).

#### 5.2.3.2 Eddy-covariance measurements

Fluxes of CO<sub>2</sub> and H<sub>2</sub>O, and subsequently latent and sensible heat exchange between the grass stand and atmosphere were measured using closed-path eddy-covariance systems Edisol (University of Edinburgh), containing infrared gas analyser Li-6262 (Li-Cor, USA), sonic anemometer Gill R2 (Gill Instruments, UK) and Edisol software package. In case of forest research stand the InSituFlux (InSituFlux, Sweden), assembled out of infrared gas analyser



LI-7000 (Li-Cor, USA), anemometer Gill R3 (Gill Instruments, UK) and EcoFlux software, was installed. The system provides time series of half an hour integral measurements of CO<sub>2</sub> and H<sub>2</sub>O fluxes.

Sonic anemometers indicating the point of fluxes and CO<sub>2</sub>, H<sub>2</sub>O vapor measurements, were placed 5 meters above the effective height of the stand. The footprint of the system covers a circular area with a radius of ca 500 m, for details see Havránková & Sedlák (2004). Post-processing of the eddy covariance data was based on the methodology paper (Aubinet et al. 2000) with several modifications according to the most recent CarboEurope and FLUXNET project's protocols. First, the spike removal and quality check of the raw signals were performed by the Quality Control (QC) Software. After gap filling the GPP and NEE values were modelled according to (Urban et al. 2007b). LUE and gLUE were calculated as follows: LUE = NEE/PPFD and gLUE = GPP/PPFD.

### 5.2.3.3 Pigment analysis

Plant leaves of grassland (n=24) and current, one- and two-years old needles of Norway spruce (*Picea abies* (L.) Karst.) trees (100 mg) (n=6) were sampled after the spectral measurements during the morning, midday and afternoon (i.e., at 9:00, 12:00 and 16:00 of local time). Samples were frozen in liquid nitrogen and foliar pigments were extracted in laboratory 80% acetone and a small amount of MgCO<sub>3</sub>. After centrifugation at 480 g for 3 min the supernatant was used for spectrophotometric (UV/VIS 550, Unicam, UK) estimation of chlorophyll *a* and *b per area* according to Lichtenthaler (1987) and also for High-Performance Liquid Chromatography (HPLC) quantification (TSP Analytical, USA) of individual carotenoids. The de-epoxidation state of the xanthophyll cycle pigments (DEPS) was calculated using conversion factors published by Farber (1997) as DEPS = (Z+A)/(V+A+Z) (Gilmore and Bjorkman 1994) where Z is zeaxanthin, A is antheraxanthin and V is violaxanthin.

### 5.2.4 Experimental setup

Experiments of three different time scales were performed in this study: (i) steady-state measurements, (ii) measurements of VIs over minutes, and (iii) over days.

*Steady-state experiment* measured the distribution of VIs over selected experimental plot of grassland ecosystem (area of about 4 m<sup>2</sup>) and analyzed whether steady state variations of VIs follow variations in CO<sub>2</sub> assimilation rate under full sunlight at midday. Within this plot we labeled 24 leaves (6 plant species, each leaf was located on separate plant), and measured their leaf CO<sub>2</sub> assimilation rate under saturating irradiance at midday ( $A_{\max}$ , measured at  $\approx 1300 \pm 10 \mu\text{mol}(\text{photons}) \text{m}^{-2} \text{s}^{-1}$ ). These leaves were lately identified on hyperspectral image, captured simultaneously with CO<sub>2</sub> observations. 10-20 of sun-lited pixels ( $\approx$  at saturating PPFD) per leaf were used to calculate the mean values of selected VIs that were correlated with  $A_{\max}$ . The experiment was done under clear sky conditions on sunny day on 18<sup>th</sup> of July 2007 at 13:00 of local time.

*“Shade removal” experiment (time scale of minutes)* tested whether the dynamical change in VIs during dark to light conditions can estimate the CO<sub>2</sub> assimilation rate of labeled grass leaves exposed to full sunlight ( $A_{\max}$ ). The experimental plot was divided into two parts (2 times 0.5 x 4 m). First part, containing 13 labeled sample leaves, was covered for 30 min by a black non-transparent blanket in order to dark adapt the grass canopy prior to hyperspectral measurement. The way of darkening enabled a lateral air convection, which prevented the physiological changes being induced by higher than ambient air temperature. Second control plot was exposed to natural radiation regime. Two AISA Eagle images of both plots were acquired at 5<sup>th</sup> and 90<sup>th</sup> second after blanket removal. Subsequently, we calculated the dynamic change in VIs computed per sample leaf (average of 10-20 pixels) during the dark-to-light transition as subtraction  $VI_{\text{DARK}} - VI_{\text{LIGHT}}$ , where  $VI_{\text{DARK}}$  and  $VI_{\text{LIGHT}}$  are values obtained from scan taken  $\sim 5$  and  $\sim 90$  seconds after removal of the blanket, respectively. These  $\Delta$ VIs were correlated with  $A_{\max}$  of sample leaves.

*Daily course experiment (time scale of days)* correlated the daily variations of mean values of VIs in AISA image of both grassland and forest ecosystems with daily variation of physiological parameters measured in half-hour interval by eddy-covariance flux systems. Grassland hyperspectral data were acquired on 2<sup>nd</sup> September 2005 in cca. 1 hour intervals from 9:30 to 16:00 of local time. The forest measurements were carried out at one hour intervals from 13:30 to 16:30 on 30<sup>th</sup> of August 2005 and from 9:30 to 16:30 of local time on 31<sup>st</sup> of August 2005.

### 5.2.5 Statistical analysis

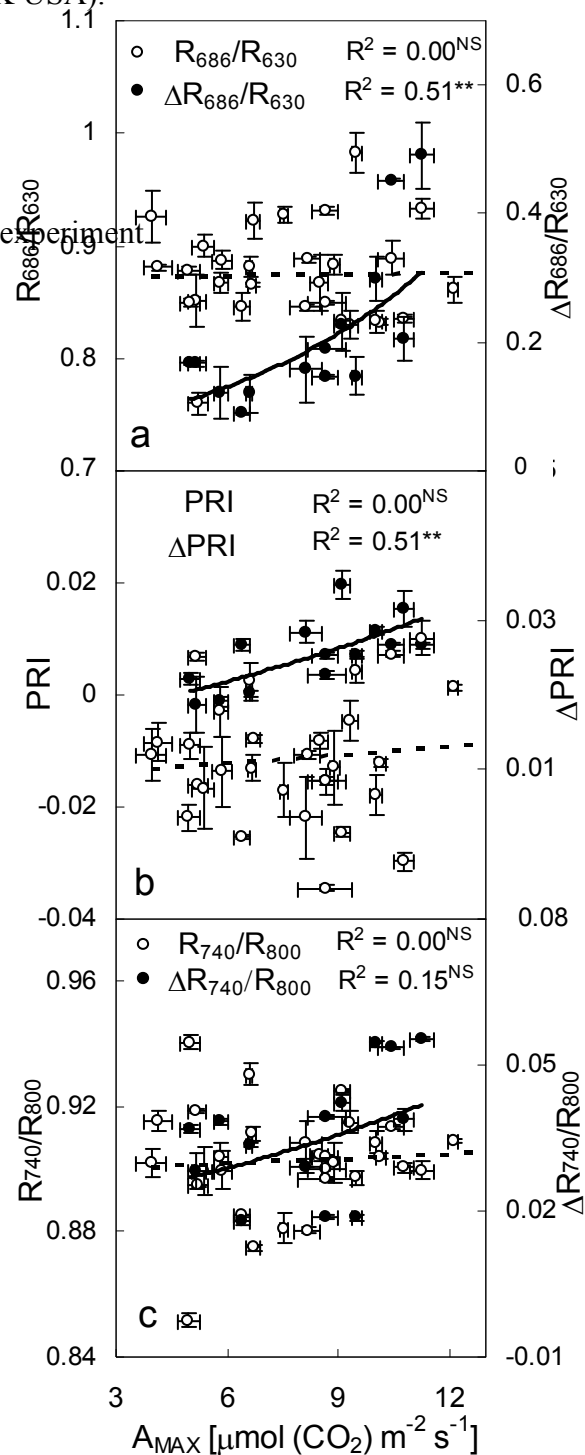
Best-fit linear regression equations were established to evaluate the relationship between the VIs and physiological parameter. Significance of the dependent variable in each model was tested using the analysis of variance (ANOVA) at two levels:  $p < 0.1$  and  $p < 0.05$ , respectively. The variation of a dependent variable explained by the regression to the independent variable was expressed with coefficient of determination ( $R^2$ ). All statistical tests were performed with Statistica 7.0 software (StatSoft Inc., Tulsa, OK USA).

## 5.3 Results

### 5.3.1 Steady-state experiment

The relationships between  $A_{max}$  of individual sampled leaves and their VIs under steady-state conditions are presented by open dots (Figs. 5.1A-C). No significant correlation was found between neither PRI nor other reflectance ratios ( $R_{686}/R_{630}$ ,  $R_{740}/R_{800}$ ) and  $A_{max}$ , which indicates that no relationship exists between  $A_{max}$  and VIs derived from hyperspectral image.

Figure 5.1. Midday relationships between light-saturated  $CO_2$  assimilation rate ( $A_{max}$ ) and selected vegetation indices (A –  $R_{686}/R_{630}$ , B – PRI (Physiological Reflectance Index), C –  $R_{740}/R_{800}$ ) under saturating steady state light conditions (open dots); and the relative change of the vegetation indices ( $\Delta$ ) during the dynamic transition of plants from dark-to-light adapted state (closed dots). Each point represents mean value of five measurements for  $A_{max}$  and 8-10 measurements (pixels) for the reflectance indices. Error bars represent standard deviations. NS means non significant relationship.



### 5.3.2 “Shade removal” experiment

Closed dots in Fig. 5.1 present relationships between  $A_{\max}$  of the sampled 24 leaves and the relative change ( $\Delta$ ) of their VIs extracted from the hyperspectral images taken 5 and 90 s after the dark blanket removal (i.e. during the dynamic transition from dark-to-light adapted state of grassland plants). Here, significant exponential relationships ( $p < 0.05$ ) were found between  $A_{\max}$  and  $\Delta(R_{686}/R_{630})$  ( $R^2 = 0.51$ ,  $y = 0.0484e^{0.1647x}$ ) (Fig. 5.1A), and  $\Delta\text{PRI}$  ( $R^2 = 0.51$ ,  $y = 0.015e^{0.0621x}$ ) (Fig. 5.1B).  $\Delta(R_{740}/R_{800})$  (Fig. 5.1C) showed no significant correlation with  $A_{\max}$ . These results indicate that when the temporal scale is included, the relative change in VIs (PRI and  $R_{686}/R_{630}$ ) positively correlates with carbon assimilation rate, probably as a result of elimination of the structural effects of leaves.

### 5.3.3 Daily course experiment

Variations in selected VIs and carbon fluxes measured within one-day temporal by eddy covariance systems were investigated for grassland and forest ecosystems jointly. This experiment was focused more on the variation of PRI and  $R_{686}/R_{630}$ , because we identified those two VIs as the most sensitive to the dynamic transition of grassland plants from dark-to-light adapted state.

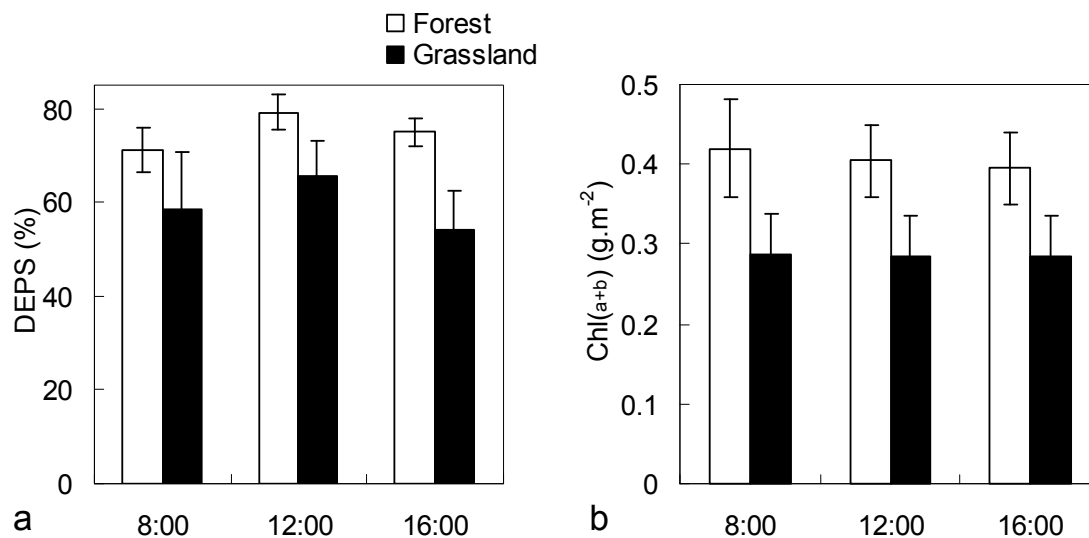


Figure 5.2. Diurnal courses of de-epoxidation state of xanthophylls cycle pigments [DEPS =  $(Z+A)/(V+A+Z)$ ], where Z is zeaxanthin, A is antheraxanthin and V is violaxanthin] (A) and total chlorophyll pigment content (Chl  $a+b$ ) (B) of grassland and forest ecosystem (black and white columns, respectively). DEPS values represent a mean value of current, 1- and 2-years old needles ( $n = 24$ ), Chl  $a+b$  values represent mean values of current needles ( $n = 6$ ). Error bars indicate standard deviations.

Fig. 5.2A shows daily courses of xanthophyll cycle pigments measured in the leaves of grassland plants and shoots of the trees. The diurnal behavior was typical for sunny days, i.e., the amount of de-epoxidised xanthophyll pigments (i.e. amount of Z and A) was highest during the midday. Chlorophyll content (Chl *a+b* per unit leaf area) did not show any significant change during the day in both grassland and in forest ecosystem (Fig. 5.2B). Forest ecosystem contained higher relative amount of xanthophyll pigments in de-epoxidised state (Fig. 5.2A), as well as a higher absolute amount of total chlorophylls (Fig. 5.2B) compared to grassland ecosystem.

Daily courses and also the relationships between the daily variations of VIs (PRI and  $R_{686}/R_{630}$ ) and the NEE and LUE measurements in grassland and forest ecosystems are shown in Fig. 5.3 and Fig. 5.4.

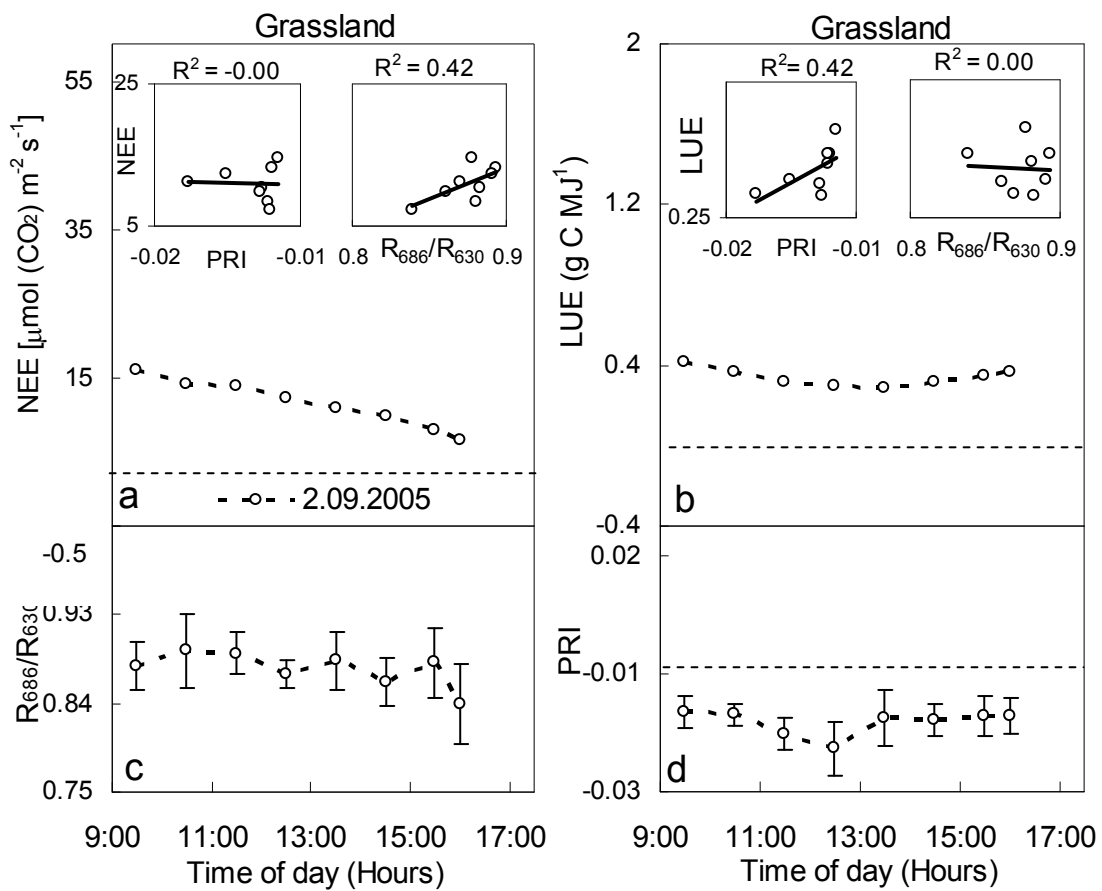


Figure 5.3. Daily courses of modelled net ecosystem exchange of CO<sub>2</sub> (NEE, A) and Light Use Efficiency (LUE, B) in grassland ecosystem and corresponding daily course of PRI (C) and  $R_{686}/R_{630}$  (D) vegetation indices over experimental plot of 4 m<sup>2</sup> measured by hyperspectral imaging sensor AISA Eagle (Specim, Finland). Each data point of eddy-covariance parameters represents an average of half-hour measurement. The PRI (Physiological Reflectance Index) and  $R_{686}/R_{630}$  data points represent average of more than 400 000 image (i.e., average of one image scan acquired in half and one hour intervals).

In the grassland, NEE gradually decreased during the day (Fig. 5.3A), while LUE showed typical daily course with the lowest values around midday (Fig. 5.3B). Different, but consistent pattern was observed for two consecutive days in forest ecosystem. NEE slightly increased during morning (till 11:00). The highest values around the midday were followed by sharp decrease in the afternoon (after 14:00) (Fig. 5.4A). Daily pattern of LUE was similar for both days, showing constant values during the day and sharp decrease after 15:00 (Fig. 5.4B). Both NEE and LUE were higher in forest compared to grassland ecosystem.

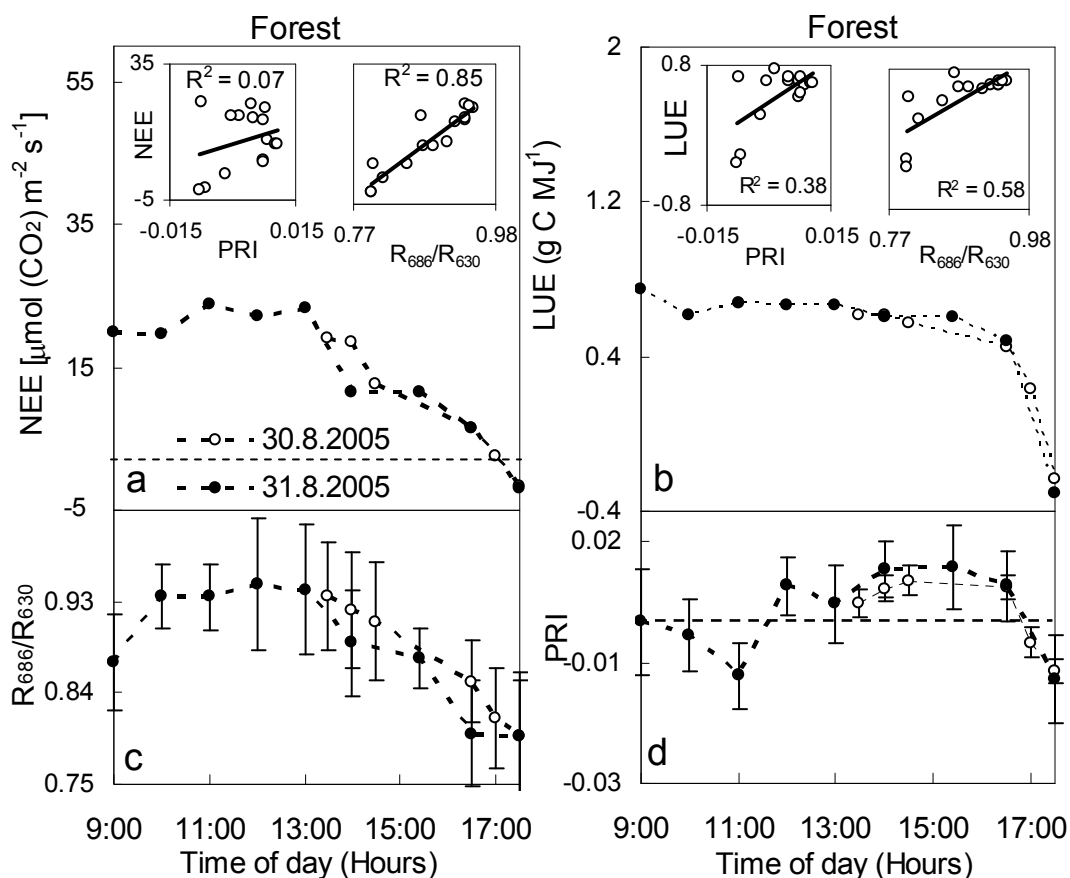


Figure 5.4. Daily courses of modelled net ecosystem exchange of  $\text{CO}_2$  (NEE, A) and radiation use efficiency (LUE, B) in forest ecosystem during two consecutive days with corresponding daily courses of  $R_{686}/R_{630}$  (C) and PRI (D) vegetation indexes (VIs) measured by hyperspectral imaging sensor AISA Eagle (Specim, Finland). Data points of eddy-covariance parameters represent averages of half-hour measurements (A,B) and data points of VIs (C,D) represent average of more than 400 000 image pixels (i.e., average of one image scan acquired in half and one hour intervals).

Daily course of  $R_{686}/R_{630}$  ratio in grassland was quite stable, with the highest values at 10:30 and 11:30 (Fig. 5.3C). In forest  $R_{686}/R_{630}$  increased in the morning hours, reached the highest values during the midday hours and then rapidly declined (Fig. 5.3D). The daily patterns of PRI variations for grassland and forest ecosystem were similar, however, the time when PRI reached its daily minimum was shifted. Grassland PRI decreased between 10:00 to

12:30 (Fig. 5.3D), reached its lowest value at the time of the highest irradiation intensity and increased again at 13:30 to its morning values. In forest ecosystem PRI decreased to the lowest value at 11:00 and then steeply increased reaching the maximum values from 13:30 to 15:30. In the late afternoon (15:30 - 17:00) it decreased again (Fig. 5.4D). In grassland we were not able to record these late afternoon measurements due to the mountainous terrain configuration. When comparing the absolute values, PRI for forest was higher than for grassland, which corresponds with higher xanthophyll cycle pigment content in de-epoxidised state of spruce needles, and with higher Chl *a+b* content.

Close statistical relationships (at  $p < 0.05$ ) between the daily variations in  $R_{686}/R_{630}$  and NEE (Fig. 5.3A, 5.4A; Tab 5.2B), were found in both ecosystems. Moreover, strong correlation was observed also between  $R_{686}/R_{630}$  and LUE in forest ecosystem (Fig. 5.4B; Tab 5.2B). PRI showed significant relationship (at  $p < 0.1$ ) only with LUE in grassland (Fig. 5.3B; Tab. 5.2A). Results of the regression analysis between the daily variations of physiological parameters derived from eddy-covariance measurements and four VIs are summarized in Tab. 5.2. Ratio  $R_{686}/R_{630}$  showed significant relationship with a high  $R^2$  for both, GPP and NEE in grassland as well as in forest. Moreover,  $R_{686}/R_{630}$  was highly correlated with gLUE and LUE in forest (Tab. 5.2B), with gLUE in grassland (Tab. 5.2A). Ratio  $R_{740}/R_{800}$  showed relatively high correlations with all examined physiological parameters for forest, but none for grassland ecosystem (Tab. 5.2A,B).

	<b>(a) Grassland (n=8)</b>				<b>(b) Forest (n=15)</b>			
VI	GPP	NEE	gLUE	LUE	GPP	NEE	gLUE	LUE
PRI	0.20	0.00	0.20	0.42*	0.08	0.07	0.08	0.38
$R_{686}/R_{630}$	0.49*	0.42*	0.49*	0.00	0.88**	0.85**	0.88**	0.58**
$R_{740}/R_{800}$	0.02	0.07	0.02	0.05	0.71**	0.69**	0.83**	0.52*

Table 5.2. Summary of coefficients of determination ( $R^2$ ) found for the linear relations between vegetation indices (VIs) and physiological parameters derived from eddy-covariance measurements in (a) grassland and (b) forest. Gross primary production (GPP [ $\mu\text{mol}(\text{CO}_2) \text{ m}^{-2} \text{ s}^{-1}$ ] = NEE + R); Net ecosystem exchange of  $\text{CO}_2$  (NEE [ $\mu\text{mol}(\text{CO}_2) \text{ m}^{-2} \text{ s}^{-1}$ ]); Gross Light Use Efficiency (gLUE = GPP/PPFD [ $\text{g C MJ}^{-1}$ ]); Radiation use efficiency (LUE = NEE/PPFD [ $\text{g C MJ}^{-1}$ ]). Values of eddy-covariance derived parameters are half-hour averages and values of VIs are averages of more than 400 000 pixels (i.e., average of one image scan acquired in half to one hour intervals), R is reflectance at subscripted wavelength and PRI is calculated as  $(R_{532}-R_{570})/(R_{532}+R_{570})$ . \* denotes for  $p < 0.1$  and \*\* for  $p < 0.05$ .

## 5.4 Discussion

According to Grace et al. (2007), VIs related to NPQ and Chl-F have potential to provide information about the diurnal, and potentially also about seasonal variations in photosynthesis. In this study, we have investigated whether PRI vegetation index and reflectance ratios that cover the emission bands of Chl-F ( $R_{686}/R_{630}$ ,  $R_{740}/R_{800}$ ), are able to follow variations in  $CO_2$  assimilation at three temporally different scales.

No significant relationship between actual states of any tested VIs and  $A_{max}$  was observed under steady state conditions (Fig. 5.1A-C), suggesting that tested VIs are incapable to follow differences in actual  $CO_2$  assimilation among different plant functional types. Our finding is in accordance with Carter et al. (1998) who also did not observe significant relationship between PRI and  $A_{max}$  under steady-state conditions at canopy level of 5-years old pine seedlings. The relationship between PRI and  $CO_2$  assimilation could be distorted by canopy structural features, especially by angular distribution of leaves, that are strongly manifested at such extremely high spatial resolution that we used. Additional confounding effects can be caused by differences in leaf structure and content of foliar pigment, which vary per plant species.

Once the temporal component has been inserted into the experimental setup, the change in VIs variability increased and consequently also the relationships between VIs and physiological parameters were identified. During dark-to-light transition, we found significant positive relationship between  $\Delta(R_{686}/R_{630})$  and PRI, and  $A_{max}$  (Fig. 5.1A,B). Since the reflectance change at wavelengths around 690 nm has been previously shown to correspond mainly with Chl-F emission from PSII (e.g. Buschmann et al. 1994; Zarco-Tejada et al. 2000a), we assume that the observed relative change of  $R_{686}/R_{630}$  derived from hyperspectral reflectance [ $\Delta(R_{686}/R_{630})$ ] corresponds to trends in “vitality index”  $R_{Fd}$ , which in other studies correlated with  $A_{max}$  of outdoor grown plant species (e.g. Lichtenthaler et al. 2007; Lichtenthaler et al. 2005). This result indicates a potential of RS methods to estimate relative changes in photosynthetic rates under contrasting illumination intensities.

Although Guo and Trotter (2004) investigated plants with contrasting photosynthetic capacities and observed that  $\Delta PRI$  (expressed in their study as PRI at low light intensity subtracted from PRI at saturating light intensity) was negatively related to  $A_{max}$ , we observed significant positive relationship between  $\Delta PRI$  and  $A_{max}$  (Fig. 5.1B). Other study has shown that larger relative change in Z pigment content was associated with lower  $A_{max}$  in both sun and shade leaves (Demmig-Adams and Adams 1992). We also observed, that larger  $\Delta PRI$  was



associated with higher chlorophyll index ratio ( $R_{750}/R_{710}$ ) (Zarco-Tejada et al. 2001) (data not shown), which might explain its significant correlation with  $A_{max}$ . Therefore, more detailed field study should be conducted to resolve the relationships between  $\Delta PRI$ , photosynthetic rates and leaf pigment composition in various outdoor growing plant species.

The strongest relationships between variations in VIs and eddy-covariance physiological parameters were found when measured during the diurnal cycle. In general, reflectance ratios using the Chl-F wavelengths ( $R_{686}/R_{630}$ ,  $R_{740}/R_{800}$ ) were performing better than with PRI (Tab. 5.2).

Number of studies investigating the link between spectral-optical properties and carbon fluxes were primarily interested in PRI as a proxy for LUE (e.g. Gamon et al. 1997; Hall et al. 2008; Hilker et al. 2008; Nichol et al. 2000; Penuelas et al. 1995) and subsequently for estimation of net primary production (NPP) using the Monteith modelling approach (Monteith 1977). Rahman (2004) successfully used PRI derived from Moderate Resolution Imaging Spectroradiometer (MODIS) satellite sensor for estimation of LUE and NPP in boreal forest. However, our results showed that even if the negative effects of shade fraction and non-green vegetation are excluded, PRI still might not be a good indicator of canopy level photosynthetic processes. Our PRI measurements correlated significantly only with LUE of natural grassland (Fig. 5.3) and still PRI was able to explain only 42% of LUE variability (Tab 5.2).

Previous studies showed that leaf level variation of PRI is driven by changes in de-epoxidation state of xanthophyll cycle pigments in antennae that reduce amount of light used in leaf  $CO_2$  assimilation and this way protect leaf from excessive radiation (e.g. Niyogi 1999; Schindler and Lichtenthaler 1996). Similar trend was observed also in our study in case of grassland ecosystem, where LUE slightly decreased during midday (Fig. 5.3B). The midday depression in LUE was not observed in the forest (Fig. 5.4B), where larger proportion of shaded compared to sun exposed needles might determine the diurnal course. Similarly, VIs extracted from hyperspectral image of forest ecosystem correspond to the top of the canopy reflectance originating mostly from sunlit shoots, while the eddy-covariance LUE is integrated within the whole canopy, including the significant proportion of shaded shoots. This discrepancy can disturb the relationships between VIs and the eddy-covariance measurements at the canopy level.

Nevertheless, Chl-F related canopy reflectance ratios ( $R_{686}/R_{630}$ ,  $R_{740}/R_{800}$ ) revealed several statistically significant regression relations with eddy-covariance parameters (Tab. 5.2). Stronger relations with carbon assimilation were observed in forest than in grassland

ecosystem (Tab. 5.2A,B), which might be partially explained by higher chlorophyll content in spruce needles and also by lower water stress, which increases stomatal conductance resulting in stronger Chl-F emission. Intensity of Chl-F is driven mainly by utilization of photosynthetically active radiation inside of thylakoids (Papageorgiou and Govindjee, 2004). Several studies have reported positive correlation of photosynthetic parameters with reflectance ratios related to Chl-F. Dobrowski et al. (2005) found in laboratory a positive relationship between the reflectance ratio  $R_{690}/R_{600}$  and  $CO_2$  assimilation ( $R^2 = 0.36$ ). Carter (1998) observed strong relation of photosynthetic capacity to the Chl-F active spectral region between 685-700 nm. The reflectance ratio  $R_{695}/R_{805}$  was found to be correlated with  $A_{max}$  of 5-years old pine seedlings measured at the canopy level in diurnal course (Carter 1998). Similarly to these previously published results, the reflectance ratio  $R_{686}/R_{630}$ , tested in this study, was found to be a statistically significant proxy of GPP, NEE, and LUE in grassland and also of gLUE in forest ecosystems. Hence, we hypothesize that  $R_{686}/R_{630}$  if approved by future long-term field-based experiments taking place in various ecosystems, might serve as a RS indicator of the ecosystem vegetation productivity parameters.

## 5.5 Conclusions

We conclude that under steady-state conditions “process-related” VIs (PRI;  $R_{686}/R_{630}$ ;  $R_{740}/R_{800}$ ) did not reveal any statistically significant relation to the carbon assimilation rate. Significant correlations were found once the relationships between VIs and physiological parameters were investigated in temporal scale. Within the dark-to-light transition experiment in minutes,  $\Delta(R_{686}/R_{630})$  and  $\Delta PRI$  of natural grassland were able to track changes in canopy carbon assimilation, measured under saturating light conditions. In diurnal course, simple reflectance ratio  $R_{686}/R_{630}$  showed the highest regression on eddy-covariance measured ecosystem parameters among the whole group of investigated VIs. More significant correlations were found for forest rather than grassland canopy. Finding strong statistical relation to GPP and NEE, we intend to propose the  $R_{686}/R_{630}$  ratio as a potential remote sensing indicator of vegetation productivity at the scale of ecosystem. In general, this study provided results relevant to further development of RS methods focusing on estimation of  $CO_2$  fluxes exchange in natural canopies, growing under changing environmental conditions.

## 5.6 Acknowledgements

This work is part of the research supported by grants 2B06068 (MŠMT ČR), 522/07/0759 (GA ČR), IAA 600870701 (GA AV), and by the Research Intention AV0Z60870520 (ISBE). All experiments described in this study were undertaken in the Czech Republic and comply with current laws of the country.

## 5.7 References

- Aubinet M et al. (2000) Estimates of the annual net carbon and water exchange of forests: The EUROFLUX methodology. In: *Advances in Ecological Research*, Vol 30, vol 30, pp 113-175
- Baroli I, Niyogi KK (2000) Molecular genetics of xanthophyll-dependent photoprotection in green algae and plants. *Philosophical Transactions of the Royal Society of London Series B-Biological Sciences* 355:1385-1393
- Bilger W, Bjorkman O, Thayer SS (1989) Light-Induced Spectral Absorbance Changes in Relation to Photosynthesis and the Epoxidation State of Xanthophyll Cycle Components in Cotton Leaves. *Plant Physiology* 91:542-551
- Black SC, Guo X (2008) Estimation of grassland CO<sub>2</sub> exchange rates using hyperspectral remote sensing techniques. *International Journal of Remote Sensing* 29:145-155
- Boelman NT et al. (2003) Response of NDVI, biomass, and ecosystem gas exchange to long-term warming and fertilization in wet sedge tundra. *Oecologia* 135:414-421
- Buschmann C, Langsdorf G, Lichtenthaler HK (2000) Imaging of the blue, green, and red fluorescence emission of plants: An overview. *Photosynthetica* 38:483-491
- Buschmann C, Nagel E, Szabo K, Kocsanyi L (1994) Spectrometer for Fast Measurements of in-Vivo Reflectance, Absorptance, and Fluorescence in the Visible and near-Infrared. *Remote Sensing of Environment* 48:18-24
- Carter GA (1998) Reflectance wavebands and indices for remote estimation of photosynthesis and stomatal conductance in pine canopies. *Remote Sensing of Environment* 63:61-72
- Carter GA, Jones JH, Mitchell RJ, Brewer CH (1996) Detection of solar-excited chlorophyll a fluorescence and leaf photosynthetic capacity using a Fraunhofer Line Radiometer. *Remote Sensing of Environment* 55:89-92
- Demmig-Adams B, Adams WW (1992) Carotenoid composition in sun and shade leaves of plants with different life forms. *Plant Cell and Environment* 15:411-419

- Demmig-Adams B, Adams WW (2000) Photosynthesis - Harvesting sunlight safely. *Nature* 403:371-+
- Dobrowski SZ, Pushnik JC, Zarco-Tejada PJ, Ustin SL (2005) Simple reflectance indices track heat and water stress-induced changes in steady-state chlorophyll fluorescence at the canopy scale. *Remote Sensing of Environment* 97:403-414
- Drolet GG et al. (2005) A MODIS-derived photochemical reflectance index to detect inter-annual variations in the photosynthetic light-use efficiency of a boreal deciduous forest. *Remote Sensing of Environment* 98:212-224
- Farber A, Young AJ, Ruban AV, Horton P, Jahns P (1997) Dynamics of xanthophyll-cycle activity in different antenna subcomplexes in the photosynthetic membranes of higher plants - The relationship between zeaxanthin conversion and nonphotochemical fluorescence quenching. *Plant Physiology* 115:1609-1618
- Filella I, Amaro T, Araus JL, Penuelas J (1996) Relationship between photosynthetic radiation-use efficiency of Barley canopies and the photochemical reflectance index (PRI). *Physiologia Plantarum* 96:211-216
- Flexas J, Briantais JM, Cerovic Z, Medrano H, Moya I (2000) Steady-state and maximum chlorophyll fluorescence responses to water stress in grapevine leaves: A new remote sensing system. *Remote Sensing of Environment* 73:283-297
- Flexas J et al. (2002) Steady-state chlorophyll fluorescence ( $F_s$ ) measurements as a tool to follow variations of net  $CO_2$  assimilation and stomatal conductance during water-stress in C-3 plants. *Physiologia Plantarum* 114:231-240
- Freedman A, Cavender-Bares J, Keabian PL, Bhaskar R, Scott H, Bazzaz FA (2002) Remote sensing of solar-excited plant fluorescence as a measure of photosynthetic rate. *Photosynthetica* 40:127-132
- Fuentes DA et al. (2006) Mapping carbon and water vapor fluxes in a chaparral ecosystem using vegetation indices derived from AVIRIS. *Remote Sensing of Environment* 103:312-323
- Gamon JA, Field CB, Bilger W, Bjorkman O, Fredeen AL, Penuelas J (1990) Remote-Sensing of the Xanthophyll Cycle and Chlorophyll Fluorescence in Sunflower Leaves and Canopies. *Oecologia* 85:1-7
- Gamon JA, Penuelas J, Field CB (1992) A Narrow-Waveband Spectral Index That Tracks Diurnal Changes in Photosynthetic Efficiency. *Remote Sensing of Environment* 41:35-44

- Gamon JA, Serrano L, Surfus JS (1997) The photochemical reflectance index: an optical indicator of photosynthetic radiation use efficiency across species, functional types, and nutrient levels. *Oecologia* 112:492-501
- Gamon JA, Surfus JS (1999) Assessing leaf pigment content and activity with a reflectometer. *New Phytologist* 143:105-117
- Gilmore AM, Bjorkman O (1994) Adenine-nucleotides and the xanthophyll cycle in leaves. 1. Effects of CO<sub>2</sub>- and temperature-limited photosynthesis on adenylate energy charge and violaxanthin de-epoxidation. *Planta* 192:526-536
- Govindjee (1995) Sixty-three years since Kautsky: chlorophyll a fluorescence. *Australian Journal of Plant Physiology* 22, 131–160.
- Grace J, Nichol C, Disney M, Lewis P, Quaipe T, Bowyer P (2007) Can we measure terrestrial photosynthesis from space directly, using spectral reflectance and fluorescence? *Global Change Biology* 13:1484-1497
- Guo JM, Trotter CM (2004) Estimating photosynthetic light-use efficiency using the photochemical reflectance index: variations among species. *Functional Plant Biology* 31:255-265
- Haboudane D, Miller JR, Pattey E, Zarco-Tejada PJ, Strachan IB (2004) Hyperspectral vegetation indices and novel algorithms for predicting green LAI of crop canopies: Modeling and validation in the context of precision agriculture. *Remote Sensing of Environment* 90:337-352
- Hall FG et al. (2008) Multi-angle remote sensing of forest light use efficiency by observing PRI variation with canopy shadow fraction. *Remote Sensing of Environment* 112:3201-3211
- Havrankova K, Sedlak P (2004) Wind velocity analysis for mountainous site Bily Kriz. *Ekologia-Bratislava* 23:46-54
- Hilker T et al. (2008) Separating physiologically and directionally induced changes in PRI using BRDF models. *Remote Sensing of Environment* 112:2777-2788
- le Maire G, Francois C, Dufrene E (2004) Towards universal broad leaf chlorophyll indices using PROSPECT simulated database and hyperspectral reflectance measurements. *Remote Sensing of Environment* 89:1-28
- Lichtenthaler HK (1987) Chlorophylls and carotenoids: pigments of photosynthetic biomembranes. In: *Methods in enzymology*, vol. 148, pp 350-382

- Lichtenthaler HK, Ac A, Marek MV, Kalina J, Urban O (2007) Differences in pigment composition, photosynthetic rates and chlorophyll fluorescence images of sun and shade leaves of four tree species. *Plant Physiology and Biochemistry* 45:577-588
- Lichtenthaler HK, Langsdorf G, Lenk S, Buschmann C (2005) Chlorophyll fluorescence imaging of photosynthetic activity with the flash-lamp fluorescence imaging system. *Photosynthetica* 43:355-369
- Lillesand TM, Kiefer RW (2000) Remote sensing and image interpretation, 4th edn. John Wiley & Sons, New York
- Louis J et al. (2005) Remote sensing of sunlight-induced chlorophyll fluorescence and reflectance of Scots pine in the boreal forest during spring recovery. *Remote Sensing of Environment* 96:37-48
- Maier SW, Günther KP, Stellmes M (2002) Remote sensing and modelling of solar induced fluorescence. 1st Workshop on Remote Sensing of Solar Induced Vegetation Fluorescence (Noordwijk, Netherlands)
- Maxwell K, Johnson GN (2000) Chlorophyll fluorescence - a practical guide. *Journal of Experimental Botany* 51:659-668
- Monteith JL (1977) Climate and Efficiency of Crop Production in Britain. *Philosophical Transactions of the Royal Society of London Series B-Biological Sciences* 281:277-294
- Morosinotto T, Caffarri S, Dall'Osto L, Bassi R (2003) Mechanistic aspects of the xanthophyll dynamics in higher plant thylakoids. *Physiologia Plantarum* 119:347-354
- Myneni RB, Hall FG, Sellers PJ, Marshak AL (1995) The interpretation of spectral vegetation indexes. *IEEE Transactions on Geoscience and Remote Sensing* 33:481-486
- Nakaji T et al. (2008) Utility of spectral vegetation indices for estimation of light conversion efficiency in coniferous forests in Japan. *Agricultural and Forest Meteorology* 148:776-787
- Nichol CJ et al. (2000) Remote sensing of photosynthetic-light-use efficiency of boreal forest. *Agricultural and Forest Meteorology* 101:131-142
- Nichol CJ et al. (2002) Remote sensing of photosynthetic-light-use efficiency of a Siberian boreal forest. *Tellus Series B-Chemical and Physical Meteorology* 54:677-687
- Niyogi KK (1999) Photoprotection revisited: Genetic and molecular approaches. *Annual Review of Plant Physiology and Plant Molecular Biology* 50:333-359

- Papageorgiou GC, Govindjee (2004) Chlorophyll a fluorescence: a signature of photosynthesis. *Advances in photosynthesis and respiration*. Vol. 19, Springer, Dordrecht, Netherlands
- Papageorgiou GC, Tsimilli-Michael M, Stamatakis K (2007) The fast and slow kinetics of chlorophyll a fluorescence induction in plants, algae and cyanobacteria: a viewpoint. *Photosynthesis Research* doi: 10.1007/s11120-007-9193-x
- Penuelas J, Filella I, Gamon JA (1995) Assessment of Photosynthetic Radiation-Use Efficiency with Spectral Reflectance. *New Phytologist* 131:291-296
- Perez-Priego O, Zarco-Tejada PJ, Miller JR, Sepulcre-Canto G, Fereres E (2005) Detection of water stress in orchard trees with a high-resolution spectrometer through chlorophyll fluorescence in-filling of the O-2-A band. *Ieee Transactions on Geoscience and Remote Sensing* 43:2860-2869
- Rahman AF, Cordova VD, Gamon JA, Schmid HP, Sims DA (2004) Potential of MODIS ocean bands for estimating CO<sub>2</sub> flux from terrestrial vegetation: A novel approach. *Geophysical Research Letters* 31
- Rahman AF, Gamon JA, Fuentes DA, Roberts DA, Prentiss D (2001) Modeling spatially distributed ecosystem flux of boreal forest using hyperspectral indices from AVIRIS imagery. *Journal of Geophysical Research-Atmospheres* 106:33579-33591
- Schaepman ME (2007) Spectrodirectional remote sensing: From pixels to processes. *International Journal of Applied Earth Observation and Geoinformation* 9:204-223
- Schindler C, Lichtenthaler HK (1996) Photosynthetic CO<sub>2</sub>-assimilation, chlorophyll fluorescence and zeaxanthin accumulation in field grown maple trees in the course of a sunny and a cloudy day. *Journal of Plant Physiology* 148:399-412
- Soukupova J et al. (2008) Annual variation of the steady-state chlorophyll fluorescence emission of evergreen plants in temperate zone. *Functional Plant Biology* 35:63-76
- Theisen AF, Rock BN, Eckert RT (1994) Detection of changes in steady-state chlorophyll fluorescence in *Pinus strobus* following short-term ozone exposure. *Journal of Plant Physiology* 144:410-419
- Urban O et al. (2007a) Temperature dependences of carbon assimilation processes in four dominant species from mountain grassland ecosystem. *Photosynthetica* 45:392-399
- Urban O et al. (2007b) Ecophysiological controls over the net ecosystem exchange of mountain spruce stand. Comparison of the response in direct vs. diffuse solar radiation. *Global Change Biology* 13:157-168

Ustin SL, Roberts DA, Gamon JA, Asner GP, Green RO (2004) Using imaging spectroscopy to study ecosystem processes and properties. *Bioscience* 54:523-534

Zarco-Tejada PJ, Miller JR, Mohammed GH, Noland TL (2000a) Chlorophyll fluorescence effects on vegetation apparent reflectance: I. Leaf-level measurements and model simulation. *Remote Sensing of Environment* 74:582-595

Zarco-Tejada PJ, Miller JR, Mohammed GH, Noland TL, Sampson PH (2000b) Chlorophyll fluorescence effects on vegetation apparent reflectance: II. Laboratory and airborne canopy-level measurements with hyperspectral data. *Remote Sensing of Environment* 74:596-608



## CHAPTER 6

Angular chlorophyll indices estimates derived from ground-based diurnal course data and multiangular CHRIS-PROBA data: two case studies

*Jochem Verrelst<sup>(1)</sup>, Alexander Ač<sup>(2,3)</sup>, Zbyněk Malenovsky<sup>(2)</sup>, Jan Hanuš<sup>(2)</sup>, Michal V. Marek<sup>(2)</sup>, Michael E. Schaepman<sup>(1)</sup>*

(1) Centre for Geo-Information, Wageningen University, Droevendaalsesteeg 3 / PO Box 47, 6700 AA Wageningen, The Netherlands

(2) Institute of Systems Biology and Ecology, Academy of Sciences of the Czech Republic, Poříčí 3b, Brno, 603 00, Czech Republic

(3) Agricultural Faculty, University of South Bohemia, Studentská 13, České Budějovice, 370 05, Czech Republic

Published in: *Proceedings 5<sup>th</sup> EARSeL Workshop on Imaging Spectroscopy. Bruges, Belgium, April 23-25 2007*

## **Abstract**

At leaf and plant level chlorophyll indices have shown strong correlations with chlorophyll content and photosynthesis-related processes. However, at canopy level additional abiotic and biotic factors confound the fidelity of these indices. In this paper we present case studies of two natural canopies at different scales where the influence of sun-target-sensor geometry and canopy structure is inter-compared for a range of chlorophyll indices.

In the first case study, surface reflectance was measured in a montane grassland ecosystem located at the Bily Kriz experimental study site (Czech republic) using a stationary mounted AISA (Airborne Imaging Spectrometer for Applications) spectrometer. The experimental set-up resulted in a ground pixel resolution of ~2mm. The effects of changing sun angles on the indices were assessed through a diurnal sampling between 9:00 and 15:00 hrs (local time). Classes of shaded and illuminated photosynthetic (PV) and non-photosynthetic vegetation (NPV) were distinguished per image using a pixelwise classification. The relative contributions of confounding factors as well as the influence of the diurnal variability on performance of the selected chlorophyll indices were evaluated.

In the second case study, surface reflectance was measured over an Alpine coniferous ecosystem in the Swiss National Park (Switzerland) using multiangular hyperspectral CHRIS-PROBA (Compact High Resolution Imaging Spectrometer onboard the Project for On-board Autonomy) satellite system with a ground pixel resolution of 17 m. The angular signature of PRI and the structure invariant pigment index (SIPI) was assessed using CHRIS data. Besides, we evaluated the influence of varying tree crown composition and varying viewing angles to the chlorophyll indices with a radiative transfer model FLIGHT.

In both cases, the PRI and the green NDVI (gNDVI) responded extremely sensitively to the considered confounding factors at canopy level. The Transformed Chlorophyll Absorption in Reflectance Index normalized by the Optimized Soil-Adjusted Vegetation Index (TCARI/OSAVI), designed to be insensitive to background and LAI variations, responded more sensitively than the conventional NDVI. No certain sensitivity was found for SIPI. The pronounced sensitivity of e.g. PRI and gNDVI, on one hand, and the inconsistency between the chlorophyll indices, on the other hand, erodes the fidelity to use these spectral indices as an effective non-destructive chlorophyll detector.

*Keywords:* Vegetation index, uncertainty, scale, hyperspectral imaging, ecosystems, model FLIGHT

## 6.1 Introduction

With the advent of hyperspectral imaging, numerous optical vegetation indices (VIs) have been proposed in the literature to retrieve chlorophyll content from spectroradiometric data. The main aim of these chlorophyll-sensitive indices - or simply chlorophyll indices - is to identify optimal mathematical formulations of spectral bands in order to maximize the sensitivity to chlorophyll content, while minimizing variations arising from other confounding factors. Within this family of indices, the Photochemical Reflectance Index (PRI) (Gamon et al. 1992) has taken the advantage of existing specific spectral feature sensitive to dynamic photosynthetic processes. At leaf and plant level, this index has shown good correlations with short-term and diurnal changes in zeaxanthin pigment concentration (Gamon et al. 1992; Filella et al. 2004) and fluorescence parameters, that are related to zeaxanthin (Evain et al. 2004), and thus to light use efficiency (LUE) parameter (Gamon et al. 2002). PRI also tracks seasonal changes in leaf-level photosynthetic capacity (Stylinsky et al. 2002) but tends to be species specific (Guo et al. 2004). However, PRI is affected not only by xanthophyll cycle activity, but also indirectly by other abiotic and biotic factors. At leaf level external factors are generally well controlled, but once up-scaling to canopy level, additional factors notably affect the relationships. Examples of airborne (Nichol et al. 2000; 2002; Rahman et al. 2001), satellite-based (Rahman et al. 2004; Drolet et al, 2004) studies and a modelling study (Barton et al. 2001) reported that PRI measures are substantially distorted by the fraction of non-photosynthetic vegetation (NPV; woody elements, e.g. branches, trunks) and the fraction of soil present in a pixel (Filella et al. 2004; Sims et al. 2002).

The problem for chlorophyll indices when up-scaled to canopy level is the propagation of increased complexity due to canopy composition and bidirectional reflectance distribution function (BRDF) effects. In its simplest form, a natural canopy can be considered as a unique and complex volumetric composition of photosynthetic vegetation (PV) elements and NPV elements and possibly soil elements, which each of them are either in sunlit or shaded state. The observed proportions of these elements depend on the sun-target-sensor geometry, and each of these elements affects the reflectance signal. Furthermore, only from the detected PV elements chlorophyll content or photosynthesis-related information can be retrieved, whereas all the other elements play role of distorters.

Apart from PRI, also other chlorophyll indices gained popularity in ecophysiological studies at canopy level. Some of these indices were specifically developed to stay invariant to influence of these confounding factors, such as the Structure-Invariant Pigment Index (SIPI)

(Penuelas et al. 1995) or the Transformed Chlorophyll Absorption in Reflectance Index normalized by the Optimized Soil-Adjusted Vegetation Index (TCARI/OSAVI) (Haboudane et al. 2002), designed to be insensitive to background and LAI variations). However, the robustness of the indices to canopy composition and BRDF effects is largely unknown and hence seriously erodes the reliability of the retrieved products. Therefore, prior to consider the use of chlorophyll indices at canopy level as an effective non-destructive chlorophyll detection method, the following key question ought to be clarified:

*Is there sufficient fidelity that the estimates of chlorophyll-related indices can be truly interpreted with respect to chlorophyll content or photosynthesis-related processes?*

To answer this question, we present case studies of two natural canopies where we quantify in either case the response of chlorophyll indices to varying sun-target-sensor geometry and canopy composition. This implies that the scope of this work was not to evaluate how well a chlorophyll index was correlated with field-measured chlorophyll estimates, but rather how sensitively an index responded to one of the aforementioned confounding factors. As a result of this analysis we categorized the indices in terms of its robustness to the tested distorters. The case studies are:

- *Diurnal ground-level AISA data of a Montane grassland (Bily Kriz, Czech republic)*  
With an AISA sensor mounted downwards a tripod at 4m height, diurnal hyperspectral data of a super spatial resolution of ~2mm over a heterogeneous meadow was acquired. The high spatial resolution enabled the discrimination of single canopy components. While a range of diurnal data acquisitions enabled the assessment of the effects of changing solar angle.
- *Angular CHRIS data of a Coniferous forest (Swiss National Park, Switzerland)*  
Spaceborne multiangular CHRIS data acquired above a heterogeneous old-growth forest provided unprecedented capabilities to assess the angular variability of narrowband indices. By using a 3D radiative transfer model called FLIGHT (North, 1996) we compared CHRIS-derived angular VI signatures with simulated VI signatures. With FLIGHT we systematically evaluated how chlorophyll indices respond to changing viewing angles and changing canopy composition.

## 6.2 Methods

Both case studies focus on the response of several chlorophyll indices as a function of sun-target-sensor and canopy composition variability. But they differ in scale and approach. The meadow study uses ground-level super-resolution AISA data to assess the effects of diurnal change on canopy composition, whereas the forest canopy case study uses CHRIS data and FLIGHT to assess the effects of variable viewing angles and canopy structure.

The selected chlorophyll indices are presented in Tab. 6.1. Since the behaviour of the NDVI is already well understood, the index is added as a reference index. The chlorophyll indices are: PRI, SIPI, gNDVI (green NDVI) and TCARI/OSAVI.

Table 6.1. Selected VIs used in this study with a central wavelength corresponding to both, AISA and CHRIS-PROBA bands.

Index	Algorithm	Measure of
NDVI (Rouse et al. 1973)	$\frac{(R_{780} - R_{672})}{(R_{780} + R_{672})}$	greenness
PRI (Gamon et al. 1992)	$\frac{(R_{530} - R_{570})}{(R_{530} + R_{570})}$	Light use efficiency
SIPI (Penuelas et al. 1995)	$\frac{(R_{780} - R_{443})}{(R_{780} + R_{705})}$	Carotenoid and Chl a Insensitive to structure
TCARI/OSAVI (Haboudane et al 2002)	$\frac{3 * [(R_{700} - R_{672}) - 0.2 * (R_{700} - R_{562}) * (R_{700}/R_{672})]}{(1 + 0.16) * (R_{800} - R_{672}) / (R_{800} + R_{672} + 0.16)}$	Chlorophyll content Insensitive to LAI and background variations
gNDVI (Smith et al. 1995)	$\frac{(R_{555} - R_{677})}{(R_{555} + R_{677})}$	Chlorophyll

Further, the eventual influence of the dissimilar AISA and CHRIS bandwidths on the VI results were evaluated with AISA data by means of a linear regression. The high correlations for each index ( $R^2 > 0.99$ ) provided confidence that the different bandwidth configuration of AISA sensor (2 nm FWHM) and CHRIS (10 nm FWHM) had a negligible effect on the computed VIs values.

In either case study, each index was normalized variance as follows:

$$\Delta VI = \frac{VI_{variable} - VI_{reference}}{VI_{reference}} * 100\% \quad (6.6.1)$$

where the reference corresponds to solar noon (12:30u) and nadir values in the case of AISA and CHRIS respectively.

### 6.3 Case study I: Sensitivity of montane grassland vegetation indices using diurnal AISA data measured at ground

#### 6.3.1 Data acquisition and study site

In the first case study we evaluated the effects of diurnal changes on the indices using ground-based nadir measurements. At 4 m above a meadow canopy an hyperspectral AISA Eagle was mounted downwards on a tripod. Five measurements were consecutively taken from 9:00 local time until 15:00 (Tab. 6.2). A montane grassland research plot, located at the Bílý Kříž experimental study site (18.54°E/49.49°N, 898 m a.s.l.) in the Beskydy Mts. (Czech republic), was chosen as test site due to its high species diversity, with around 25 herbaceous species (phytocenological analysis in 2004). The most abundant species at the measured plot were *Festuca rubra agg.*, *Hieracium sp.*, *Plantago sp.*, *Nardus stricta* and *Jacea pseudophrygia*. The Beskydy Mts. are characterized as cool and humid with annual precipitation of about 1000 – 1400 mm. The Leaf Area Index (LAI) of the grass canopy was during the data acquisition between 3 and 3.5. The inclination of the plot was slight, with orientation to south-east.

Table 6.2. AISA sensor configuration during diurnal measurement.

Sampling	Image area	Sun zenith angles	Local time	Spectral bands	Spectral range
~2.2 mm @ 4 m altitude	1 x 3 m (500 x 1500 pixels)	5 nominal angles @ - 51°, 35°, 26°, 29° and 38°	5 nominal times @ 9:00, 11:00, 12:30, 14:00 and 15:00	260 bands with 2nm width	450-940 nm

#### 6.3.2 Classification and resampling

In order to identify the diurnal variability occurring at ~2mm scale, the five meadow images were classified using the Maximum Likelihood classifier into four classes: i) fully sun-exposed green vegetation, ii) partly shaded vegetation (S: green leaves under diffuse light), iii) vegetation under “deep shade” (DS: dark parts deeply penetrated in the canopy), and iv) non-photosynthetic vegetation (NPV: flowers, dry leaves) (Fig. 6.1). The influence of the confounding classes NPV and shade (S and DS) on the indices will be further analyzed. Next, the original spatial resolution was resampled to a much coarser resolution (0.1 × 0.2m). With this classified image not only the effects of NPV and shade on the indices can be assessed, but also the effects of the diurnal course per canopy class.

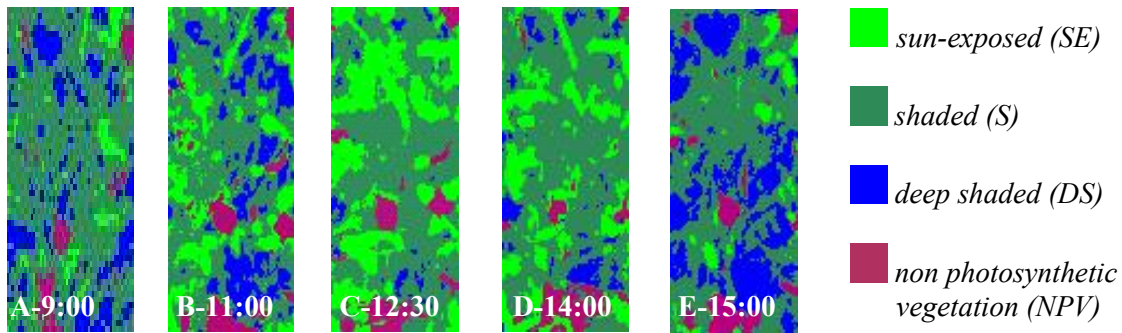


Figure 6.1. Automatic classification of the representative area in diurnal course (pixel size of 0.1 x 0.2m; N=8145 pixels). The overall classification accuracy was between 83.1-87.8% with kappa coefficient between 0.78 – 0.83.

For each index, the influence of each single confounding class (CC: S, DS or NPV) was evaluated by plotting per resampled pixel the relative influence against the fraction of that confounding class. The relative VI influence is compared to the VI value of the joined fractions of SE and CC:

$$VI_{\text{Relative difference}} = VI_{(SE + CC) \text{ fraction}} - VI_{CC \text{ fraction}} \quad (6.6.2)$$

where  $VI_{SE \text{ fraction}}$  is the index value of the sun-exposed (SE) pixels and  $VI_{CC \text{ fraction}}$  is the index value of a given confounding class.

From each of these plots a linear regression was drawn and significance of the slope was tested. Subsequently, the steepness of the slope indicates the dependency on a given class. Finally, for each index the normalized diurnal course (Eq. 6.6.1) was determined, both for the mixed pixels as well for the sunlit-exposed class.

## 6.4 Results

Regarding the nadir-detected diurnal variability of the meadow classes, most of the observed changes were due to changes in sun-exposed vegetation (4-32%) trading off with vegetation under deep shade (4-25%) as a result of changing solar angles (Fig. 6.2). The fraction of NPV (between 5-7%) and shaded vegetation (between 58-66%) stayed relatively constant during the daily course. The observed high fraction of green vegetation under diffuse light (S pixels) is likely due to the grass structure dominated by erectophyl plant types.

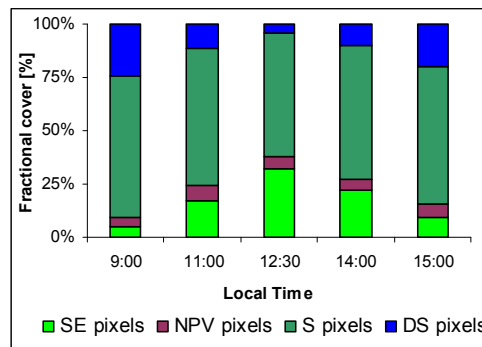


Figure 6.2. Histogram showing diurnal variation in defined classes.

The contribution of the distorters (i.e., S, DS, and NPV) was assessed for each index by evaluating the slopes of the linear regressions (Fig. 6.3). A negative slope indicates a decrease of the index values at canopy level due to a given class (see performance of NPV). In case of TCARI/OSAVI even all distorters had a negative impact on the signal. A positive slope means that a given class is responsible for an increase in the index response at canopy level (in most cases of S and DS).

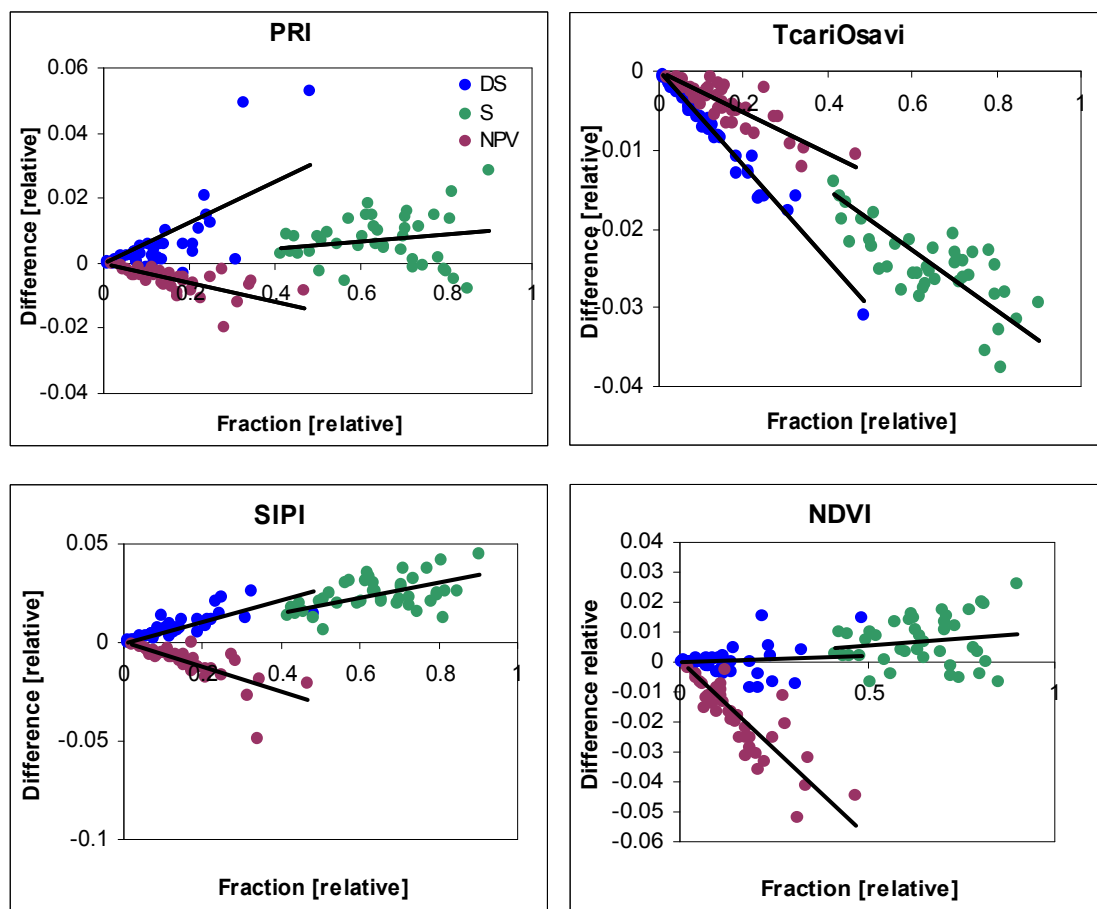


Figure 6.3. Sensitivity of PRI (A), TCARI/OSAVI (B), SIPI (C) and NDVI (D) to deep shade (DS, blue), shade (S, green) and non-photosynthetic vegetation (NPV, red) at 12:30 (local time).



When comparing the slopes of all diurnal data (Tab. 6.3), the gNDVI index responded strongly to the confounding factors, with oscillating negative and positive slopes during the day for the S and DS fractions. The slopes of the other indices were more consistent during the day period. PRI and TCARI/OSAVI were sensitive to DS fraction, while NDVI and SIPI were less affected by the considered distorters. In general, each VI showed higher sensitivity to DS than to S fraction. Hence, we recommend being careful when interpreting chlorophyll indices results for canopies with significant fraction of deep shade.

Table 6.3. Slopes of linear regressions of compared VIs in the diurnal course. Asterisks show statistical significance of linear regression at  $p < 0.05$ (\*) and  $p < 0.01$ (\*\*) levels.

Time	distorter	PRI	TCARI/OSAVI	NDVI	gNDVI	SIPI
9:00	DS	0.135**	-0.126**	0.086**	0.193*	0.035*
	S	0.034*	-0.078**	0.051	0.009	0.016
	NPV	-0.003	-0.070**	-0.06**	-0.352**	-0.123**
12:30	DS	0.062	-0.060**	0.022	-0.231**	0.054**
	S	0.010	-0.037**	0.033	-0.078**	0.037**
	NPV	-0.030**	-0.027**	-0.117**	-0.382**	-0.060**
15:00	DS	0.096**	-0.092**	0.069**	0.010	0.025*
	S	0.027**	-0.058**	0.048*	0.037	-0.006
	NPV	-0.011	-0.052**	-0.088**	-0.358**	-0.142**

The stronger sensitivity of PRI and gNDVI can be explained by wavelengths of only visible part used for their computation. Low vegetation reflectance in the visible wavelengths can cause big differences between two adjacent bands when normalized. However, a similar sensitivity of TCARI/OSAVI, which also uses a NIR wavelength, was in this context unexpected, because TCARI/OSAVI was designed to be a robust index for LAI and background variability.

#### 6.4.1 Diurnal course

When observing the sun angle effects for all pixels (Fig. 6.4A) then each VI showed an increasing trend with increasing SZA, except for TCARI/OSAVI. The reason for this increase is higher fraction of shaded vegetation. Similar observations were found at canopy level for NDVI (Haboudane et al. 2002; Rouse et al. 1973). The fluctuating behaviour of

TCARI/OSAVI can be partly explained by the negative sensitivity to shade. PRI has a remarkable higher variability that can be potentially explained by the high sensitivity to the deep shade vegetation (Tab. 6.3). Also, because at noon the PRI value was close to zero (normalization value: 0.015), a similar change as for instance for the NDVI (normalization value: 0.9), will result in a much higher variability.

The NDVI, SIPI and gNDVI values showed a slight decrease with decreasing SZAs when isolating only green sun-exposed pixels (Fig. 6.4B). Conversely, PRI showed again a pronounced angular response, closely followed by TCARI/OSAVI. Whether this variability can be related to the varying diurnal concentration of the zeaxanthin pigment remains questionable. In fact, diurnal chlorophyll measurements on the same grassland plot one year earlier (2005) did not exhibit any significant diurnal course.

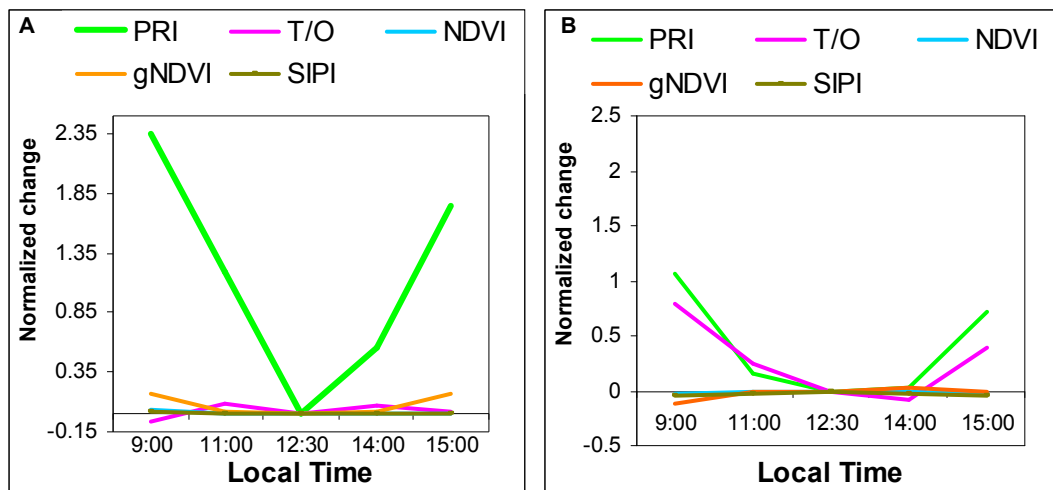


Figure 6.4. Noon-normalized diurnal courses of VIs for all pixels (A) and for sun-exposed pixels only (B).

Finally, from each angular signature the standard deviation (SD) of normalized VIs values was calculated as a quantitative measure of their inter-comparability (Tab. 6.4). Considering all pixels as well as solely sunlit pixels the PRI outreached the other indices. The SD works properly as long as the index does not fluctuate around the normalized value, as is the case for the TCARI/OSAVI of all pixels. TCARI/OSAVI and gNDVI showed considerable variability while NDVI and SIPI stayed rather invariant.

Table 6.4. Normalized standard deviations as calculated from values in figure 6.4.

Normalized SDs	PRI	TCARI/OSAVI	NDVI	gNDVI	SIPI
All pixels	9.32	0.54	0.11	0.85	0.08
Sulit pixels	4.77	3.5	0.1	0.57	0.2

## 6.5 Case study II: Sensitivity of coniferous forest vegetation indices using multiangular CHRIS-PROBA data and FLIGHT modelling

### 6.5.1 Data and study site

This second case study capitalizes on the use of a unique combination of hyperspectral and directional data set provided by CHRIS-PROBA. The CHRIS data set ideally has the capabilities to assess the angular response of various narrowband vegetation indices. Its specifications are shown in Tab. 6.5. The used CHRIS image set, acquired on June 27 2004 10:41h AM local time under partly cloudy conditions (1/8<sup>th</sup> cloud cover), was geometrically and radiometrically corrected following an approach dedicated for rugged terrains (Kneubühler et al. 2005). Five scenes of the test site had a geometric accuracy of 1-2 pixels. The generated ‘surface reflectance’ represents hemispherical-directional reflectance factor (HDRF) (Schaeppman-Strub et al. 2006). The +21° scene is the (near-) nadir scene while the -55° scene happened to be viewing predominantly back scattering (Fig. 6.3).

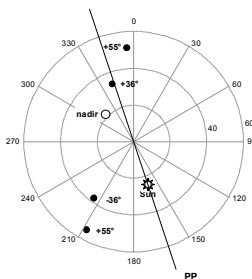


Table 6.5. CHRIS configurations for Land Mode 3

Sampling	Image area	Spectral bands	Spectral range
~17 m @ 556 km altitude	13 x 13 km (744 x 748 pixels)	18 bands with 6-33nm width	447-1035 nm

Figure 6.5. Polar plot of CHRIS acquisition and illumination geometry as of June 27, 2004. PP: principal plane

The study site is located in the eastern Ofenpass valley, which is part of the Swiss National Park (SNP) in South East Switzerland (10°13'48"E/46°39'45"N). The Ofenpass represents a dry inner-alpine valley with rather limited precipitation (900-1100 mm/a) on an average altitude of about 1900 m a.s.l.. The south-facing slope of the Ofenpass valley is considered as the core test site. The evergreen coniferous forest is dominated by mountain pine (*Pinus Montana ssp. arborea*). The forest structure is characterized by varying density and a relatively high fraction of woody elements (ca. 30%) due to the advanced age of the pine forest and nature management practice that stopped 70 years ago. Average LAI is 2.2 (1.0 SD). The understory is characterized by low and dense vegetation composed mainly of *Vaccinium*, *Ericaceae*, and *Seslaraiia* species.

In a previous work using CHRIS data of the SNP coniferous forest (Verrelst et al. 2007) several vegetation indices gave sign of a pronounced anisotropic behaviour, particularly indices related to chlorophyll and other foliar pigment. It was suggested that an eventual increased proportion of NPV could significantly affect those chlorophyll VIs. In this study it was assessed whether the above suggested hypothesis is valid by using a radiative transfer model FLIGHT (Flight, 1996), where viewing angles and canopy composition can be systematically controlled.

#### FLIGHT modeling

With FLIGHT, evaluation of the Bidirection Reflectance Factor (BRF) is achieved by deterministic photon ray tracing within the discontinuous environment of a simulated forest canopy. The model allows the representation of complex vegetation structures and a correct treatment of spectral mixing resulting from multiple scattering within the scene. FLIGHT simulates a 3D forest canopy by geometric primitives with defined shapes and positions of individual stands with associated shadow effects. Within each crown envelope foliage is approximated by volume-averaged parameters with optical properties of both leaf (PV) and woody scattering elements (NPV) (North, 1996).

We simulated canopy reflectance consisting of stands with crown envelopes of various PV-NPV mixtures as a function of field-measured canopy variables and CHRIS acquisition geometries. The distribution of PV and NPV elements within the crown was random. We firstly modelled canopy reflectance for stands with solely NPV elements, followed by stands consisting of PV-NPV mixtures with consecutive PV increments of 20%, up to finally stands with solely PV elements. As for FLIGHT parameterization the averaged field measurements of four core test sites within the forest were used (Tab. 6.4). The foliage optical properties were modelled by PROSPECT (Jacquemoud and Baret, 1992) coupled with FLIGHT (Kotz et al. 2004) while the spectral properties of the woody parts and understory were characterized by spectrometric field measurements. The spectral properties of the vegetated understory were kept constant. This implies that even for a 100% NPV stand, due to the relatively low LAI and fractional cover, the signal still behaved as a typical vegetation signature.

Name	Value/ Range	PV	NPV
Fractional cover (%)	0.64		
Leaf Area Index	2.4		
Fraction of green foliage (%)		100%	0%
Fraction of bark (%)		0%	100%
Incident zenith ( $^{\circ}$ ), $\theta_i$	24.0		
Reflected zenith ( $^{\circ}$ ), $\theta_r$	-54.6, -37.8, +21.2 (nadir), +33.3, +51.1		

Table 6.6. Averaged input variables for FLIGHT parameterization collected at four test sites. (Remaining input variables are described in Flight, 1996)

Once having the simulations completed, indices can be calculated as a function of PV-NPV mixture and viewing angle. By increasing the NPV fraction at greater zenith angles the assumption of a likely greater contribution to an angular VI signature can be assessed.

Further, a sensitivity study was conducted by calculating per-index the variance of varying canopy composition and viewing angle combinations. This was done as follows. First, for each PV-NPV combination the normalized angular change was compared to a reference angle (nadir) according to equation (6.6.1).

Next, from the generated  $\Delta VI$ 's for each viewing angle the variance ( $\sigma^2$ ) of the PV-NPV mixtures was calculated. Since each index is normalized to a standard reference point the variance could be interpreted as a standardized measure of canopy structure spread in comparison to viewing angles. As such, quantitative comparison between the indices was possible. Finally, the above procedure was repeated but then by normalizing each PV-NPV combination to a reference of 60-40% of PV-NPV and then calculating the variance of the viewing angles.

## 6.6 RESULTS

The hypothesis that a greater contribution of NPV at greater viewing angles affects the angular signature of chlorophyll indices was tested for PRI and SIPI in Fig. 6.6. The upper left figure shows the angular PRI signature normalized against the nadir value as measured by CHRIS for the study site. The upper right figure shows normalized FLIGHT-modelled PRI's derived from various PV-NPV combinations. The values were normalized against a reference of 80%PV at nadir position. The FLIGHT results clearly show that when increasing the NPV content at greater zenith angles, the PRI response tend to fall down, virtually reaching a shape as observed by CHRIS. With SIPI, however, rather invariant responses were observed, both by CHRIS, both by FLIGHT with changing NPV fractions.

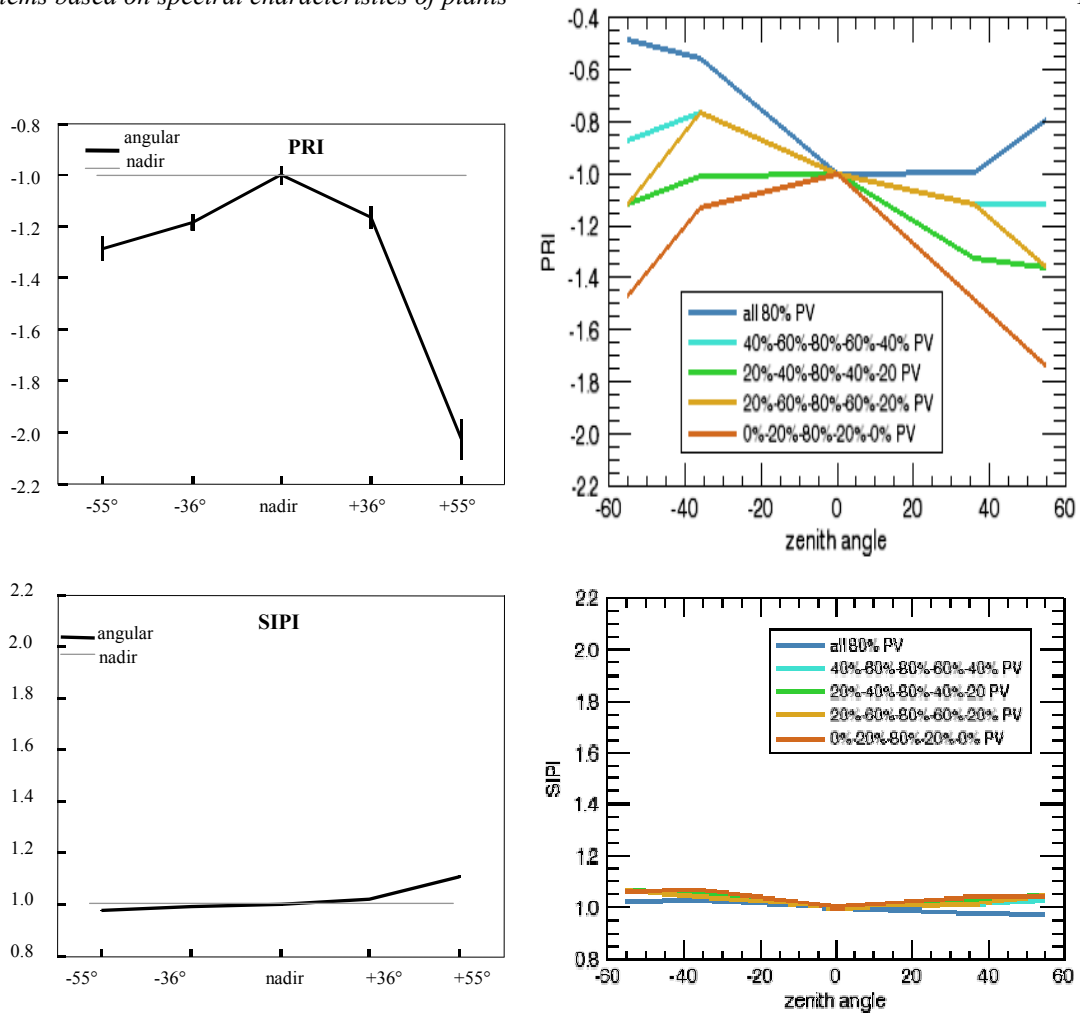


Figure 6.6. Averaged angular PRI and SIPI from forest acquired by CHRIS with error bars of  $\pm 1$  SEM (a). PRI derived from FLIGHT-BRFs with varying fractions of PV and NPV along the CHRIS viewing geometry (b). (% NPV = 100 - % PV)

### 6.6.1 Chlorophyll indices sensitivity analysis

The sensitivity analysis consisted of two parts: (1) normalizing the indices that are calculated for all combinations (viewing angle – canopy composition) to a standard value, and (2) calculating the variability of these normalized indices by means of the standard deviation ( $SD = \sqrt{\sigma^2}$ ). The results of first part of the sensitivity assessment are shown in Fig. 6.7 where for each PV-NPV combination the angular response was normalized to nadir position. These graphs clearly show that PRI and TCARI/OSAVI responded strongly anisotropic when increasing the PV fractions, while SIPI and NDVI responded rather invariant.

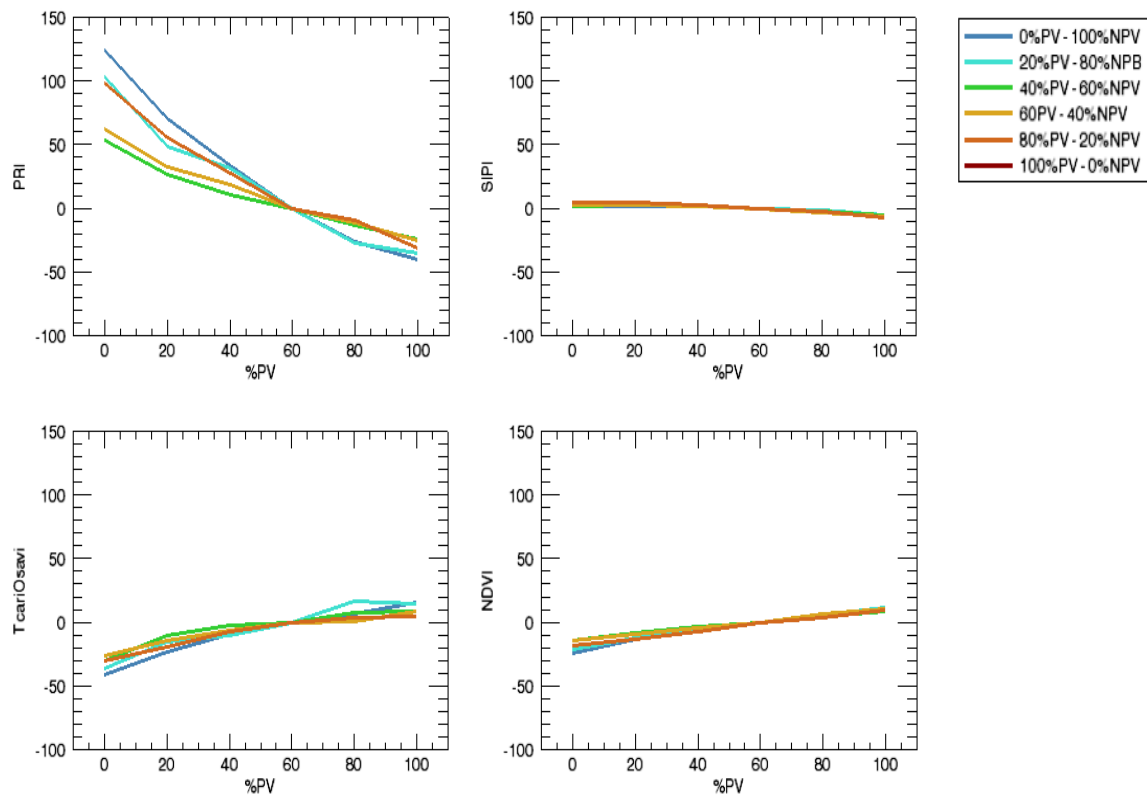


Figure 6.7. Normalized angular signatures of PRI, SIPI, TCARI/OSAVI and NDVI calculated from FLIGHT-BRFs for stands various PV-NPV mixtures.

Based on the above results for each index and for each viewing angle the SD of the PV-NPV mixtures were calculated (Fig. 6.8A). The figure indicates that gNDVI was most sensitive to varying canopy composition, particularly in backscatter direction, followed by PRI and TCARI/OSAVI, respectively. Only SIPI did not show any variability.

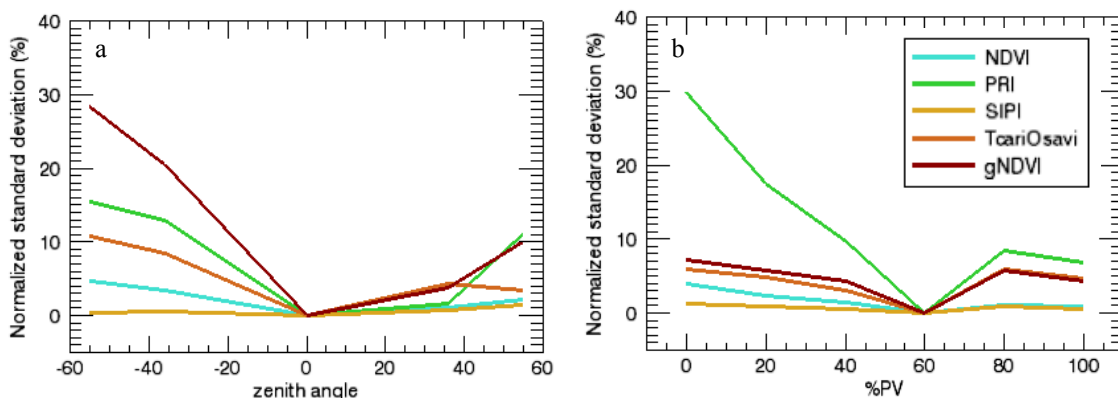


Figure 6.8. Standard deviations of VIs calculated from the (a) per-angle PV-NPV variability and (b) per-PV-NPV mixture angular variability.

When calculating the SDs of the viewing angles per PV-NPV mixture (the same approach as in Fig. 6.4), the SD was greatest for PRI (Fig. 6.8B). TCARI/OSAVI and gNDVI

responded as second and third most sensitive indices - more than NDVI - while again SIPI responded invariantly.

From the SDs presented in both figures (6.8A) and (6.8B), a final per-index SD was calculated in case of (a) for variable viewing angles and (b) for variable canopy composition (Tab. 6.7). When summing up these two SDs, a per-index value of total spread was generated, enabling a quantitative comparison. This comparison was done by ranking the indices from the largest total SD to the lowest total SD. Based on such ranking the PRI and gNDVI can be labelled as ‘*extremely*’ sensitive, the TCARI/OSAVI can be labelled as ‘*moderately*’ sensitive and SIPI can be labelled as ‘*insensitive*’ to the assessed abiotic and biotic factors.

Index	SD (SD[PV-NPV mixtures per viewing angle])	SD (SD[viewing angles per PV-NPV mixtures])	Summed SDs
PRI	6.97	10.34	17.32
gNDVI	11.74	2.48	14.22
TCARI/OSAVI	4.23	2.26	6.49
NDVI	1.83	1.38	3.21
SIPI	0.52	0.41	0.93

Table 6.7. Ranked SDs of the in Figure 6.8 calculated SDs.

## 6.7 Conclusions

The reflectance properties of individual leaves are insufficient to describe the remotely sensed response of vegetation at canopy scale, as it is rather function of an assemblage of PV and NPV elements that are either sunlit or shaded. It was recognized in recent literature that perturbations due to additional abiotic and biotic factors are the key factors inhibiting successful understanding of the retrieved PRI measure (Barton and North, 2001; Filella et al. 2004).

Triggered by the above studies, this work attempted to evaluate at canopy level the fidelity of PRI compared to other chlorophyll indices as estimators of chlorophyll content or photosynthesis-related processes. The influences of variable sun-target-sensor geometry and canopy composition on the indices were assessed from ground-based and spaceborne hyperspectral data over alpine meadow and montane coniferous forest, respectively. Combining the findings of the both studies led to the following conclusions:

- **PRI** responded extremely sensitively to sun-target-sensor geometry and canopy structure. Caution is, therefore, recommended when interpreting PRI estimates. In heterogeneous natural canopies, with a mixture of PV-NPV elements, PRI becomes less effective as indicator of chlorophyll-related processes (e.g., LUE, stress or



fluorescence indication). Also, a BRDF correction is desired when using PRI in multitemporal studies.

- **gNDVI** responded extremely sensitively to the variances in case of the alpine meadow. The observed steep slopes and oscillating diurnal behaviour considerably weakened the fidelity of this index.
- In the meadow case **TCARI/OSAVI** was found to be relatively highly sensitive to shaded vegetation. With FLIGHT the TCARI/OSAVI varied twice as much as NDVI. The overall impression arises conclusion that this index has a fidelity that is in-between the gNDVI and NDVI.
- **SIPI** responded rather insensitively to variability in canopy composition and variability in sun-target-sensor geometry. Nevertheless, this invariance raises questions how accurately SIPI is capable to track chlorophyll variation.

It was shown in both case studies that particularly PRI and gNDVI, but also TCARI/OSAVI, were influenced by external abiotic and biotic factors. This lack of fidelity at canopy level suggests that the general applicability and performance of selected chlorophyll indices should be still tested. Therefore, prior to developing new indices further research on the behaviour of existing indices is desired. In particular, attention should be paid to investigate how much variability in the measures is explained by pigment variability itself and how much by additional factors. Then a follow-up work should be devoted to develop for each index a quality assessment such as the degree of confidence. Such an indicator should be provided jointly with the retrieved chlorophyll map.

## 6.8 References

- Barton CVM & PRJ North (2001) Remote sensing of light use efficiency using the photochemical reflectance index: Model and sensitivity analysis. *Remote Sensing of Environment* 78:264–273
- Björkman O, Demmig-Adams B (1995) Regulation of photosynthetic light energy capture, conversion, and dissipation in leaves of higher plants. In: *Ecophysiology of photosynthesis*, edited by Schulze ED & Caldwell MM, Springer, Berlin, 17–4.
- Drolet GG, Huemmrich KF, Hall FG, Middleton EM, Black TA, Barr AG, Margolis GA (2004) A MODIS-derived photochemical reflectance index to detect inter-annual

- variations in the photosynthetic light-use efficiency of a boreal deciduous forest. *Journal of Geophysical Research* 106:33579–33591
- Evain S, Flexas J, Moya I (2004) A new instrument instrument for passive remote sensing: 2. Measurement of leaf and canopy reflectance changes at 531 nm and their relationship with photosynthesis and chlorophyll fluorescence. *Remote Sensing of Environment* 91:175-185
- Filella I, Amaro T, Araus JL, Penuelas J (1996) Relationship between photosynthetic radiation-use efficiency of barley canopies and the photochemical reflectance index (PRI). *Physiologia Plantarum* 96:211-216
- Filella I, Penuelas J, Llorens L, Estiarte M (2004) Reflectance assessment of seasonal and annual changes in biomass and CO<sub>2</sub> uptake of a Mediterranean shrubland submitted to experimental warming and drought. *Remote Sensing of Environment* 90: 308-318
- Gamon JA, Penuelas J, Field CB (1992) A narrow-waveband spectral index that tracks Diurnal Changes in Photosynthetic Efficiency. *Remote Sensing of Environment* 41:35-44
- Gamon JA, Serrano L, Surfus JS (2002) The photochemical reflectance index: an optical indicator of photosynthetic radiation use efficiency across species, functional types and nutrient levels. *Oecologia* 112:492-501
- Guo J, Trotter CM (2004) Estimating photosynthetic light-use efficiency using photochemical reflectance index: variations among species. *Functional Plant Biology* 31:255-265
- Haboudane D, Miller JR, Tremblay N, Zarco-Tejada PJ, Dextraze L (2002) Integrated narrow-band vegetation indices for prediction of crop chlorophyll content for application to precision agriculture. *Remote Sensing of Environment* 81:416-426
- Jacquemoud S, Baret F (1990) PROSPECT: A model of leaf optical properties spectra. *Remote Sensing of Environment* 44: 281-292
- Kötz B, et al. (2004) Radiative transfer modeling within a heterogeneous canopy for estimation of forest fire fuel properties. *Remote Sensing of Environment* 92: 32-344
- Nichol CJ, Huemmrich KF, Black TA, Jarvis PG, Walthall CL, Hall FG (2000) Remote sensing of photosynthetic-light-use efficiency of boreal forest. *Agricultural and Forest Meteorology* 101:131-142
- Nichol CJ, Lloyd J, Shibistova O, Arneth A, Roser A, Knohl A, Matsubara Sm, Grace J (2002) Remote sensing of photosynthetic-light-use efficiency of a Siberian boreal forest. *Tellus* 54B:677-687

- Penuelas J, Baret F, Filella I (1995) Semi-empirical indices to assess carotenoids/chlorophyll a ratio from leaf spectral reflectance. *Photosynthetica* 31:221-230
- North PRJ (1996) Three-dimensional forest light interaction model using a monte carlo method. *IEEE Transactions on Geoscience and Remote Sensing* 34:946-956
- Rahman AF, Cordova VD, Gamon JA, Schmid HP, Sims DA (2004) Potential of MODIS ocean bands for estimating CO<sub>2</sub> flux from terrestrial vegetation: A novel approach. *Geophysical Research Letters* 31:L10503
- Rahman AF, Gamon JA, Fuentes DA, Roberts DA, Prentiss D (2001) Modeling spatially distributed ecosystem flux of boreal forest using hyperspectral indices from AVIRIS imagery. *Journal of Geophysical Research* 106:33579– 33591
- Sims DA, Gamon JA (2002) Relationships between leaf pigment content and spectral reflectance across a wide range of species, leaf structures and developmental stages. *Remote Sensing of Environment* 81:337-354
- Stylinsky CD, Gamon JA, Oechel WC (2002) Seasonal patterns of reflectance indices, carotenoid pigments and photosynthesis of evergreen chaparral species. *Oecologia* 131: 366-374
- Verrelst J, Schaepman ME, Koetz B, Kneubühler M (2007) Angular sensitivity of vegetation indices derived from CHRIS/PROBA data in two Alpine ecosystems. *Remote Sensing of Environment* (in revision)

## Curriculum Vitae

**Name** Ač  
**First name** Alexander  
**Date of birth** 4<sup>th</sup> 11, 1980  
**Place of Birth** Jablonec nad Nisou, Czech Republic  
**Address** Bratislava, Slovakia  
**E-mail** acalex@usbe.cas.cz

### Education

1992-1999 Gymnasium Bilíkova, Bratislava, Slovakia  
1999-2004 Mgr. (equivalent to M.Sc.): Pavol Jozef Šafárik University (Košice), Faculty of Sciences, Environmental Ecology (1999 – 2004)  
2004 – present Ph.D. studies: University of South Bohemia (České Budějovice), Agricultural faculty

### Academic and professional appointments:

2004 – 2005 Institute of Landscape Ecology ASCR  
2005 – present Institute of Systems Biology and Ecology ASCR

### Important research visits and fellowships:

2003 Sokrates Erasmus exchange programme at the Aristotle University of Thessaloniki (Greece)  
2006 to 2007 PhD fellowship – Wageningen University (Netherlands)

### Share on grants within the framework of dissertation thesis:

2008-2010 *ForChange* – Indication of state and changes of forest ecosystems in the context of global change by means of analysis of ecophysiological processes and observation by means of remote sensing methods. MŽP SP/2D1/70/08

2006-2011 *Interviron* – Quantification and interpretation of ecosystem response to environmental pressure v the Czech Republic. MŠMT 2B06068.

## List of publications

### *Peer reviewed journals*

1. Urban O, Ač A, Kalina J, Priwitzer T, Šprtová M, Špunda V, Marek MV (2007) Temperature dependences of carbon assimilation processes in four dominant species from mountain grassland ecosystem. *Photosynthetica*, 45:392-399
2. Lichtenthaler HK, Ač A, Marek MV, Kalina J, Urban O (2007) Differences in pigment composition, photosynthetic rates and chlorophyll fluorescence images of sun and shade leaves of four tree species. *Plant Physiology and Biochemistry*, 45:577-588
3. Verrelst J, Ač A, Malenovský Z, Hanuš J, Marek M, Schaepmann ME (2007) Chlorophyll Vegetation Indices Estimates Derived from Ground-Based Diurnal Course Data and Multiangular CHRIS-PROBA Data. In Reusen, I., Cools, J., (Eds.) "Imaging Spectroscopy: innovation in environmental research" 5<sup>th</sup> EARSeL SIG IS workshop, Bruges, Belgium, 23-25 April, Proceedings – CD ROM."
4. Ač A, Malenovský Z, Hanuš J, Tomášková I, Urban O, Marek MV (2009) Near distance imaging spectroscopy investigating photosynthetic activity of grassland in the daily course, *Accepted in Functional Plant Biology*
5. Ač A, Malenovský Z, Urban O, Hanuš J, Košvancová M, Navrátil M, Vašková M, Olejníčková J, Marek M (2009) Are simple reflectance ratios related to chlorophyll fluorescence able to track changes in carbon fluxes of grassland and forest ecosystems? *Planned for submission to Oecologia*

**Conference and workshop contributions**

1. **Ač A**, Malenovský Z, Pokorný R, Hanuš J, Marek MV (2006) Field imaging spectroscopy investigating PRI spatial distribution of montane grassland canopy in diurnal course. In: European Geosciences Union General Assembly 2006 Vienna, Austria, April 2-7.
2. **Ač A** (2006) Spatial distribution of carbon sinks activity using high resolution imaging spectroscopy. In: The annual conference of PhD students, University of South Bohemia in České Budějovice, May 3-4.
3. **Ač A** (2006) Daily courses of selected vegetation indices for chlorophyll estimation of the montane grassland using high spatial/spectral resolution imaging spectroscopy. In: 15 years of EU-supported ecophysiological research in the Czech Republic, Olomouc, September, 18-21.
4. **Ač A**, Malenovský Z, Hanuš J, Marek MV (2007) Daily courses of selected optical indices for chlorophyll fluorescence estimation of the montane grassland using high spatial/spectral resolution imaging spectroscopy. In: 3<sup>rd</sup> International workshop on remote sensing of vegetation fluorescence, Florence, Italy, February 7-9.
5. **Ač A**, Olejníčková J, Mistra KB, Malenovský Z, Hanuš J, Trtílek M, Nedbal L, Marek MV (2008) Towards remote sensing of vegetation processes. In Kooistra, L., Ligtenberg, A., (Eds.). "Proceedings of International Workshop Sensing a Changing World. CGI report CGI-08-005, Wageningen University and Research Centre, Wageningen, The Netherlands. ISSN 1568-1874.
6. **Ač A**, Hanuš J, Marek MV (2009) Separating the effects of light and temperature on hyperspectral reflectance and chlorophyll fluorescence measured simultaneously. In: 8<sup>th</sup> International Conference Ecophysiological aspects of plant responses to stress factors, Krakow, Poland, September 16-19.
7. Navrátil M, Špunda V, Jančíková H, **Ač A** (2009) Photochemical reflectance index for estimation of activity of xanthophyll cycle in *Picea abies*. In: 8<sup>th</sup> International Conference Ecophysiological aspects of plant responses to stress factors, Krakow, Poland, September 16-19.